UNIVERSITÀ DEGLI STUDI DI MILANO
Department of Pharmacological and Biomolecular Sciences

PhD SCHOOL OF BIOCHEMICAL, NUTRITIONAL
AND METABOLIC SCIENCES

PhD IN BIOCHEMISTRY
XXVI CYCLE

POTENTIAL MITOCHONDRIAL REGULATORS: FUNCTIONAL VALIDATION BY INTEGRATED APPROACHES

Disciplinary Scientific Sector BIO/10

Elisabetta Brioschi
Student ID: R09260

Co-Tutor: Dott. Nico Mitro
Tutor: Dott. Emma De Fabiani
Coordinator: Prof. Francesco Bonomi

Index:

1. Introduction:

1.1 Metabolism

Metabolism is the set of life-sustaining chemical transformations within the cells of living organisms. These enzyme-catalyzed reactions allow organisms to grow and reproduce, maintain their structures, and respond to their environments. Metabolism is usually divided into two categories; anabolism and catabolism. Anabolism is the set of constructive metabolic processes where the energy released by catabolism is used to synthesize complex molecules. Anabolism involves three basic stages. Firstly, the production of precursors such as amino acids, monosaccharaides, isoprenoids and nucleotides; secondly, their activation into reactive forms using energy from adenosine triphosphate (ATP); and thirdly, the assembly of these precursors into complex molecules such as proteins, polysaccharides, lipids and nucleic acids. Catabolism is the set of metabolic processes that break down large molecules. These include breaking down and oxidizing food molecules. The most common set of catabolic reactions in animals can be separated into three main stages. In the first, large organic molecules such as proteins, polysaccharides or lipids are digested into their smaller components outside cells. Next, these smaller molecules are taken up by cells and converted to yet smaller molecules, usually acetyl coenzyme A (acetyl-CoA), which releases some energy. Finally, the acetyl group on the CoA enters in the citric acid cycle producing water, carbon dioxide and reducing the coenzyme nicotinamide adenine dinucleotide (NAD^+) and flavin adenine dinucleotide (FAD) into NADH and $FADH_2$. These coenzymes transfer their electrons to the electron transport chain, which coupled with the oxidative phosphorylation produce water and ATP.

1.2 Energetic metabolism

Glycolysis is the metabolic pathway that converts glucose into pyruvate; it occurs in the cytosol of the cell. The free energy released in this process is used to form the high-energy compounds ATP and NADH. The net yield of the glycolysis for one glucose molecule is two pyruvate molecules, two ATP, two NADH, two H_2O and two H^+. Glycolysis is a determined sequence of ten enzyme-catalyzed reactions. The intermediates provide entry points to glycolysis. For example, most monosaccharaides, such as fructose and galactose, can be converted to one of these intermediates. Glycolysis occurs, with variations, in nearly all organisms, both aerobic and anaerobic. The wide occurrence of glycolysis indicates that it is one of the most ancient known metabolic pathways [1].

In the aerobic metabolisms during the fasted state, the main destiny of the pyruvate molecules produced in the glycolysis is to entry into the tricarboxylix acid (TCA) cycle. In eukaryotic cells, the TCA cycle occurs in the matrix of the mitochondrion (Fig. 1.2.1). The TCA cycle is a series of eight chemical reactions used by all aerobic organisms to generate energy through the oxidation of acetate derived from carbohydrates, fats and proteins into carbon dioxide (CO_2) and chemical energy in the form of ATP. The net yield for each molecule of glucose oxidized is two GTP (guanosine triphosphate), six NADH, two $FADH_2$ (flavin adenine dinucleotide), six H^+ e four CO_2. In addition, the cycle provides precursors of certain amino acids as well as the reducing agent NADH that is used in numerous other biochemical reactions. Its central importance to many biochemical pathways suggests that it was one of the earliest established components of cellular metabolism.

The acetyl-CoA, necessary for the TCA cycle is obtained not only by the glycolysis but also by the β-oxidation of the fatty acids. Fatty acids are transported across the

outer mitochondrial membrane by carnitine acyl transferases, and then couriered across the inner mitochondrial membrane by carnitine. Once inside the mitochondrial matrix, the fatty acyl-carnitine reacts with CoA to release the fatty acid and produce acetyl-CoA. Once inside the mitochondrial matrix, fatty acids undergo β-oxidation (Fig. 1.2.1). During this process, two-carbon molecules acetyl-CoA are repeatedly cleaved from the fatty acid. Acetyl-CoA can then enter the TCA, which produces NADH and $FADH_2$. Since β-oxidation cleaves two-carbon molecules repeatedly, it works well for even carbon chain length saturated fatty acids. For odd-carbon chain length fatty acids and unsaturated fatty acids, a slightly different pathway is taken.

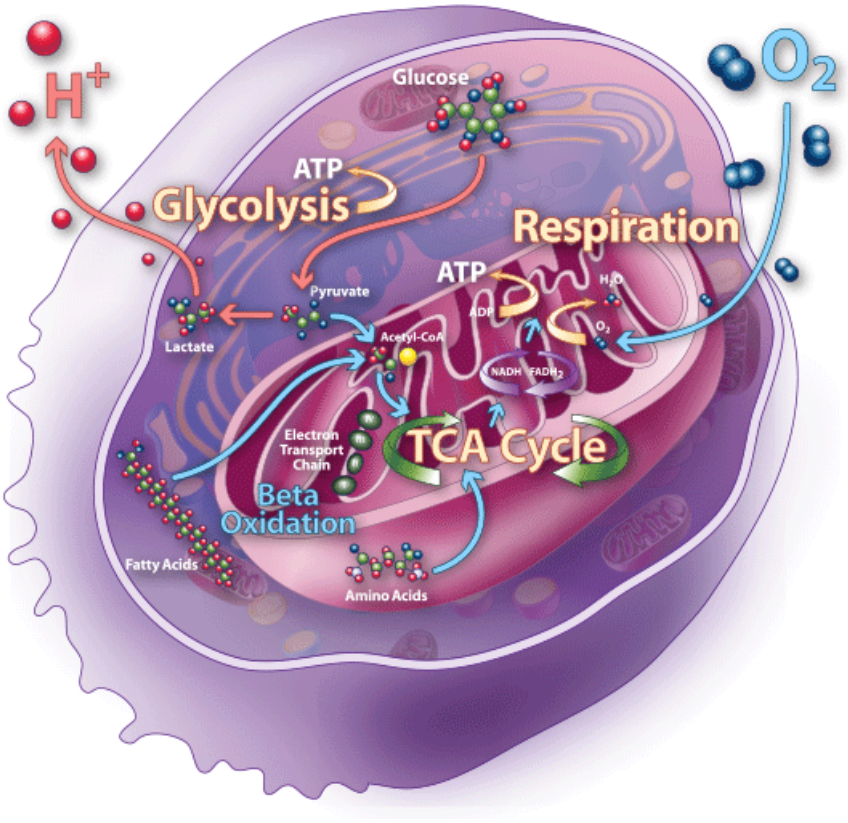

Figure 1.2.1: Mitochondria are involved in many pathways belonged to energetic metabolism.

All the oxidative degradation pathways described converge in the final step of the cellular respiration. During this process, all the energy produced is used to generate ATP. The oxidative phosphorylation (OXPHOS) represents the top of the energetic

metabolism for aerobic organisms. During OXPHOS, electrons are transferred from electron donors to electron acceptors such as oxygen, in redox reactions. These redox reactions release energy, which is used to form ATP. In eukaryotes, these redox reactions are carried out by a series of protein complexes within the cell's intermembrane wall mitochondria. The energy released by electrons flowing through this electron transport chain is used to transport protons across the inner mitochondrial membrane, in a process called electron transport. This generates potential energy in the form of a pH gradient and an electrical potential across this membrane. This store of energy is tapped by allowing protons to flow back across the membrane and down this gradient, through a large enzyme called ATP synthase (ATPase). This enzyme uses this energy to generate ATP from adenosine diphosphate (ADP), in a phosphorylation reaction. This reaction is driven by the proton flow, which forces the rotation of a part of the enzyme; the ATPase is a rotary mechanical motor.

1.3 Mitochondria

Mitochondria are ubiquitous membrane-bound organelles that are characteristic of the eukaryotic cell. Their functions are mediated by thousands of mitochondrial-specific proteins encoded by both the nuclear (nDNA) and mitochondrial (mtDNA) genome [2, 3]. The organelle is formed by a soluble matrix surrounded by a double membrane, an ion impermeable inner membrane, and a permeable outer membrane (Fig. 1.3.1) [4].

Early biochemists documented the significance of mitochondria for aerobic oxidation of metabolic fuels, as they are the location of the electron transport chain (ETC) and OXPHOS that provides the majority of cellular energy in the form of ATP [5, 6].

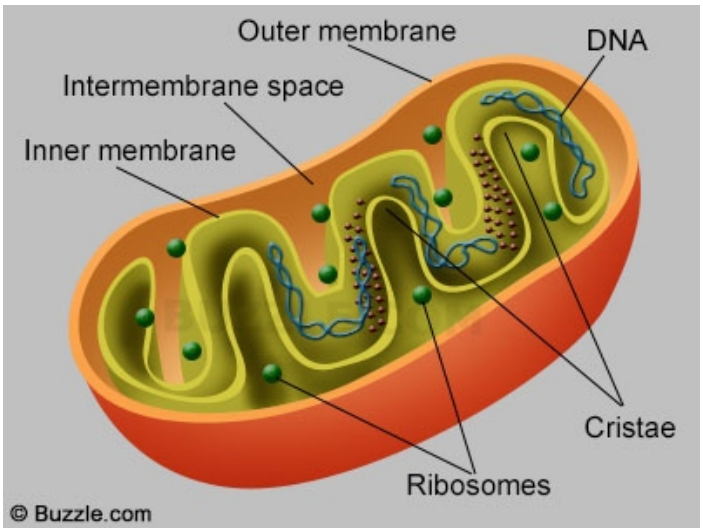

Figure 1.3.1: The basic structure of mitochondria. They are composed of an innemr membrane, an outer membrane and among them the intermembrane space. They have own circular molecule of DNA and ribosomes. The inner membrane is organized in cristae in order to increase the surface.

It is now well established that they contribute to many other important functions including oxidative catabolism of amino acids, ketogenesis, ornithine cycle activity ("urea cycle"), the generation of reactive oxygen species (ROS) with important signaling functions [7, 8], the control of cytoplasmic calcium [9, 10], and the synthesis of all cellular Fe/S clusters, protein cofactors fundamental for cellular functions such as protein translation and DNA repair [11]. The rate-limiting first step in steroidogenesis is also located in mitochondria, associating mitochondrial function to endocrine homeostasis [12-15]. This collection of organelle functions justifies the variability in pathophysiology, severity, and age of onset of the increasing number of disorders associated to alterations in specific mitochondrial pathways [11, 16-18].

1.3.1 Evolution of mitochondria

To comprehend nuclear–mitochondrial connections, we must take into consideration the early steps in the endosymbiontic event that generated the eukaryotic cell about 2

billion years ago [19]. In the beginning, the proto-nucleus–cytosol was restricted by energy. This limitation was relieved by its symbiosis with an oxidative α-protobacterion, the proto-mitochondrion [20]. Consequently, growth and replication of the nucleus turn out to be regulated by mitochondrial energy production and thus calorie availability. This required the regulation of nuclear replication and gene expression by mitochondrial energetics. This was accomplished by joining alteration of nDNA chromatin structure and function by modification via high-energy intermediates: phosphorylation by ATP, acetylation by acetyl-CoA, deacetylation by NAD^+ and methylation by S-adenosyl-methionine. Equally, the nucleus had to acquire mechanisms for modulating mitochondrial growth and replication. This was made complex by the successive transfer of genes from the proto-mtDNA to the nDNA, with the cytosolic translation products being directionally imported back into the mitochondrion [19]. This process continued over a billion years with the result that the nDNA-encoded genes of the mitochondrial genome are now disseminated throughout the chromosomes [19]. Hence, new mechanisms had to develop to coordinate the expression of the mitochondrial genes based on nuclear necessities for energy for growth and reproduction. As a result, this evolved in the development of inter-chromosomal coordinate transcriptional regulation. Over the subsequent 1.2 billion years, the nucleus–cytosol became increasingly specialized in specifying structure while the mitochondrion became entirely dedicated to energy production [20].

1.3.2 The dynamic morphology of mitochondria

Mitochondria are organized in a reticulum that is in continuous communication through dynamic fusion and fission events, moving actively throughout the cell

thanks to interactions with the cytoskeleton. The mitochondrial reticulum is constituted of an outer and an inner membrane, between which is the intermembrane space, and a matrix limited by the inner membrane (Fig. 1.3.1). The area of the inner membrane is greater than that of the outer membrane due to the presence of cristae, inner membrane invaginations that include all the transmembrane proteins of the ETC as well as the mitochondrial ATPase [21-23]. The mitochondrial matrix contains also the components of the TCA cycle and of the β-oxidation pathway. Mitochondrial fusion and fission not only merges the mitochondrial inner and outer membranes but also mixes mitochondria matrices and redistributes the mtDNAs [20].

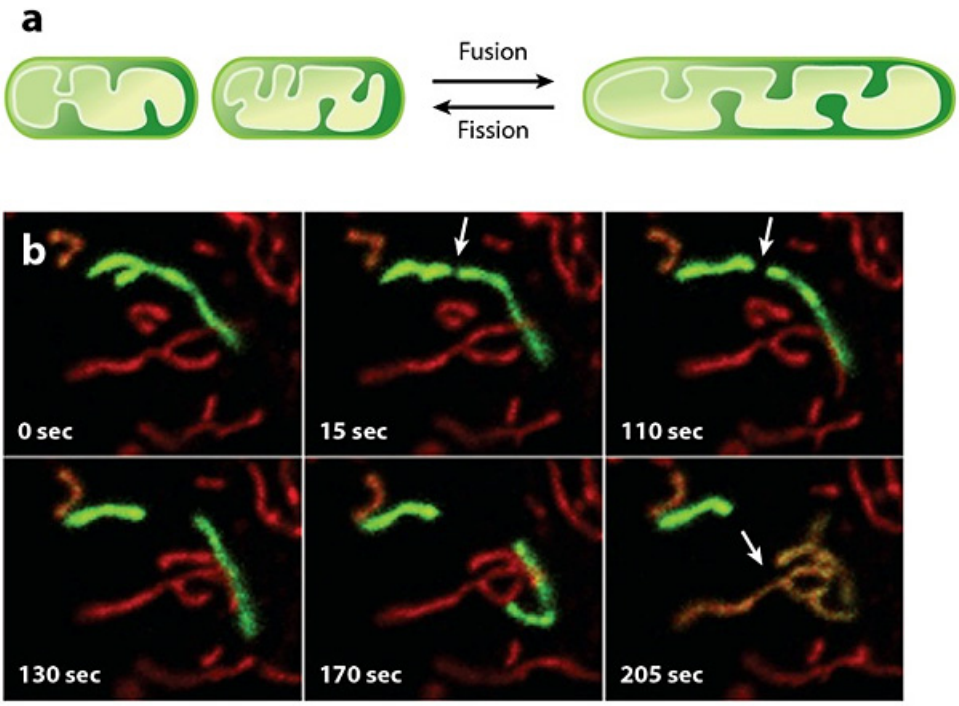

Figure 1.3.2: Overview of mitochondrial fusion and fission. A: A schematic showing mitochondrial fusion and fission. During fusion, there is merging of the mitochondrial outer membrane and inner membrane, resulting in mixing of the mitochondrial matrices. B: Live imaging illustrating that mitochondrial fusion results in content mixing. The mitochondria are labeled with DsRed and photoactivatable GFP. A mitochondrion is photoactivated (green) in the first frame and undergoes fission (arrow, second and third frames) followed by fusion (arrow, last frame)[24].

The mammalian mitochondrial fusion machinery includes three major proteins: mitofusin 1 (Mfn1), 2 (Mfn2), and the Optic Atrophy-1 Protein (Opa1) [25-27], while

the mitochondrial fission machinery engages dynamic-related protein 1 (Drp1), fission 1 (Fis1), and mitochondrial fission factor (Mff) [28-31]. Mitochondrial fission and fusion activities are both mediated by large guanosine triphosphatases (GTPases) in the dynamin family [32]. Their mutual actions divide and fuse the two lipid bilayers that surround mitochondria (Fig. 1.3.2). Fission is driven by the Mff-mediated recruitment of Drp1 from cytosol to mitochondria in mammals [33], often at sites where mitochondria make contact with the endoplasmic reticulum [34]. Fusion between mitochondrial outer membranes is mediated by membrane-anchored dynamin family members named Mfn1 and Mfn2 in mammals, whereas fusion between mitochondrial inner membranes is mediated by a single dynamin family member called Opa1 in mammals [35]. Mitochondrial fission and fusion machineries are controlled by proteolysis and posttranslational modifications [32]. Frequencies of mitochondrial fission and fusion depend on variations in metabolism. Mitochondria are more fused when they have to rely on oxidative phosphorylation by withdrawing glucose as a carbon source [36]. Amplified fusion may be essential to increase the fidelity for oxidative phosphorylation by encouraging complementation among mitochondria. Starvation-induced autophagy may boost fusion by increasing the dependence on oxidative phosphorylation through the metabolism of lipids and proteins [36]. Otherwise, starvation may induce a specific stress response called stress-induced mitochondrial hyperfusion [37], or it may prevent fission in order to protect mitochondria from autophagic catabolism [38, 39]. Each of these outcomes is coherent with a model in which mitochondrial dynamics support the maximization of the oxidative phosphorylation under stressful conditions.

1.3.3 mtDNA

Contrary to the nuclear genome, characterized of repetitive sequence families, introns, and vast intergenic regions, the mtDNA of mammals and other vertebrates shows remarkable economy of sequence organization [4]. The vertebrate mitochondrial genome is a closed circular molecule of ~16.5 kb whose entire protein coding capacity is dedicated to the synthesis of 13 proteins that are essential subunits of respiratory complexes I, III, IV, and V [4]. The genes encoding complex II are entirely nuclear. The mtDNA also encodes the 22 tRNAs and 2 ribosomal RNAs essential for the translation of these respiratory subunits within the mitochondrial matrix. Mitochondrial genes miss introns and are arranged end on end with little or no intergenic regions [4]. Some respiratory protein genes overlay, and the adenine nucleotides of UAA termination codons are not encoded in the mtDNA but rather are delivered by polyadenylation following RNA processing [40]. Protein coding and rRNA genes are interspersed with tRNA genes that are assumed to determine the cleavage sites of RNA processing. The only substantial noncoding region is the D-loop, named after the triple-stranded structure or displacement loop that is formed by association of the nascent heavy (H)-strand in this region (Fig. 1.3.3) [4]. The D-loop comprises the origin of heavy (H)-strand DNA replication and is also the site of bidirectional transcription from opposing heavy (HSP) and light (LSP) strand promoters [41]. Since mtDNA is a compartmentalized extra-chromosomal component, its inheritance model diverges from that of nuclear genes. Somatic mammalian cells generally have 10^3-10^4 copies of mtDNA with ~2–10 genomes per organelle [42]. These genomes replicate in a relaxed fashion that is independent of the cell cycle that is defined by nuclear DNA replication [43, 44]. Some mtDNA molecules experience multiple rounds of replication while others do not replicate.

This, along with random sampling during cell division, permits the separation of sequence variants during mitosis [45]. Transcription of mtDNA is completely dependent on nucleus-encoded gene products. The transcription initiation complexes are comprised of a mitochondrial RNA polymerase (POLRMT), Transcription factor A (Tfam) and one of the two TFB isoforms (TFB1M and TFB2M) that function as dissociable specificity factors that contact both the polymerase and Tfam.

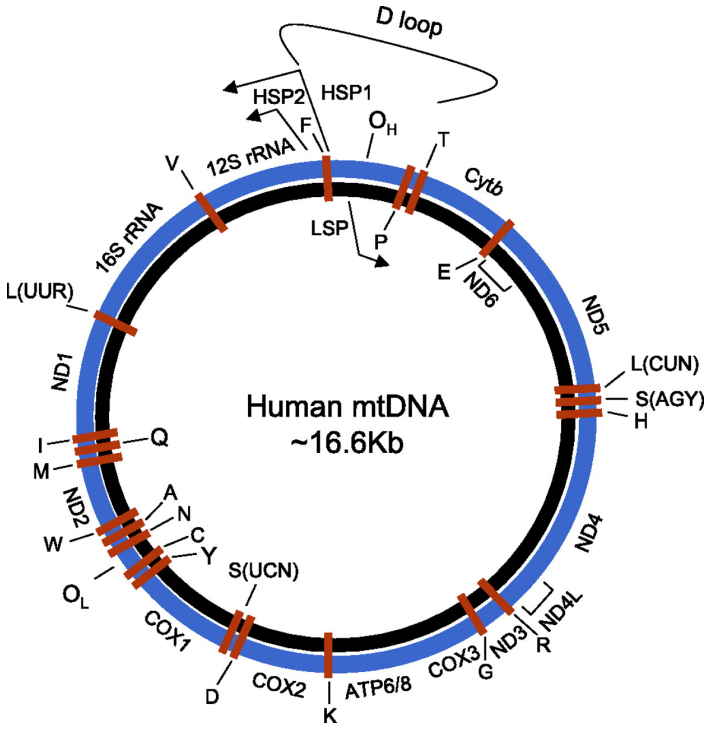

Figure 1.3.3: Schematic representation of the human mitochondrial genome. Genomic organization and structural features of human mtDNA are depicted in a circular genomic map showing heavy (blue) and light (black) strands assigned as such based on their buoyant densities. Protein coding and rRNA genes are interspersed with 22 tRNA genes (red bars denoted by the single-letter amino acid code). Duplicate tRNA genes for leucine (L) and serine (S) are distinguished by their codon recognition (parentheses). The D-loop regulatory region contains the L- and H-strand promoters (LSP, HSP1, and HSP2), with arrows showing the direction of transcription. The origin of H-strand replication (OH) is within the D-loop, whereas the origin of L-strand replication (OL) is displaced by approximately two-thirds of the genome within a cluster of five tRNA genes (W, A, N, C, Y). Protein coding genes include the following: cytochrome oxidase (COX) subunits 1, 2, and 3; NADH dehydrogenase (ND) subunits 1, 2, 3, 4, 4L, 5, and 6; ATP synthase (ATPS) subunits 6 and 8; cytochrome b (Cyt b). ND6 and the 8 tRNA genes transcribed from the L-strand as template are labeled on the inside of the genomic map, whereas the remaining protein coding and RNA genes transcribed from the H-strand as template are labeled on the outside [4].

In mammals, mtDNA is maternally inherited [45, 46]. Usually, paternal mtDNA is lost during the first few embryonic cell dissections and does not give mtDNA to the

progeny, although there are reports of the occurrence of the paternal heredity in somatic tissues [47]. Once, recombination between maternal and paternal genomes has been recognized [48]. Furthermore, because mtDNA is a multicopy genome, an individual may show more than a single sequence, a condition named heteroplasmy. A harmful sequence variant may be tolerated in low copy because the defective gene product(s) it encodes do not reach the threshold for disrupting cellular function. Conversely, sequence variants are recognized to separate rapidly from heteroplasmy to homoplasmy in passing from one generation to the next [49]. This could end with offspring in which the detrimental variant prevails, running to a defective mitochondrial phenotype.

1.3.4 Oxidative phosphorylation

The ETC is constituted of four large multisubunit complexes (complexes I to IV) with more than 85 individual gene products and ATPase (complex V). The proteins that compose the different complexes are both nuclear and mitochondrial encoded except the complex II that is completely nuclear. In Table 1 the number of subunits for each complex that are nucleus or mitochondria encoded are reported [50].

	Complex I	**Complex II**	**Complex III**	**Complex IV**	**Complex V**
mtDNA	7	0	1	3	2
nDNA	39	4	10	10	14

Table 1: Number of nuclear- and mitochondrial-encoded electron transport chain proteins.

The ETC transfers electrons from donors (NADH at complex I, $FADH_2$ at complex II) to a final acceptor, molecular oxygen, forming H_2O at complex IV [51]. Two electrons (reducing equivalents from hydrogen) are transferred from NADH + H^+ to

the OXPHOS complex NADH dehydrogenase (complex I) or from $FADH_2$ to the succinate dehydrogenase (SDH, complex II) to reduce ubiquinone (coenzyme Q_{10}, CoQ) to ubiquinol $CoQH_2$ [20]. The electrons from $CoQH_2$ are transferred successively to complex III (bc_1 complex), cytochrome c, complex IV (cytochrome c oxidase, COX), and finally to oxygen ($1/2O_2$) to give H_2O [20]. The energy that is liberated during the electrons' flow is used to pump protons out across the mitochondrial inner membrane through complexes I, III, and IV creating a proton electrochemical gradient; the remainder is dissipated as heat (Fig. 1.3.4). The energy contained in the proton electrochemical gradient generated by the ETC is then coupled to ATP production as protons flow back into the matrix through the mitochondrial ATPase (Complex V). Matrix ATP is then exchanged for cytosolic ADP by the inner membrane adenine nucleotide translocators [20].

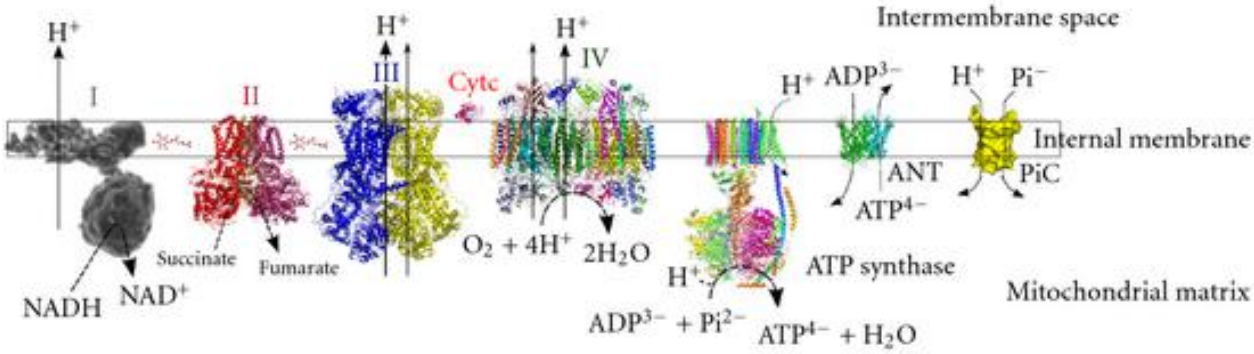

Figure 1.3.4: The mammalian oxidative phosphorylation (OXPHOS) system. Depicted are the four respiratory complexes (I–IV), electron carriers coenzyme Q and cytochrome c, the ATP synthase complex, the ADP/ATP carrier and the phosphate carrier (PiC). Arrows at complexes I, III, and IV illustrate the proton pumping to the intermembrane space.

Thus, OXPHOS results from electron transport, the generation of a proton gradient, and subsequent proton flux coupled to the mitochondrial ATPase [51]. Each of these steps can vary in efficiency; for example, the exact stoichiometry between electron flow and proton pumping, or between proton pumping and ATP synthesis varies depending on the probability of loss of electrons from the ETC before reaching

complex IV and on non-ATPase-coupled proton leak through the inner mitochondrial membrane (e.g., via uncoupling proteins (UCPs)) [51]. The high electronegative potential produced by the proton gradient also forces the rapid entry of Ca^{++} into the mitochondrial matrix, protecting its concentration in the cytoplasm. In the mitochondrial matrix, Ca^{++} can stimulate flux through the TCA cycle by rising dehydrogenase activities [10]. The exit of Ca^{++} from the matrix is driven by electroneutral exchange with Na^{+} or H^{+}.

The efficiency by which dietary reducing equivalents are converted to ATP by OXPHOS is known as the coupling efficiency [20]. This is determined by the efficiency by which protons are pumped out of the matrix by complexes I, III, and IV and the efficiency by which proton flux through complex V is converted to ATP [20]. The uncoupler compounds like 2,4-dinitrophenol (DNP) or carbonyl cyanide rn-chlorophenylhydrazone (CCCP) and the nDNA-encoded UCP1 and 2 render the mitochondrial inner membrane leaky for protons, by-passing complex V and dissipating the energy as heat [19].

1.3.5 ROS and mitochondria

The ETC is a strong font of ROS. ROS production is more expected to happen when the proton gradient is large and electron carriers are highly reduced, e.g., when ADP is rate limiting for ATP generation or when availability of O_2 is restrictive. Uncoupling proteins are pondered to be natural regulators of this process, replying to and governing ROS production by alleviating the establishment of a large proton gradient. Under normal physiological conditions, ROS production is highly structured, at least in part controlled by complex I [52-54]. Though, when the ETC turns out to be highly reduced, the excess electrons can be delivered directly to O_2 to

produce superoxide anion (O_2^-). The O_2^- generated by complex I is discharged into the mitochondrial matrix where it is transformed to hydrogen peroxide (H_2O_2) by the matrix manganese superoxide dismutase, MnSOD (Sod2 gene). Superoxide produced from complex III is liberated into the mitochondrial intermembrane space where it is converted to H_2O_2 by Cu/ZnSOD (Sod1) which is located in the mitochondrial intermembrane space and cytosol [20]. Mitochondrial H_2O_2 can diffuse into the nucleus–cytosol. If H_2O_2 faces a reduced transition metal or is mixed with O_2^-, the H_2O_2 can be further reduced to hydroxyl radical, the most potent oxidizing agent of the ROS. ROS can impair cellular proteins, lipids, and nucleic acids. Hereafter, excessive mitochondrial ROS generation can exceed the antioxidant protections of the cell, and the cumulative injury can ultimately lead to cell death [20].

1.3.6 Apoptosis and mitochondria

Apoptosis mediates catabolism of eukaryotic cells and it is a process crucial for the development and the turnover of tissues, for the mechanisms of cellular defense and protection from cancer. All apoptotic pathways converge to the activation of caspases, proteases that orchestrate the efficient cell elimination without causing inflammation. Two pathways have been characterized by which caspases are activated: the extrinsic pathway that is mediated by some membrane receptors, which directly activate caspase 8, and the intrinsic pathway that originates from the mitochondria. Mitochondria control an apoptotic phase, which precedes the activation of caspases and which is regulated by proteins belonging to the family of B-cell lymphoma 2 (Bcl-2). It is well documented, that the role of mitochondria in the activation of caspases is accomplished through the release of these proteins from the intermembrane space to the cytosol. When cytochrome c is released from

mitochondria binds to the apoptotic protease activating factor 1 (APAF1), initiating the assembly of the apoptosome, which is responsible for the activation of caspase 9 [55]. In literature it is well established, that during the apoptotic phenomenon mitochondria fragment into many small units, although it is not yet fully clear whether this occurs before or simultaneously with activation of caspases. It has been demonstrated that the blocking of this unregulated fission inhibits the release of cytochrome c and delays cell death, connecting the morphogenic machinery of these organelles to the programmed cell death [56]. Excessive mitochondrial fission appears to be a necessary requirement in intrinsic apoptotic pathway, at least for the release of cytochrome c and the caspase activation. On the other hand, apoptosis can be inhibited, by the mitochondrial fusion. Some proteins involved in mitochondrial fusion machinery are in some way linked to apoptosis. The silencing of Mfn1 and Mnf2 results in excessive mitochondrial fragmentation and increased sensitivity to proapoptotic stimuli [57].

An early mark of apoptosis is the mitochondrial membrane potential decrease [58]. It activates, the mitochondrial permeability transition pore (mtPTP), the mitochondrial self-destruct system [59]. mtPTP is also stimulated when the biochemical condition of the mitochondria and cell regress, specifically when mitochondrial energy production declines, ROS generation increases, and excessive Ca^{++} is discharged into the cytosol and taken up by the mitochondrion [20]. When the mtPTP is activated, it unlocks a channel in the mitochondrial inner membrane, short circuits proton electrochemical gradient, and initiates programmed cell death (apoptosis) [60].

1.4 Transcriptional control mechanisms of mitochondria

Although we know very little about specific mechanisms that control different modalities of mitochondrial biogenesis, it is clear that these mechanisms require coordination between the nuclear and mitochondrial genomes. Transcription of the mitochondrial genome is under the control of a single transcription factor, Tfam, which is encoded by the nuclear genome [51]. In turn, Tfam expression is controlled by the nuclear transcription factors 1 (NRF-1) and 2 (NRF-2), which specifically activate abundant nuclear-encoded genes implicated in mitochondrial respiration [61, 62] (Fig. 1.4.1). Thus, through NRF-stimulated expression of Tfam, the transcription of the mitochondrial genome is stimulated in coordination with that of nuclear-encoded mitochondrial genes [51]. The expression of many other mitochondrial genes is coordinated by additional nuclear transcription factors, like peroxisome proliferator-activated receptor α (PPARα), PPARδ, estrogen-related receptor (ERR) α /γ, and Sp1 (Fig. 1.4.1), which can stimulate the mitochondrial genes' expression in a tissue-dependent and physiological context-dependent manner [50]. A high level of transcriptional coordination is required to ensure coupling of mitochondrial activity to other metabolic activities within the cell and to mediate appropriate parallel changes in all components of multiprotein complexes [51]. This coordination is achieved through the action of transcriptional coactivators and corepressors. The most-known coactivators of mitochondrial gene transcription are members of the PPARγ coactivator (PGC) family, including PGC-1α, PGC-1β [63, 64], and PPRC, a related serum-responsive coactivator [65] (Fig. 1.4.1). These act in response to cellular energy-requiring states such as cell growth, hypoxia, glucose deprivation, and exercise [50] to promote transcription factors involved in mitochondrial remodeling and/or biogenesis, thus restoring cellular energetics. For instance, PCG-1α is highly

expressed in muscle, liver, and brown fat, and its expression is further increased in these tissues in response to exercise, fasting, and cold exposure, respectively [51]. Although PGC-1α and β do not seem to be essential for mitochondrial biogenesis during development [66], they are required for the expression of the entire set of proteins necessary for mitochondrial OXPHOS and fatty acid β-oxidation pathways in muscle and brown adipose tissue [67-76]. Additionally, PGC-1α and PGC-1β are critical for the rapid bursts in mitochondrial proliferation that is associated with perinatal heart and brown adipose tissue development [66]. These considerations sustain the idea that mitochondrial adjustment to specific energy needs is regulated by PGC-1α and PGC-1β. Conversely, mitochondrial development during cell proliferation is more likely to rely on serum-responsive coactivators such as PPRC [77]. The role of corepressors in the transcriptional control of energy metabolism genes is less extensively studied [51]. Nevertheless, evidence in cultured cells and in mouse models supports the critical role of the corepressor RIP140 in controlling mitochondrial energy metabolism in both adipose tissue and muscle [78-82]. RIP140 inhibits UCP1 through interaction with specific enhancer elements and also avoids expression of genes associated with β-oxidation and respiratory chain assembly. RIP140 also interacts directly with many of the transcription factors coactivated by PGC-1α [83]. The mechanisms that control the balance between PGC-1 coactivators and RIP140 and other corepressors are not clear but are likely to represent key regulatory mechanisms of energetic adaptation [51].

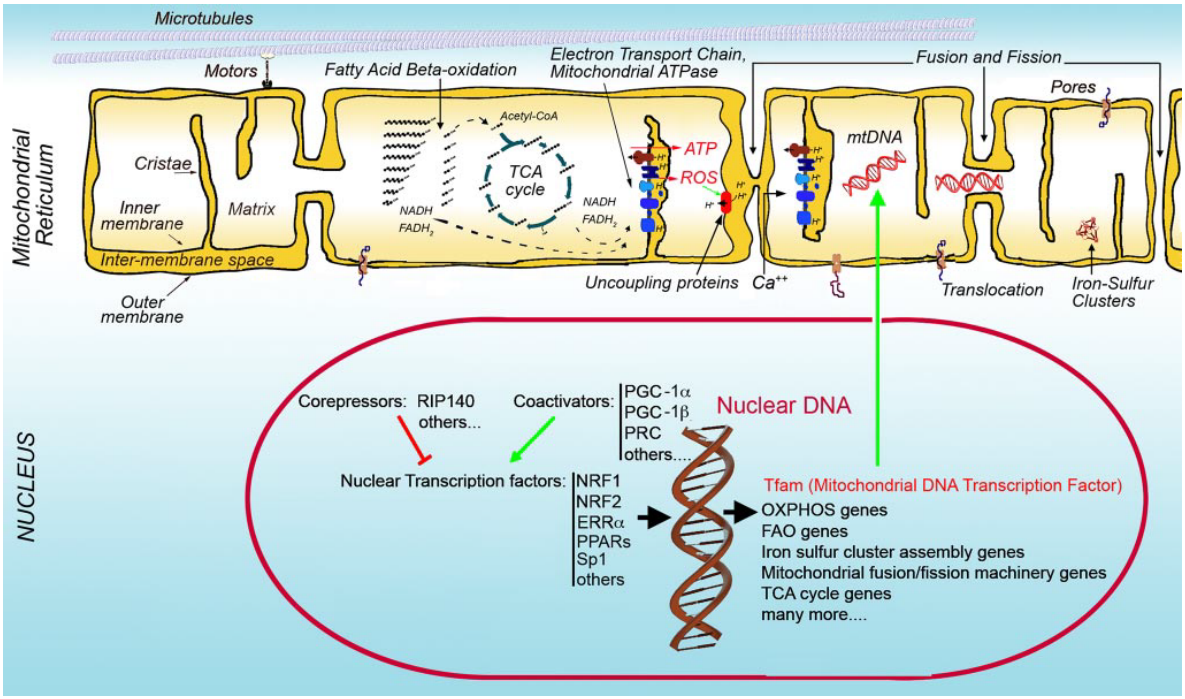

inner membrane is folded into cristae. The organization and distribution of the mitochondrial reticulum is controlled by interactions with cytoskeletal elements such as microtubules. The matrix contains the enzymatic machinery for fatty acid β-oxidation, which generates acetyl-CoA from acyl chains, and reducing equivalents in the form of NADH and $FADH_2$ in the process. Acetyl-CoA fuels the TCA cycle, which also produces NADH and $FADH_2$. These donate electrons to the ETC, leading to the generation of a proton gradient across the inner mitochondrial membrane. Dissipation of this gradient through the mitochondrial ATPase generates ATP. Delay of electron transport by the ETC results in the production of ROS, which can activate UCPs that dissipate the proton gradient without producing ATP. The electrochemical gradient also causes cytoplasmic $Ca^{++}$to enter the matrix, buffering cytoplasmic Ca^{++} levels and promoting TCA cycle flux. Mitochondria are also crucial in the generation of iron-sulfur clusters that form the prosthetic group of numerous proteins involved in multiple cellular pathways. The mitochondrial reticulum undergoes continuous fusion and fission reactions that involve both the inner and outer mitochondrial membranes, allowing redistribution of matrix content, such as mtDNA, within the reticulum. Both mitochondrial and nuclear DNA encoded the proteins composing all mitochondrial machineries. The master transcription factor operating on mtDNA is Tfam, which is encoded in the nuclear genome. The expression of mitochondrial genes in the nucleus is driven by numerous transcription factors, which are in turn controlled by specific coactivators and corepressors that respond to cellular energy demands [51].

1.4.1 Tfam

Tfam was first recognized as a high mobility group (HMG)-box protein that promote transcription through specific binding to recognition sites upstream from both light (LSP) and heavy (HSP) strand promoter [84]. Structurally, it consists of two tandemly arranged HMG motifs and a COOH-terminal tail [4]. Tfam looks like other HMG

proteins, as it can bend and unwind DNA, properties potentially connected to its ability to promote transcription upon binding DNA [85, 86]. Tetrameric binding of Tfam to its recognition site is known to stimulate bidirectional transcription by facilitating symmetrical interactions with other transcriptional components [87]. In addition to specific promoter recognition, Tfam binds nonspecifically to apparently random sites on mtDNA [85, 88]. This property, along with its abundance in mitochondria, suggests that it plays a role in the stabilization and maintenance of the mitochondrial chromosome [4]. The transcriptional activation function of Tfam belongs to a COOH-terminal activation domain that is necessary both for transcriptional ability and for specific binding to promoter recognition sites [89]. Tfam knockout mice show embryonic lethality and a reduction of mtDNA corroborating a crucial role for the protein in mtDNA maintenance in mammals [90]. Intriguingly, Tfam levels associate well with increased mtDNA in ragged-red muscle fibers, fibers showing an excessive proliferation of abnormal mitochondria, and decreased mtDNA levels in mtDNA-depleted cells [91]. This evidence correlates with the observation that transgenic mice overexpressing human Tfam show increased mtDNA copy number [92]. The mtDNA amount determined in somatic tissues and in embryos is relative to those of Tfam expressed in each, advocating that Tfam could be a limiting factor of mtDNA copy number. Thus its properties implicate Tfam as an ideal target for regulatory pathways that control both mtDNA maintenance and transcriptional expression [4].

In addition to its role in transcription initiation, Tfam binds abundantly and non-specifically around the entire mitochondrial genome [93]. In vivo, mtDNA exists as discrete, punctate protein–DNA structures named nucleoids. Tfam is a major component of the nucleoid [94-96], where it an architectural [97] or scaffolding [92]

role, apparently through its strong affinity for non-specific DNA sequences [88]. Several models have been stated to clarify how Tfam regulates genome compaction and promoter activity [97-102]. Fig. 1.4.2 provides a series of illustrations of Tfam dimer-mediated genome compaction with increasing Tfam loading by a non-specific, cooperative mechanism as Tfam abundance increases [93]. Because the abundance of Tfam in nucleoids can vary considerably without affecting nucleoid volume [103-105], the loops formed at low Tfam occupancy were considered to be the primary mechanism for the maintenance of mtDNA contour length [93]. As Tfam concentration increases, cooperatively drives Tfam loading at proximal sites, increasing the rigidity and density of the structure [93].

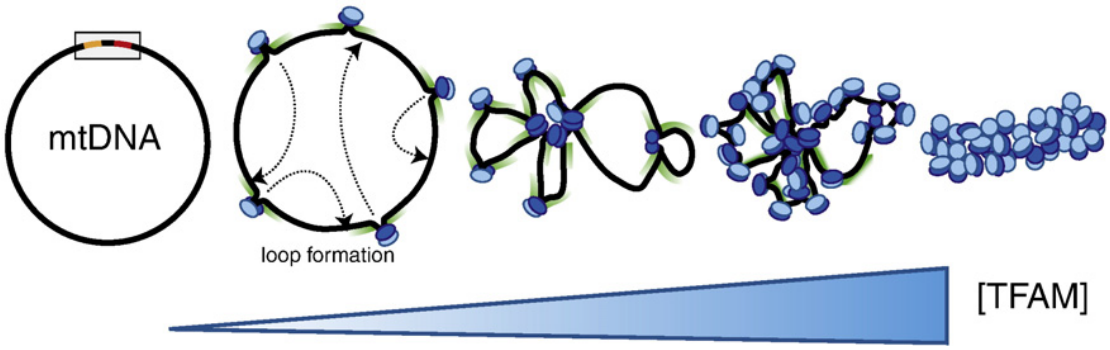

Figure 1.4.2: Tfam binding: dimerization, formation of loop structures, and genome compaction. Tfam concentration increases from the left to the right of the illustration (indicated by blue triangle). All binding events are considered non-specific and are not to scale. Because this model assumes dimeric Tfam bound to DNA, the subunit bound to DNA is shown in dark blue and the unbound subunit is in light blue. At low concentrations Tfam dimers bind to form loop structures that reduce DNA contour length (both subunits are shown in dark blue, indicating DNA binding by both subunits in the dimer to form a loop). Cooperative binding stimulates preferential Tfam loading at sites proximal to previously bound Tfam molecules (sites shown in green), until maximal compaction is achieved at highest Tfam concentrations. Limited genome access at these maximally compacted molecules could minimize transcription or replication activity [93].

The additional structural rigidity is likely imparted by topological changes in the genome, with some contour length reduction occurring through bending and supercoiling [85, 93, 106, 107]. Based on the evidences that high Tfam:mtDNA ratios

decline mtDNA copy number [108, 109] *in vivo*, true saturation of Tfam would likely drive to biologically inactive (quiescent) genomes [98]. The large number of genomes within the cell would allow for some molecules to exist in this **"**off**"** state; tissues with lower relative oxidative metabolism, or those in which primary cells are not dividing, might be able to maintain a greater percentage of quiescent mtDNA without ending in some sort of illnesses [93]. The mtDNA:Tfam ratio is controlled by the mitochondrial Lon protease that regulates the mtDNA copy number and transcription by selective degradation of Tfam [109].

1.4.2 NRF-1/ NRF-2

NRF-1 is a nuclear encoded transcription factor linked to the expression of many genes involved in mitochondrial respiratory function as the vast majority of nuclear genes that encode subunits of the five respiratory complexes [110-112]. Moreover, considerable data sustains a potential integrative role of NRF-1 in coordinating respiratory subunit expression with that of the mitochondrial transcriptional machinery [4]. As illustrated in Figure 1.4.3, NRF-1 activates the Tfam promoter [61], a major regulator of mitochondrial transcription. NRF-1 is also related to the expression of key enzymes of the heme biosynthetic pathway [113, 114]. Moreover, NRF-1 acts on genes whose functions are not restricted to the bigenomic expression of the respiratory apparatus (Fig. 1.4.3) [4]. For example, NRF-1 regulates key constituents of the protein import and assembly machinery in mitochondria. This proposes a broader function for the factor in coordinating mitochondrial biogenesis beyond the transcriptional expression of the respiratory chain. This hypothesis is strengthened by reports that relate rises in NRF-1 mRNA or DNA binding activity with generalized effects on mitochondrial biogenesis [4]. It is worth to notice that

NRF-1 targets are not limited to genes involved in mitochondrial function. Among these are genes encoding metabolic enzymes, components of signaling pathways, and gene products necessary for chromosome maintenance and nucleic acid metabolism among others.

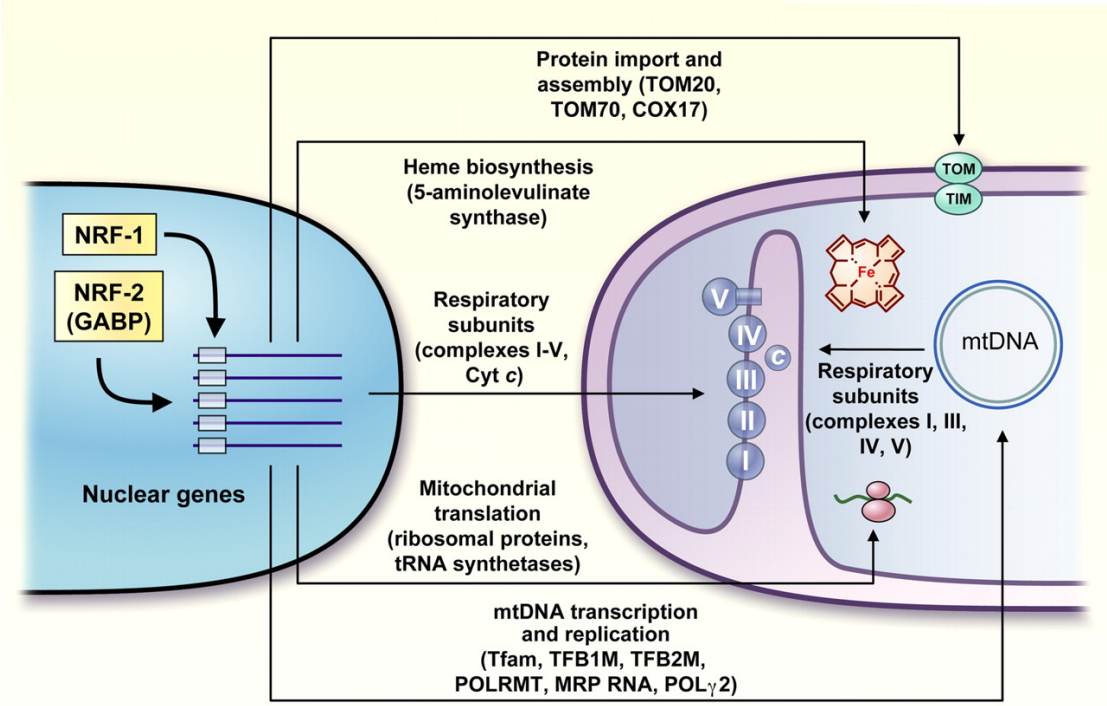

*Figure 1.4.3:*Diagrammatic summary of the nuclear control of mitochondrial functions by NRF-1 and NRF-2 (GABP). NRFs contribute both directly and indirectly to the expression of many genes required for the maintenance and function of the mitochondrial respiratory apparatus. NRFs act on genes encoding cytochrome c, the majority of nuclear subunits of respiratory complexes I–V, and the rate-limiting heme biosynthetic enzyme 5-aminolevulinate synthase. In addition, NRFs promote the expression of key components of the mitochondrial transcription and translation machinery that are necessary for the production of respiratory subunits encoded by mtDNA. These include Tfam, TFB1M, and TFB2M as well as a number of mitochondrial ribosomal proteins and tRNA synthetases. Recent findings suggest that NRFs are also involved in the expression of key components of the protein import and assembly machinery [50].

A second nuclear factor designated as NRF-2 or GABP was recognized based on its specific binding in the cytochrome oxidase subunit IV (COXIV) promoter [62]. In addition to the COX promoters, functional NRF-2 sites have been identified in a number of other genes connected to respiratory chain expression [110, 111]. Hence, like NRF-1, NRF-2 contributes in the coordination of the expression profile of

essential respiratory chain proteins with key components of the mitochondrial transcription machinery [4]. Such a mechanism may serve to ensure the coordinate bigenomic expression of respiratory subunits.

1.4.3 PGC-1α

PGC-1α, the best-studied member of a family of transcriptional coactivators, was identified in a differentiated brown fat cell line on the basis of its interaction with PPARγ, an important regulator of adipocyte differentiation [115]. The remarkable induction of PGC-1α mRNA in brown fat upon cold exposure sustains its role in thermogenic regulation [116, 117]. A relevant aspect of the thermogenic program is the stimulation of mitochondrial biogenesis, and PGC-1α is a great inducer of this process [4]. Ectopic overexpression of the coactivator in cultured myoblasts and other cells stimulates respiratory subunit mRNAs and increases COXIV and cytochrome c protein levels as well as the steady-state level of mtDNA [63]. As illustrated in Figure 1.4.4, NRF-1 has been identified as an important target for the induction of mitochondrial biogenesis by PGC-1α. The coactivator binds NRF-1 and can trans-activate NRF-1 target genes involved in mitochondrial respiration [4]. In addiction, a dominant negative allele of NRF-1 inhibits the effects of PGC-1α on mitochondrial biogenesis providing *in vivo* evidence for a NRF-1-dependent pathway [63]. PGC-1α may connect nuclear regulatory events to the mitochondrial transcriptional machinery through its transcriptional activation of Tfam. As with respiratory subunit genes, the coactivator targets the NRF-1 and NRF-2 recognition sites within Tfam promoter leading to increased mRNA expression [118]. Estrogen related receptor α (ERRα) and NRF-2α recognition sites are conserved in the promoters of a number of oxidative phosphorylation genes, including cytochrome c and β-ATP synthase, and PGC-1α can

drive expression through these sites [119, 120] (Fig. 1.4.4). In addition to its role on the respiratory chain and mitochondrial transcription, PGC-1α stimulates mitochondrial oxidative functions by promoting the expression of genes of the mitochondrial fatty acid oxidation and heme biosynthetic pathways [4] (Fig. 1.4.4).

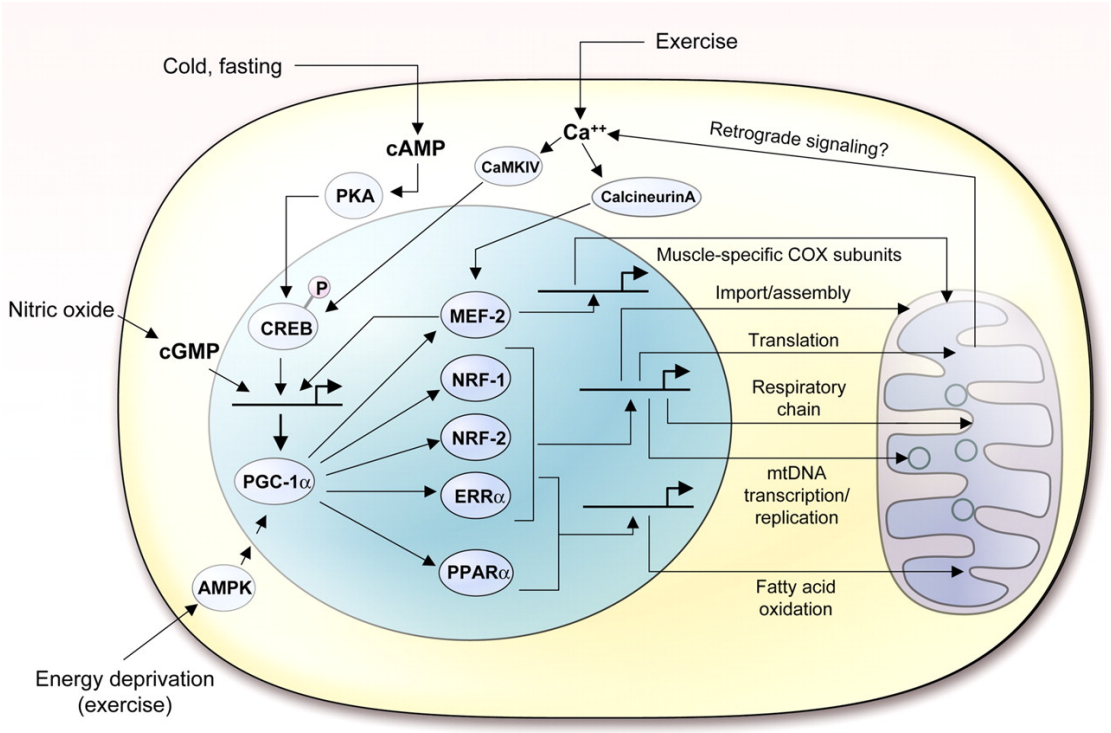

Figure 1.4.4: Illustration summarizing PGC-1α-mediated pathways governing mitochondrial biogenesis and function. Depicted in the nucleus (shaded sphere) are the key transcription factors (NRF-1, NRF-2, ERRα, PPARα, and MEF-2) that are PGC-1α targets and act on nuclear genes governing the indicated mitochondrial functions. Some of the physiological effector pathways mediating changes in the transcriptional expression or function of PGC-1α are also shown. The CREB activation of PGC-1α gene transcription in response to cold (thermogenesis), fasting (gluconeogenesis), and exercise has been well documented. The physiological mechanisms of PGC-1α induction by nitric oxide are not established but may involve the production of endogenous nitric oxide by eNOS. A potential pathway of retrograde signaling through calcium is also included [50].

Physiological expression of PGC-1α at the transcriptional level can be modulated through cAMP-dependent signaling [4]. The PGC-1α promoter has a potent cAMP response element (CRE) that works as a target for CREB-mediated transcriptional activation [121]. PGC-1α along with Tfam and NRF-1 are induced via cGMP-dependent signaling resulting from elevated levels of nitric oxide (NO) [122] (Fig.

1.4.4). The NO induction of PGC-1α is correlated with increased mitochondrial biogenesis in several cell lines [4]. The induced mitochondrial mass is complemented by increased oxidative phosphorylation-coupled respiration consistent with an induced in functional mitochondria [123]. A number of reports associate the expression of PGC-1α to exercise-induced mitochondrial biogenesis in skeletal muscle [124-128]. In each case, PGC-1α mRNA and/or protein increase as an adaptive response to endurance exercise of varying intensity and duration.

1.5 Patophysiology

In the last 20 years, mitochondrial dysfunction has been recognized as an important promoter of human pathologies. Mitochondrial defects play a direct role in certain well-defined neuromuscular diseases and are also thought to contribute indirectly to many degenerative diseases [4]. Mutations in mitochondrial genes for respiratory proteins and translational RNAs, particularly tRNAs, show themselves in a wide range of clinical conditions, most of which affect the neuromuscular system [60, 129]. These mtDNA mutations are often maternally inherited, and in some cases, patients with certain mitochondrial myopathies display excessive proliferation of abnormal mitochondria in muscle fibers, the so-called ragged red fiber [130]. In addition, a subset of mitochondrial diseases exhibits a Mendelian inheritance pattern typical of nuclear gene defects [4]. These can impair respiratory protein subunits, assembly factors, and gene products necessary for mtDNA maintenance and stability [131, 132]. In addition to single gene defects, dispersed lesions in mtDNA that accumulate over time may be involved in human pathologies including neurodegenerative diseases [133], diabetes [134], and ageing [135].

1.5.1 Neurodegenerative diseases

It has been widely speculated that free radical production by the mitochondrial respiratory chain contributes to the neuropathology observed in dementia and other degenerative diseases [4]. Although there is positive evidence for oxidative stress associated with neuropathology, it has been difficult to prove whether this is a cause or a consequence of neuronal death [136]. Parkinson's disease (PD) is the most common movement disorder and is characterized primarily by the loss of dopaminergic neurons in the substantia nigra pars compacta leading to a dopamine deficit in the striatum (). The consequent dysregulation of basal ganglia circuitries explains the most prominent motor symptoms, including rigidity, resting tremor and postural instability. A pathological hallmark of sporadic PD is the occurrence of proteinaceous deposits within neuronal perykarya (Lewy bodies) and processes (Lewy neurites), mainly constituted of α-synuclein, ubiquitin, neurofilaments and molecular chaperones [137]. Little is known about the etiopathogenesis of PD. Accumulating evidence suggests that PD-associated genes directly or indirectly impinge on mitochondrial integrity, for example the MTPT compound (1-methyl-4-phenyl-1,2,3,6-tetrahydropyridine), an ETC complex I inhibitor, was found to induce Parkinson in humans [138, 139]. Moreover, oxidative stress is found to have a role in neuronal degeneration of the dopaminergic neurons [140]. The most common sporadic form of PD looks like a complex multifactorial disorder with variable influences of environmental factors and genetic susceptibility. A major breakthrough in PD research was the identification of genes that are responsible for monogenic familial forms. Mutations in the genes encoding α-synuclein and LRRK2 (leucine-rich repeat kinase 2) are accountable for autosomal dominant forms of PD, apparently by a gain-of-function process. Increased α-synuclein expression as well as α-

synuclein deficiency may be associated with mitochondrial irregularities like ultrastructural abnormalities, impaired COX and complex IV activity, reduced complex I/III activity, a decline in the mitochondrial membrane potential, oxidation of mitochondria-associated metabolic proteins, and an amplified sensitivity to mitochondrial toxins [141-146]. LRRK2 can bind to the outer mitochondrial membrane in mammalian brain and about 10% of overexpressed LRKK2 was found in association with the outer mitochondrial membrane. Nevertheless, it remains to be investigated whether LRRK2 has an influence on mitochondrial integrity [140].

Loss-of-function mutations in the genes encoding parkin and PINK1 mediate autosomal recessive PD. Sporadic and monogenic forms share important clinical, pathological and biochemical characters, notably the progressive demise of dopaminergic neurons in the substantia nigra [140]. Several studies examined mitochondrial features in tissues from parkin-mutant patients. An important reduction (by about 60%) in complex I activity was discovered both in patients with parkin mutations and sporadic PD patients, whereas complex IV activity was only impaired in sporadic PD patients. Cultured fibroblasts from parkin mutant patients presented morphological and functional mitochondrial deficiencies, for instance a reduction in the membrane potential (by 30%), complex I activity (by 45%), ATP production (by 58%) and a rise in rotenone-induced mitochondrial fragmentation [147]. In another report parkin mutant fibroblasts were characterized by a 22% decrease in the mtDNA copy number and an increased vulnerability to oxidative stress-induced mtDNA impairment [148]. The consequences of PINK1 deficiency on mitochondrial function and morphology are multidimensional, including decreases in mitochondrial membrane potential, complexes I and IV activities, ATP production, mitochondrial

import and mtDNA levels, increases in ROS production and abnormal ultrastructural mitochondrial morphology [18, 149-151].

1.5.2 Aging

The accumulation of mutations in mtDNA is also thought to contribute to human aging [4]. Alterations in mtDNA, comprising increased occurrence of point mutations and deletions, have been documented in aged individuals [152] and mice [153]. The declining in the somatic mtDNA mutations rate by introducing catalase into the mitochondrial matrix lengthens mouse life span [154]. These observations along with the known age-related reduction in oxidative energy metabolism has suggested that mtDNA mutations impair the respiratory chain driving to a decreased oxidative phosphorylation [135].

1.5.3 Type 2 diabetes

There has also been considerable interest in mitochondrial dysfunction as a contributing factor in the onset of type 2 diabetes (T2D)[155]. Although the primary cause of this disease is unknown, it is clear that insulin resistance plays an early role in its pathogenesis and that defects in insulin secretion by pancreatic β cells are instrumental in the subsequent progression to hyperglycemia. Indeed, several lines of evidence indicate that insulin resistance is an early feature of T2D. Petersen et al. found that in comparison with matched young controls, healthy lean elderly subjects had severe insulin resistance in muscle, as well as significantly higher levels of triglycerides in both muscle and liver [156]. These changes were accompanied by decreases in both mitochondrial oxidative activity and mitochondrial adenosine

triphosphate (ATP) synthesis. These data support the hypothesis that insulin resistance in humans' skeletal muscle arises from defects in mitochondrial fatty acid oxidation, which in turn lead to increases in intracellular fatty acid metabolites (fatty acyl CoA and diacylglyerol) that disrupt insulin signaling (Fig. 1.5.1) [134].

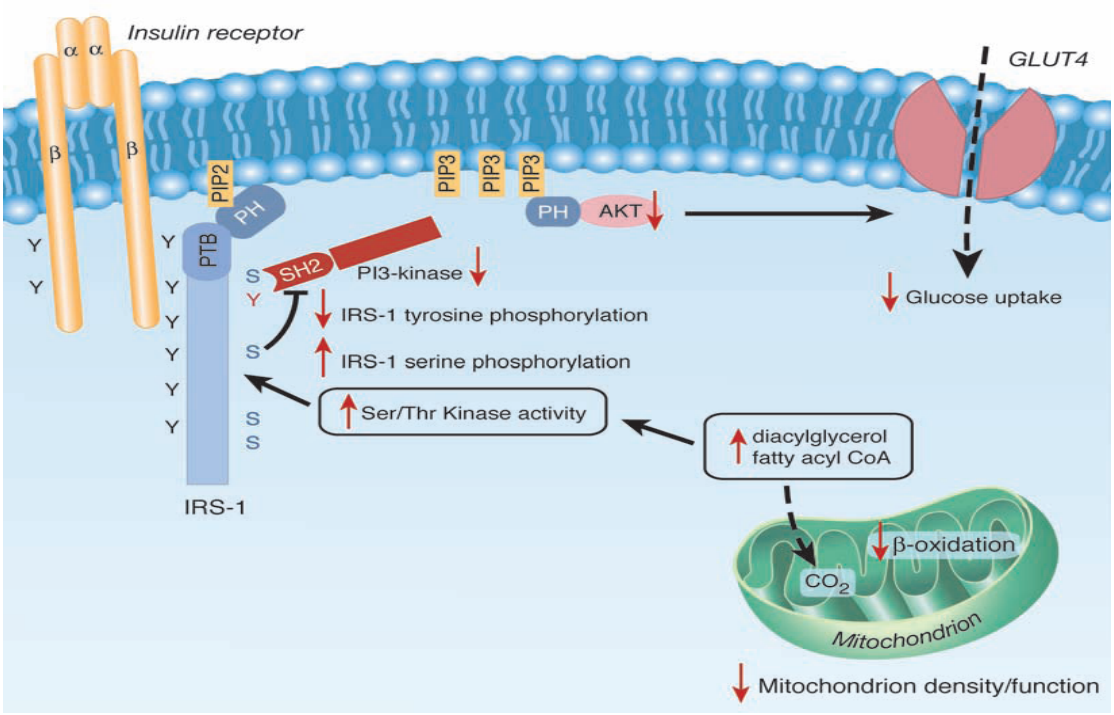

Figure 1.5.1: Potential mechanism by which mitochondrial dysfunction induces insulin resistance in skeletal muscle. In the depicted model, a decrease in mitochondrial fatty acid oxidation, caused by mitochondrial dysfunction and/or reduced mitochondrial content, produces increased levels of intracellular fatty acyl CoA and diacylglycerol. These molecules activate novel protein kinase C, which in turn activates a serine kinase cascade possibly involving inhibitor of nuclear factor kB kinase (IKK) and c-Jun N-terminal kinase 1, leading to increased serine phosphorylation (pS) of insulin receptor substrate–1 (IRS-1). Increased serine phosphorylation of IRS-1 on critical sites (e.g., IRS-1 Ser^{307}) blocks IRS-1 tyrosine (Y) phosphorylation by the insulin receptor, which in turn inhibits the activity of phosphatidyl inositol 3-kinase (PI 3-kinase). This inhibition results in suppression of insulin-stimulated glucose transport, the process by which glucose is removed from the blood. PIP3 indicates phosphatidylinositol 3,4,5-trisphosphate; PTB, phosphotyrosine binding domain; PH, pleckstrin homology domain; SH2, src homology domain [134].

Insulin resistance in healthy aged individuals with no family history has been correlated with a decline in mitochondrial oxidative phosphorylation [156]. The expression of a number of genes involved in oxidative metabolism is reduced in diabetic subjects as well as in those predisposed to diabetes because of family history

[157, 158]. In addition, in comparison with insulin-sensitive controls, the insulin-resistant subjects were found to have a lower ratio of type I to type II muscle fibers. Type I fibers are mostly oxidative and contain more mitochondria than type II muscle fibers, which are more glycolytic. Conceivably, these individuals may have fewer muscle mitochondria, possibly because of decreased expression of nuclear-encoded genes that regulate mitochondrial biogenesis, such as PGC-1α [63] and PGC-1β [159]. Microarray studies support this hypothesis since PGC-1α–responsive genes are down-regulated in the skeletal muscle of obese Caucasians with impaired glucose tolerance and T2D [158], and PGC-1α and PGC-1β are themselves down-regulated in the skeletal muscle of both obese diabetic and overweight non diabetic Mexican-Americans [157]. Alternatively, the reduction in mitochondrial oxidative phosphorylation activity in insulin-resistant individuals could be due not to mitochondrial loss but rather to a defect in mitochondrial function. This hypothesis is supported by muscle biopsy studies. In one study, the activity of mitochondrial oxidative enzymes was found to be lower in T2D subjects [160], and in another, the activity of mitochondrial rotenone-sensitive nicotinamide adenine dinucleotide oxidoreductase was found to be lower [161]. Because obese individuals have also been shown to have smaller mitochondria with reduced bioenergetic capacity compared with lean controls [161], the mitochondrial abnormalities in these subjects might be related to obesity rather than to insulin resistance.

Although insulin secretion is also modulated by a number of stimuli that operate outside this pathway, it is clear that oxidative mitochondrial metabolism is central to glucose-stimulated insulin secretion [162]. The critical role of mitochondria is evident from the rare hereditary disorders in which diabetes with β cell dysfunction has been traced to specific mutations in the mitochondrial genome [162, 163]. Given the

central role of mitochondria in glucose sensing, it is possible that decreased mitochondrial function in β cells, might predispose individuals to develop β cell dysfunction and T2D.

These associations of mitochondrial dysfunction with human degenerative disease raise the basic question of how mammalian cells control mitochondrial biogenesis. It has become increasingly apparent that transcriptional mechanisms contribute to the biogenesis of mitochondria including the expression of the respiratory apparatus. Unfortunately, little is known about the link between mitochondria and many diseases, about the mitochondrial regulation and about the cross-talk between the nucleus and the mitochondria.

2. Aim:

As sites of the main oxidative reactions and of the electron transport chain, mitochondria are the organelle committed to metabolic energy production required for all cellular functions. Mitochondria possess an own genome, whose replication and transcription is nuclear-mediated through the Tfam. Most of the mitochondrial proteins are nuclear-encoded, too. Consequently the nuclear-mitochondrial crosstalk is at the base for mitochondrial biogenesis and function. The mitochondrial biogenesis is the process through which new mitochondria are created and a hallmark of this event is the increase in the mtDNA content. For the mitochondrial function or activity instead, we intend all the processes mitochondria have to deal with, and the most important one is the ATP production. Because of the ubiquitous presence of mitochondria in all tissues, their density and function have a significant impact on whole-body metabolism. Deficiency in energy metabolism has emerged as a possible explanation for the etiology of complex diseases over the past 20 years [20]. The primary limiting factor for growth and reproduction of all biological systems is energy and the first report that mtDNA mutations can cause disease [164-169] have been followed by reports that a broad spectrum of metabolic and degenerative diseases can have a mitochondrial etiology. In fact, a mitochondrial dysfunction is associated to many disorders such as insulin resistance, diabetes and Parkinson's diseases. The contribution of mitochondria to the pathogenic mechanisms underlying these pathologies is not completely characterized. Finding new mitochondrial regulators is a major challenge, both for basic science and for translational medicine. The goal of this project is to find new regulators that control mitochondrial biogenesis and function and validate them in C2C12, a skeletal muscle cell line, with the final aim to gain further insights on the mechanisms by which mitochondria are involved in

pathophysiology.

Since most of the pathologies associated with mitochondrial dysfunction are characterized by reduced density and function of these organelles, we decided to focus our attention on the isolation of new "positive" mitochondrial regulators; in other words factors capable of inducing mitochondrial function.

In all the experiments reported in this thesis we decided to use a gain of function approach instead of a loss of function strategy. Based on current knowledge, it might be expected that reduced expression of a given "potential" regulator does not necessarily lead to a marked phenotype. In this regard, the muscle-specific overexpression of the co-activator PGC-1α (a well characterized mitochondrial regulators) in mice induces an impressive switch toward oxidative-type muscle fibers containing large amounts of mitochondria [170, 171]. On the other hand PGC-1α$^{-/-}$ null mice displayed normal numbers of these fibers, and although mitochondrial gene expression and activity were blunted, mitochondrial fractional volume was unchanged in one study and only slightly decreased in another [71, 72].

To define potential mitochondrial regulators we performed a preliminary high throughput screening in HEK 293 cells, a cell line that allow high transfection efficiency. Afterwards, we characterized the new mitochondrial factors in the mouse skeletal muscle cell line C2C12, that are enriched in mitochondria. A mitochondrial regulator should increase both the mitochondrial biogenesis and function; thus we developed some biochemical-functional assays to evaluate these effects. We analyzed the mitochondrial DNA content as a hallmark of mitochondrial biogenesis and the oxygen consumption rate, the expression level of OXPHOS proteins and the ATP amount as a hallmark of mitochondrial function.

3. Materials and Methods:

3.1 Cell Culture

3.1.1 Cell Lines

We used the human epithelial kidney HEK293 cells (ATCC) and the murine skeletal muscle myoblasts C2C12 cells (ATCC).

3.1.2 Medium

Maintenance Medium: Both cell lines were grown using the Dulbecco's Modified Eagle's Medium from Sigma (DMEM, D5671) added of 10% Fetal Bovine Serum (Euroclone), 2mM L-Glutamine (Life Technology) and 100U/ml Penicillin and 100ug/ml Streptomycin (both Life Technology).

Transfection Medium: We used for both cell lines the Dulbecco's Modified Eagle's Medium from Sigma (DMEM, D5671) without any addition.

3.2 Expression Vectors

3.2.1 pCDNA3

pCDNA3 empty vector (Open Biosystem) was used as negative control. A plasmid bearing the sequence encoding PGC-1α in the pCDNA3 vector (Open Biosystem) was used as positive control.

3.2.2 pCMV

This is the vector in which is cloned the cDNA coding for the green fluorescent protein (GFP), source Open Biosystem. We used this plasmid as a control of transfection degree.

3.2.3 pCMV Sport 6.1

This is the vector in which are cloned all the cDNAs coding for the 22 potential mitochondrial regulators. We bought all these plasmids already assembled with the different genes from Open Biosystem. All the genes coding for the different candidates are murine except for genes 2 and 22 that are human.

3.3 Reporter System

3.3.1 Wild Type TFAM Reporter System (WT TFAM)

This reporter system has the luciferase expression under the control of the Tfam promoter. The promoter is composed of the region for the binding of NRF-1, Sp1 and NRF-2. We used this reporter system in the HTS experiment, but also to evaluate the Tfam activation by Zc3h10.

3.3.2 Mutated TFAM Reporter System (MUT TFAM)

This reporter system has the luciferase expression under the control of a mutated form of the Tfam promoter. The promoter is deleted of the NRF-1 binding site. We used this reporter system to evaluate the Tfam activation by Zc3h10.

3.3.3 pTKLUC Reporter System

This reporter system has the luciferase expression under the control of the TK (thymidine kinase) promoter. We used this reporter system to sustain the hypothesis that exist a specific interaction between the Zc3h10 protein and the Tfam promoter and not with Zc3h10 protein and the backbone of the plasmid.

3.3.4 Zc3h10 Reporter System

This reporter system was purchased by SwitchGear Genomics and has the luciferase expression under the control of the Zc3h10 promoter. The promoter region cloned comprehends 907 bases. We used this reporter system to evaluate some possible inducer of the Zc3h10 promoter activity.

3.4 Bioinformatic Analysis

3.4.1 Biological process and molecular function classification

This classification was performed using the free Panther Software (www.pantherdb.org). The genes were inserted as Enter IDs and the software provided the classification according to GeneOntology.

3.4.2 BioGPS analysis

All the genes were inserted in BioGPS dataset (biogps.org) and their expression levels in the C2C12 cells and in the murine gastrocnemius were checked.

3.4.3 PubMed Analysis

All the proteins encoded by the different genes were checked using PubMed (www.ncbi.nlm.nih.gov), in order to understand which function they have and if they are already known as mitochondrial regulators.

3.5 Transient Transfections

3.5.1 HEK 293 Cotransfection in 96 well plates, "in-plate transfection"

Materials:

- 96 multi-well plate black (PerkinElmer)
- C2C12 myoblasts (5000cell/well)
- cDNA 80ng/well (pCDNA3, PGC-1α, candidates 1-22, and GFP)
- reporter gene (WT Tfam-LUC) 20 ng/well
- Fugene6 Transfection Reagent (Promega)
- Transfection medium: DMEM Serum free, Sigma
- Maintenance medium: DMEM Sigma + 1% pen-strep + 1% L-Gln + 10% fbs

Quantities per well:

- 100ul plated/well
- cDNA: 80ng/well
- reporter gene: 20ng/well
- Fugene 1:5
- cells: 5000 cells/well

Protocol:

- Add in each well with a matrix pipette 2ul of reporter gene from a solution concentrated 10ng/ul
- Add in each well with a matrix pipette 4ul of each cDNAs from a solution concentrated 20ng/ul
- Add in each well with a matrix pipette 3.5ul of DMEM serum free
- Add in each well with a matrix pipette 0.5ul of Fugene
- Centrifuge the plates for 2 min a 750 rpm
- Wait 20 minutes (the cDNA and Fugene have to form a complex)

- Add 90ul of cells concentrated 56000cell/ml.
- Wait 40 minutes (the transfection has to happen)
- Check the transfection efficiency 24h after transfection going to the fluorescent microscope and measuring how many green fluorescent cells you can see. (only for cells transcfected with GFP)

3.5.2 C2C12 Myoblasts Transfection in 96 well plates

Materials:

- 96 multi-well plate black (PerkinElmer)
- C2C12 myoblasts (10000cell/well)
- cDNA 125 ng/well (pCDNA3, PGC-1α, Zc3h10, and GFP)
- Fugene6 Transfection Reagent (Promega)
- Transfection medium: DMEM Serum free, Sigma
- Maintenance medium: DMEM Sigma + 1% pen-strep + 1% L-Gln + 10% fbs

Quantities per well:

- 100ul plated/well
- cDNA: 125ng/well
- Fugene 1:5
- cells: 10000 cells/well

Quantities per mix:(1 mix = 10 wells)

- Final Volume: 1ml /mix
- Transfection Volume: 275µl/mix
- cDNA: 1250ng/mix
- Fugene 1:5: 6.25ul
- Cells: 100000 cells/mix
- cell volume: 75ul
- cell concentration: 1300000cell/ml

Protocol:

- Add 189.5ul of DMEM serum free into a 2ml tubes
- Add 4.25ul of each cDNAs from a solution concentrated 300ng/ul
- Add 6.25ul of Fugene
- Wait 20 minutes (the cDNA and Fugene have to form a complex)
- Add 75ul of cells concentrated 1300000cell/ml.

- Wait 40 minutes (the transfection has to happen)
- Add 725ul of DMEM Sigma + 1% pen-strep + 1% L-Gln + 10% fbs
- Plate 100ul each well.
- Check the transfection efficiency 24h after transfection going to the fluorescent microscope and measuring how many green fluorescent cells you can see. (only for cells transcfected with GFP)

3.5.3 C2C12 Myoblasts Transfection in 24 well plates

Materials:

- 24 multi-well plate
- C2C12 myoblasts (20000cell/well)
- cDNA 700 ng/well (pCDNA3, PGC-1α, candidates 1-22, and GFP)
- Fugene6 Transfection Reagent (Promega)
- Transfection medium: DMEM Serum free, Sigma
- Maintenance medium: DMEM Sigma + 1% pen-strep + 1% L-Gln + 10% fbs

Quantities per well:

- 500 ulplated/well
- cDNA: 700 ng/well
- Fugene 1:5
- cells: 20000 cells/well

Quantities per mix:(1 mix = 3.25 wells)

- Final Volume: 1,625 ml /mix
- Transfection Volume: 679 µl/mix
- cDNA: 2240 ng/mix
- Fugene 1:5: 11.2 ul
- Cells: 100000 cells/mix
- cell volume: 178 ul

Protocol:

- Add 482 ul of DMEM serum free into a 2ml tubes
- Add 7.5 ul of each cDNAs from a solution concentrated 300ng/ul
- Add 11.2 ul of Fugene

- Wait 20 minutes (the cDNA and Fugene have to form a complex)
- Add 178 ul of cells concentrated 560000 cell/ml.
- Wait 40 minutes (the transfection has to happen)
- Take the mix to the final volume with DMEM Sigma + 1% pen-strep + 1% L-Gln + 10% fbs
- Plate 500 ul in each well.
- Check out the transfection efficiency 24h after transfection going to the fluorescent microscope and measuring how many green fluorescent cells you can see. (only for cells transcfected with GFP)

3.5.4 C2C12 Myoblasts Transfection in 6 well plates

Materials:

- 6 multi-wells plate
- C2C12 myoblasts (500.000 cell/well)
- cDNAs3.36 ug/well (pCDNA3, PGC-1α, Zc3h10, and GFP)
- Fugene6 Transfection Reagent (Promega)
- Transfection medium: DMEM Serum free, Sigma
- Maintenance medium: DMEM Sigma + 1% pen-strep + 1% L-Gln + 10% fbs

Quantities per well:

- 2 ml plated/well
- cDNA: 3.36 ug/well
- Fugene 1:5
- cells: 500000 cells/well

Quantities per mix:(1 mix = 6.5wells)

- Final Volume: 13 ml /mix
- Transfection Volume: 1 ml/mix
- cDNA: 21.84 ug/mix
- Fugene 1:5: 109.2ul
- Cells: 3500000 cells/mix
- cell volume: 928ul
- cell concentration: 3500000 cell/ml

Protocol:

- Add 2.418 ml of DMEM serum free into a 50ml tubes
- Add 73ul of each cDNAs from a solution concentrated 300ng/ul
- Add 109.2ul of Fugene
- Wait 20 minutes (the cDNA and Fugene have to form a complex)
- Add 928 ul of cells concentrated 3500000 cell/ml.
- Wait 40 minutes (the transfection has to happen)
- Take the mix to the final volume with DMEM Sigma + 1% pen-strep + 1% L-Gln + 10% fbs
- Plate 2 ml in each well.
- Check out the transfection efficiency 24h after transfection going to the fluorescent microscope and measuring how many green fluorescent cells you can see. (only for cells transcfected with GFP)

3.5.5 C2C12 Myoblasts Cotransfection in 96 well plates

Materials:

- 96 multi-well plate black (PerkinElmer)
- C2C12 myoblasts (3000cell/well)
- cDNA 132ng/well (pCDNA3, PGC-1α, Zc3h10, and GFP)
- report system 66ng/well (WT Tfam-LUC, MUT Tfam-LUC, pTK-LUC or Zc3h10-LUC)
- Lipofectamine 2000, Sigma
- Transfection medium: DMEM Serum free, Sigma
- Maintenance medium: DMEM Sigma + 1% pen-strep + 1% L-Gln + 10% fbs

Quantities per well:

- 100ul plated/well
- cDNA: 132ng/well
- reportersystem:66ng/well
- Lipo: 5ul
- cells: 3000 cells/well

Quantities per mix:(1 mix = 10 wells)

- Final Volume: 1ml /mix
- Transfection Volume: 100µl/mix
- cDNA: 1320ng/mix
- reportersystem: 660 ng/mix
- Lipo5ul
- Cells: 100000 cells/mix
- cell volume: 50ul
- cell concentration: 600000cell/ml

Protocol:

- Add 29.6ul of DMEM serum free into a 2ml tubes
- Add 8.8ul of each cDNAsfrom a solution concentrated 150ng/ul
- Add 6.6ul of the reporter system from a solution concentrated 100 ng/ul
- Add 4ul of Lipofectamine
- Wait 20 minutes (the DNA and Fugene have to form a complex)
- Add 50ul of cells concentrated 600000cell/ml.
- Wait 40 minutes (the transfection has to happen)
- Add 900ul of DMEM Sigma + 1% pen-strep + 1% L-Gln + 10% fbs
- Plate 100ul each well.
- Check the transfection efficiency 24h after transfection going to the fluorescent microscope and measuring how many green fluorescent cells you can see. (only for cells transcfected with GFP)

3.6 Mitochondrial activity evaluation (HTS validation)

The mitochondrial activity was analyzed 60 hours after cotransfection of HEK293cells in 96 multi-well plates.

Materials:

- MitoTracker Red CM-H_2Xros
- PBS 1X
- Hoechst 33258
- H_2O
- EnVision (Perkin Elmer, Waltham, MA)

Protocol:

- Remove media from wells
- Wash once cells with PBS 1X
- Stained cell with 50 ul of a solution of MitoTracker Red CM-H_2Xros 400nM in PBS 1X for 30 minutes at 37°C.
- Remove the staining and wash once cells with PBS 1X
- Read the fluorescence without any solution in the wells (dry cells)

  (EnVision protocol: Bottom Mirror: FITC Bottom

  Excitation filter: FITC 580nm

  Emission filter: FITC 620nm)
- Stained cell with 50 ul of a solution of Hoechst 3325 diluited1:1000 in H_2O for 3 minutes at RT.
- Remove the staining and wash once cells with PBS 1X
- Read the fluorescence without any solution in the wells (dry cells)

  (EnVision protocol: Bottom Mirror: DAPI Bottom

  Excitation filter: FITC 320nm

  Emission filter: FITC 460nm)

The mitochondrial activity values obtained by MitoTracker Red CM-H_2Xros staining were than divided for the number of cells measured by Hoechst 3325 staining.

3.7 quantitative Real Time PCR (qRT-PCR)

3.7.1 mtDNA

Total DNA from C2C12 myoblasts was extracted 60 hours after transfection and purified with NucleoSpin® Tissue extraction kit (Macherey-Nagel, Milano, Italia) and quantitated with Nanodrop (Thermo Scientific, Wilmington, DE). Each sample was diluted at 5 ng/ul. Specific DNA sequences were amplified and quantitated by real time PCR, using iScript^{TM} One Step RT-PCR for Probes (Bio-Rad, Milano, Italia), following the manufacturer's instructions. Experiments were performed in triplicate and repeated at least twice with different cell preparations. Calculate the mtDNA levels comparing the target gene (Mitochondrial) values with the houskeeping gene (Nuclear) values. The qRT-PCR protocol is composed of 40 cycles of amplifications each consisting of a denaturation step at 95° C for 15 seconds and an annealing/extension step at 60° C for 60 seconds. The oligonucleotides used for real-time PCR were synthesized by Eurofin MWG Operon (Ebersberg, Germany) and were:

m36B4	fwd	AGATGCAGCAGATCCGCAT
	rev	GTTCTTGCCCATCAGCACC
	probe	CGCTCCGAGGGAAGGCCG
m mtCOX II	fwd	TGGTGAACTACGACTGCT
	rev	CTGGGATGGCATCAGTTT
	probe	TGGCAGAACGACTCGGTTATCAACT

3.7.2 mRNA

Total RNA from murine skeletal muscle was extracted with TRIzol Reagent® (Invitrogen) and purified with commercial kit (Macherey-Nagel, Milano, Italia) and quantitated with Nanodrop (Thermo Scientific, Wilmington, DE). Specific mRNA

was amplified and quantitated by real time PCR, using One Step for probes kit (Bio-Rad, Milano, Italia) following the manufacturer's instructions. Data were normalized to 36B4 mRNA and quantitated setting up a standard curve.

Experiments were performed in triplicate. Primers for real-time PCRs were designed with IDT software available on line. The qRT-PCR protocol is composed of 10 min at 50°C for reverse transcription, 40 cycles of amplifications each consisting of a denaturation step at 95° C for 10 seconds and an annealing/extension step at 60° C for 30 seconds. The oligonucleotides used for qRT-PCR were synthesized by EurofinMWG Operon (Ebersberg, Germany) and were:

m36B4	fwd	AGATGCAGCAGATCCGCAT
	rev	GTTCTTGCCCATCAGCACC
mZc3h10	fwd	CCTACGAATGTAACTTGGCTCC
	rev	CTGCTCCAGAAGTACCTCATTG

3.8 Oxygen Consumption Evaluation

Materials:

- Trypsin
- Oxygen Consumption Buffer, 50 ml total PBS with:
    - 25 mM D-Glucose
    - 1 mM Na pyruvate
    - Fatty acid free BSA 2% w/v (g/100ml)
- Oligomycin 2.5 mM
- CCCP 10 mM

Protocol:

- Remove media from wells

- Detach cells with Trypsin
- Centrifuge cells at 2000 rpm for 3 min
- Discard supernatant
- Resuspend cells in 1 ml of oxygen consumption buffer
- Evaluate the basal level of oxygen consumption
- To measure the uncoupled respiration, treat cells with oligomycin 2.5 uM
- To measure the maximal respiration, treat cells with CCCP 3.75 uM
- Remove the sample from the chamber and use 200 ul for normalizing values with the proteins quantification

Centrifuge remaining cells for WB analysis

3.9 Measurement of promoter activity

3.9.1 Measurement of Tfam promoter activity and pTK-LUC

The Tfam promoter activity or the pTK-LUC was analyzed 24 hours after transfection of C2C12 myoblasts in 96 multi-well plates.

Materials:

- Britelite (Perkin Elmer)
- EnVision (Perkin Elmer, Waltham, MA)

Protocol:

- Remove the medium from each well
- Add 50ul of fresh Britelite prepared according the company's instruction
- Wait 2 minutes and read the luminescence with the EnVision device

3.9.2Measurement of Zc3h10 promoter activity

Materials:

- Renilla (Promega)
- EnVision (Perkin Elmer, Waltham, MA)

Protocol:

- Remove the medium from each well
- Wash cells with 50 ul of PBS
- Add 20ul of Renilla Luciferase assay Lysis buffer prepared according to manufacturer's instruction
- Wait 15 minutes and read the luminescence with the EnVision device

3.10 Protein Extraction and Dosage

Material:

- C2C12 myoblasts
- 96 multi-well plates
- RIPA buffer
- BSA 2 mg/ml
- KIT BCA Kit (Pierce)

RIPA Buffer preparation:

TrisHCl pH 7,4 50mM

NP-40 1%

Na-desossicolate 0,25%

NaCl 150 mM

EDTA 1mM

Protease Inhibitors, 10ul/ml (Sigma)

H_2O to reach the desired volume

Proctocol:

- Prepare in a 96 wells plate a standard curve in duplicate following the table:

curvepoints	Pointsconcentration mg/ml	ulfrom 2mg/ml BSA stock	ul H_2O	ulLysis Buffer
A	1	5 ul	x	5 ul
B	0,75	3,75	1,25	5 ul
C	0,5	2,5	2,5	5 ul
D	0,25	1,25	3,75	5 ul
E	0,125	0,62	4,38	5 ul
F	0	x	5 ul	5 ul

- Centrifuge cells and remove the supernatant
- Add 200ul RIPA buffer to lysate cells
- If some gelatinous conglomerate is present, centrifuge for 3 min at 14000 rpm and keep the supernatant
- Aliquote5 ul of the supernatant of each samples in the wells
- Prepare the BCA reagent: 50 Reagent A : 1 Reagent B
- Add 200ul of BCA Reagent in each well
- Incubate 30 min a 37°C
- Read the absorbance at 550 nm
- Calculate the total mg of protein for each sample

3.11 Western Blot

The proteins used for this analyses were collected from the same sample used for the Oxygen consumption, after this measurement

3.11.1 OXPHOS WB

Solutions preparation:

1. SDS-sample buffer 2X:

   20% Glycerol

   4% SDS

   100 mMTris pH 6.8

   0.002% BBF

2. Running buffer 10X:

   144g Glycine

   30g Tris

   Bring to 8.4 pH

   10g of SDS

   Add water to reach 1L

3. Running Buffer 1X:

   100ml of Running Buffer 10X

   900 ml of H_2O

4. CAPS buffer:

   4.52g CAPS (Sigma)

   Add 1.6L of H_2O

   Bring to pH 11

   Add H_2O to reach 2L volume

5. PBS:

   8g NaCl

   0.2g KCl

   1.44g Na_2HPO_4

   0.24g KH_2PO_4

   Add H_2O to reach 1L volume

Material:

- SDS – sample buffer 2X
- Running Bffer 1X
- CAPS Buffer
- MitoProfile® Total OXPHOS Rodent WB Antibody Cocktail (ab110413)
- mouse anti beta actin Antibody (Sigma)
- Secondary anti-mouse Ab conjugated with horseradish peroxidase
- PBS 1X
- Tween-20
- Milk powder
- ECL western blot substrate (Pierce)

Protocol:

- Load 10 ug of samples proteins (previously resuspended 1ug/ul in SDS – sample buffer 2X, in order to lysate cells) in each well
- Separate proteins on a 10 wells Tris-Glycine 12.5 % PAA gel at 110 V in the Running Buffer 1X
- Soak gel and a PVDF membrane in CAPS buffer for 30 min
- Transfer to the PVDF membrane in CAPS buffer for 2 hours

- Overnight block in 5% milk/PBS 4° C
- Incubate blot with MitoScienceAb cocktail diluted 1:250 in 1% milk/PBS for 2 hours or with the anti beta actin antibody diluted 1:1000 in 1% milk/PBS for 1 hour
- Wash 3 times in PBS/0.05% tween-20 for 5 min
- Incubate blot with secondary anti-mouse Ab diluted 1:5000 in 1% milk/PBS for 2 hours
- Wash 3 times in PBS/0.05% tween-20 for 5 min
- Develop with ECL western blot substrate

3.11.2 Zc3h10 WB

Solutions preparation:

1. SDS-sample buffer 2X:

   20% Glycerol

   4% SDS

   100 mMTris pH 6.8

   0.002% BBF

2. Running buffer 10X:

   144g Glycine

   30g Tris

   Bring to 8.4 pH

   10g of SDS

   Add water to reach 1L

3. Running Buffer 1X:

   100ml of Running Buffer 10X

   900 ml of H_2O

4. Transfer buffer 10X:

   288g Glycine

   60.4 Tris Base

   Add H_2O to reach 1L volume

5. Transfer Buffer 1X:

   100ml of Transfer Buffer 10X

   200ml of Methanol

   Add H_20 to reach 1L volume

6. PBS:

   8g NaCl

   0.2g KCl

   1.44g Na_2HPO_4

   0.24g KH_2PO_4

   Add H_2O to reach 1L volume

7. TBS-T (1L):

   50mM Tris

   150mM NaCl

   Adjust pH with HCl to pH 7.6

   1ml of Tween 20

Material:

- SDS – sample buffer 2X
- ZC3H10 primary antibodie (AVIVA)
- mouse anti beta actin Antibody (Sigma)
- Secondary anti-mouse Ab conjugated with horseradish peroxidase (Sigma)
- Secondary anti-rabbit Ab conjugated with horseradish peroxidase (Sigma)

- PBS 1X
- PBS-T 0,05 %
- BSA
- TBS-T 0,1 %
- ECL western blot substrate (Pierce)

Protocol:

- Load 25 ug of samples proteins (previously resuspended 1ug/ul in SDS – sample buffer 2X) in each well
- Separate proteins on a 10 wells Tris-Glycine 12.5 % PAA gel at 110 V in the Running Buffer 1X
- Transfer to the NitroCellulose membrane in transfer buffer for 1 hour and half at 350 mA
- Block in 5% BSA/PBS-T at RT for 2 hs
- Incubate blot with ZC3H10 antibody diluted 1:1000 in 3% BSA/TBS-T for O/N
- Wash 3 times in TBS-T 0,1% for 5 min 3 times
- Incubate blot with secondary anti-rabbit Ab diluted 1:50000 in 3% BSA/TBS-T for 1 hour
- Wash 3 times in TBS-T 0,1% for 5 min 3 times

Develop with ECL western blot substrate

3.12 Evaluation of ATP Production

The ATP production was analyzed 60 hours after transfection of C2C12 myoblasts in 96 multi-well plates.

Solutions preparation:

1. Oligomycin 5 uM in serum free DMEM media
2. DMSO 5 uM in serum free DMEM media
3. Standard curve solutions: ATP 50, 5, 0.5, 0.05, 0.005, 0.0005 uM in PBS
4. ATP buffer solution

Protocol:

- Treat samples with the solutions 1 or 2 at 37° C for 24 hours (100 uL/well)

After 24 hours:

- Keep the PBS 1X at RT
- Remove the medium from each well
- Aliquote 50 uL of standard curve solutions in the respective wells
- Aliquote 50 uL of PBS in samples wells
- Aliquote 50 uL of solution 4 in each well
- Shake the 96 well plate for 2 minutes using an orbital shaker
- Measure the luminescence (EnVision, PerkinElmer)

To calculate the cytosol ATP production, subtract the luminescence signal obtained from the oligomycin treated samples to the signal obtained from the respective vehicle treated samples.

3.13 Evaluation of ROS production

The ROS production was analyzed 60 hours after transfection of C2C12 myoblasts in 96 multi-well plates.

Solutions preparation:

1. Solution H_2O_2 10mM in PBS

   . 2ul $H_2O_2$0.9M (H_2O_2 3% bought in pharmacy)

   . 178ul PBS 1X at 37°C

2. Solution H_2DCFDA 10mM

   Add 8.6ul of DMSO to the lyophilized probe (Invitrogen cod. c6827)

3. Solution H_2O_2 25uM and H_2DCFDA 5uM in PBS:

   . 3ul H_2DCFDA 10mM

   . 15ul H_2O_2 10mM

   . 5982ul PBS 1X at 37°C

4. Solution H_2DCFDA 5uM in PBS:

   . 3ul H_2DCFDA 10mM

   . 5997 PBS 1X at 37°C

5. Blank solution DMSO 0.05%:

   . 3ul DMSO

   . 5997ul PBS 1X at 37°C

6. Blank with H_2O_2solution (H_2O_2 25uM in PBS without probe)

   . 1.25ul H_2O_2 10mM

   . 499ul PBS 1X at 37°C

Protocol:

- Warm the PBS 1X at 37°C
- Prepared all the solution

- Remove the medium from each well
- Treat each well with the appropriate solution 3-6
- Leave for 30 minutes at 37°C
- Remove the treatment solutions from each well
- Wash once with pre-warmed PBS 1X
- Read the fluorescence without any solution in the wells (dry cells)

  (EnVision protocol: Bottom Mirror: FITC Bottom

  Excitation filter: FITC 485nm

  Emission filter: FITC 535nm)
- Add 30ul of Ripa Buffer in each well
- Vortex the wells
- Protein Dosage using the BCA kit (cod. 23227 Pierce BCA Protein Assay Kit)

  We decided to normalize the Ros detection data dividing them by the number of proteins.

3.14 Evaluation of membrane potential

The mitochondrial membrane potential was analyzed 60 hours after transfection of C2C12 myoblasts in 96 multi-well plates.

Solutions preparation:

1. Solution JC-1 3uM in PBS

   . 2.34ul JC-1 7.7mM

   . 5998ul PBS 1X at 37°C
2. Solution JC-1 3uM and CCCP 10uM

   . 1ul CCCP 10mM in DMSO

. 999ul solution 1

3. Blank solution (for JC-1):

   . 2.34ul DMSO

   . 5998ul PBS 1X at 37°C

4. Blanksolution (for CCCP):

   . 1ul DMSO

   . 999ul solution3

Protocol:

- Warm the PBS 1X at 37°C
- Prepared all the solution
- Remove the medium from each well
- Treat each well with the appropriate solution 1-4
- Leave for 30 minutes at 37°C
- Remove the treatment solutions from each well
- Wash once with pre-warmed PBS 1X
- Read the fluorescence without any solution in the wells (dry cells)

  EnVision protocols:

  GREEN MONOMERS

  Bottom Mirror: FITC Bottom

  Excitation filter: FITC 485nm

  Emission filter: FITC 535nm

  RED J-AGGREGATE

  Bottom Mirror: FITC Bottom

  Excitation filter: FITC 485nm

  Emission filter: FITC 600nm

- Add 30ul of Ripa Buffer in each well
- Vortex the wells
- Protein Dosage using the BCA kit (cod. 23227 Pierce BCA Protein Assay Kit)

To calculate the mitochondrial membrane depolarization you have to calculate the JC-1 ratio, you have to divide the red J-Aggregates value for the green monomer value.
We decided to normalize the depolarization data dividing the JC-1 ratio values by the number of proteins.

3.15 Zc3h10 expression levels in different mice organs

C57Bl/6J mice were purchased from Charles River Laboratories, Calco, Italy. Four male mice at 10 weeks of age were sacrificed and the different organs were collected. All animal studies were approved by the local ethical committee and followed the Italian and European Community legislation.
The tissues were kept in nitrogen tillthe mRNA was extracted as explained before.

3.16 *Statistical* analysis

Statistical analyses were performed with Student's *t* test or one-way ANOVA followed by Dunnett's Post Test when needed using GraphPadPrism version 5.0 for Macintosh (GraphPad, San Diego, California).

4. Preliminary Results:

4.1 High Throughput Screening

Since all factors known to influence mitochondrial number or OXPHOS appear to modulate the expression of Tfam, evaluation of its promoter activity can be used as a screening system to identify genes and genetic pathways that regulate mitochondrial biogenesis. To aid functional annotation of the genome, the Genomics Institute of the Novartis Research Foundation (GNF) has developed technology to assess the role of genes in a high-throughput manner in cell-based phenotypic assays. Specifically, GNF has assembled genome-wide cDNA and siRNA collections, arrayed them in 384-well format (1 gene/well), developed robotics/automation and procedures to manipulate, transfect cells, and evaluate gene activity in transfected cells in a high-throughput screen (HTS) fashion (Fig. 4.1.1). This technology has been used to discover new oncogenes, transcriptional co-activators that regulate metabolism, modulators of apoptosis, p53, Wnt signaling, etc.[172-177].

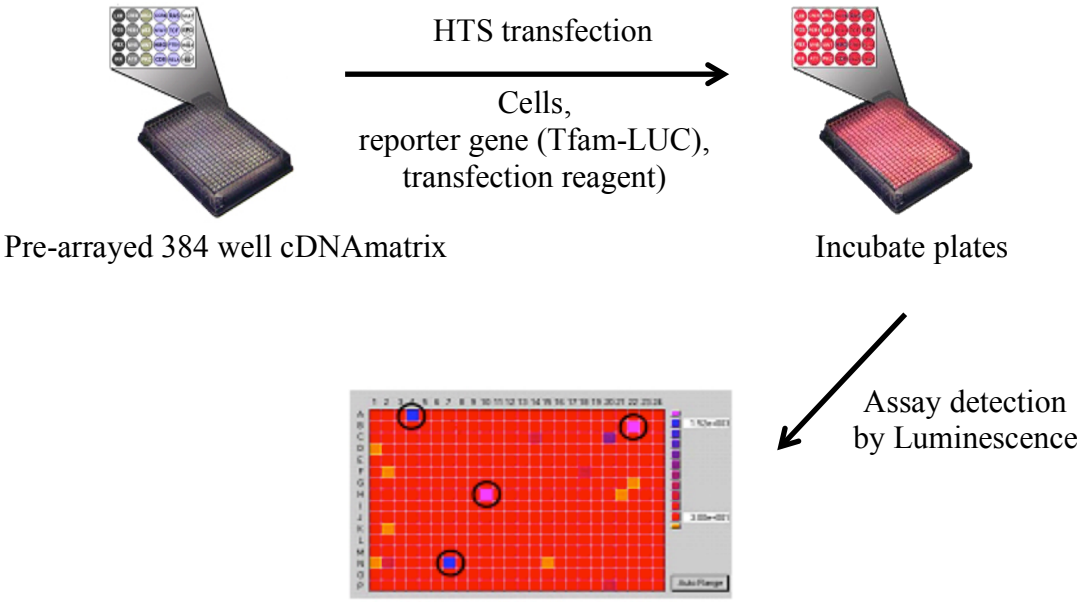

Figure 4.1.1: Scheme of the Tfam-Luc transfection used in the screen.

In collaboration with the GNF we applied this technology was to identify genes that modulate mitochondrial number and function. To this end two cDNA libraries, which account for 70% of known genes, were overexpressed in mammalian expression vectors by transient transfection in HEK 293 cells. One of these libraries contains 16,000 fully sequenced cDNAs (MGCv2, mouse and human), while the other one includes 11,000 5' and 3' sequenced cDNAs (Origene, mouse and human). These collections have been arrayed onto 384-well plates for functional screening, with a single cDNA spotted per well to facilitate deconvolution of results. Individual cDNAs were co-transfected with a luciferase reporter to measure the activity of mitochondrial transcription factor A (Tfam; Fig. 4.1.2).

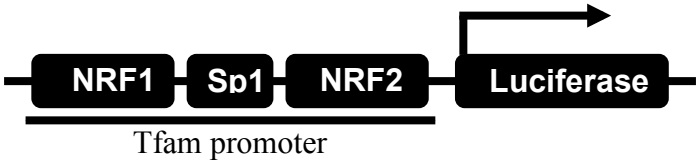

Figure 4.1.2: Scheme of the Tfam-Luc reporter system.

Since all factors known to influence mitochondrial number or oxidative phosphorylation such as PGC-1α, NAD^+-dependent histone/protein deacetylases such as sirtuins and in particular SIRT1, NRF1 and p160 myb binding protein appear to modulate Tfam expression levels, evaluation of Tfam promoter activity can serve as a marker to identify genetic pathways that regulate mitochondrial biogenesis. Pilot experiments with this reporter performed in screening mode (384-well, robotic manipulations) indicate that the signal to noise ratio is robust and appropriate for HTS (Fig. 4.1.3).

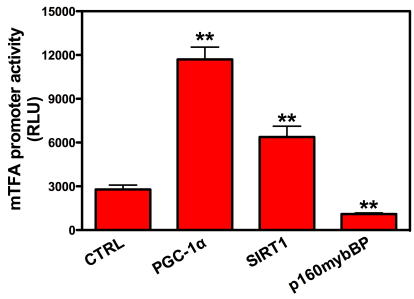

Figure 4.1.3: validation of Tfam promoter in HEK 293 cells. PGC-1α and SIRT1 were used as positive control and p160 myb binding protein as negative. Data are presented as relative light unit (RLU). Statistical analysis was performed using one way ANOVA followed by Tukey post test, **P<0.001.

Libraries were screened in duplicate and data statistically evaluated to select hits. cDNA was considered a hit if it regulated Tfam expression as much as positive known regulators of mitochondrial functions such as PGC-1α (positive, [63]) and p160 myb binding protein (negative, [178]). All hits were checked against GNF's genomic screening database to exclude genes that induce Tfam activity in a not specific manner. The genomic HTS yielded 441 clones able to induce and 300 clones able to reduce Tfam promoter activity (Fig. 4.1.4 A and B).

A)

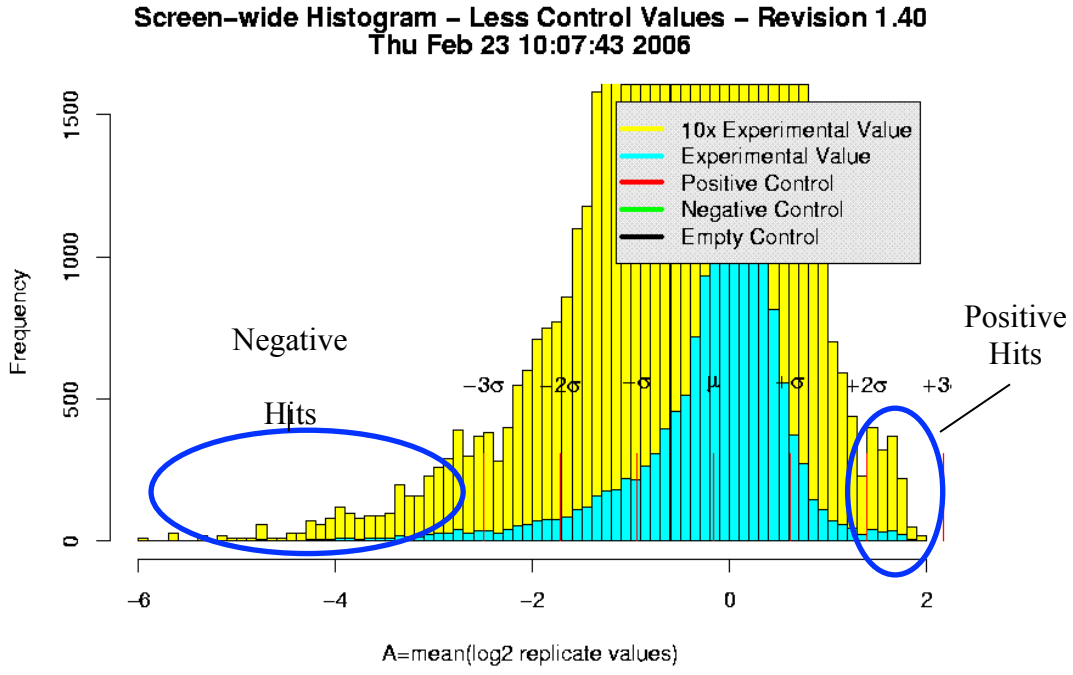

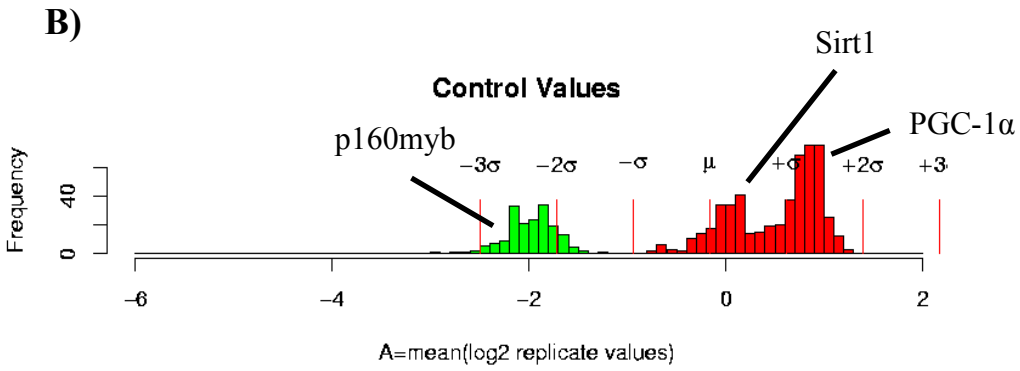

Figure 4.1.4: graphical representation of the mitochondrial screen data analysis. A) Data plot in a Log2 based scale. The distribution of the data shows the positive and the negative hits (blue circle) at the upper and the lower bound of the X axis. B) This graph shows the score ofpositive (PGC-1**α**) and negative (p160 myb) controls in the screen determining the cut off to choose the hits.

4.2 FACS Analysis

As already mentioned, we focused our attention only on the 441 positive candidates, as our final aim is to discover new positive mitochondrial regulators. All hits from the cDNA screen were confirmed in HEK 293 cells by flow cytometry analyses of cells transfected with a single cDNA and stained with Mitotracker® Green and Mitotracker® CM-H_2X-ROS as markers for mitochondrial density and function, respectively. Notably, by applying these screening assays, we were able to identify factors already known to promote mitochondrial biogenesis like CREB (cAMP response element binding protein [179]) among the positive hits.

Starting from 441 genes, 131 positive candidates were confirmed to modulate mitochondrial density and activity in HEK293 cells.

5. Results:

5.1 Bioinformatic Analysis

In order to better investigate 131 genes, we classified them according to their biological and molecular function (GeneOntology classification). By using Panther software (www.pantherbd.org) we were able to classify 126 candidates, so we decided to exclude the five missing genes from the analysis, as either they did not have aliases or they were not recognized by the software.

5.1.1 Biological process classification

By classifying the 126 candidates according to their biological function, we found that the 40% of the encoded proteins are involved in cellular and metabolic processes (Fig. 5.1.1 and Table 5.1). Hence, we decided to classify these two components in more depth. The genes classified as belonging to metabolic processes are mainly involved in nucleic acid metabolic processes or in protein metabolic processes (Fig.5.1.1 B and Table 5.2). On the other hand, the genes that according to GO classification belong to cellular processes are mainly involved in cell cycle or in cell communication (Fig. 5.1.1 C and Table 5.3).

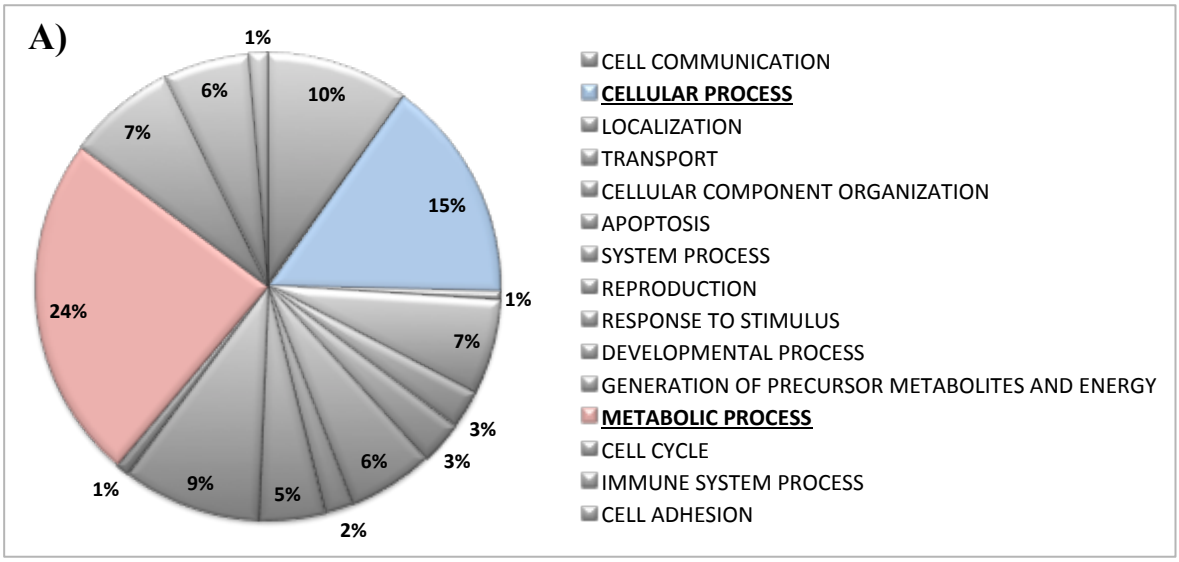

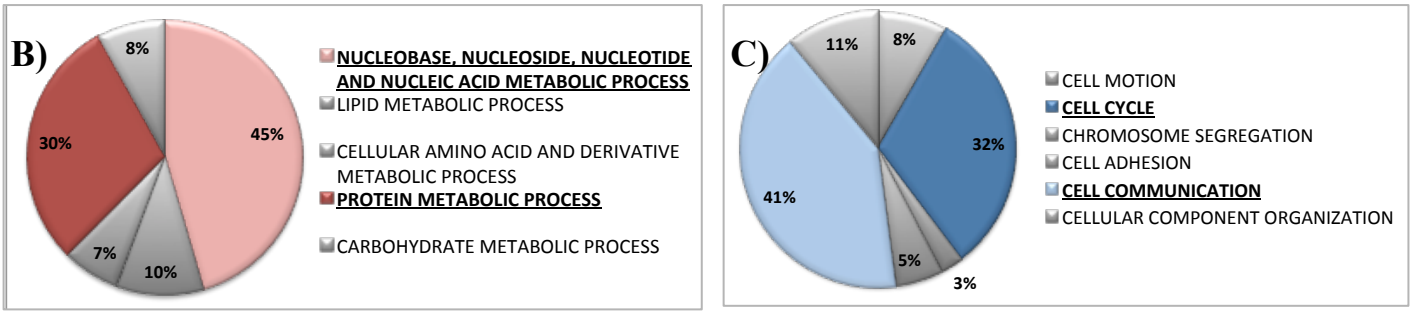

Figure 5.1.1: The 126 genes were classified according to GeneOntology biological processes (A), metabolic processes (B) and Cellular processes (C) using www.pantherdb.org.

BIOLOGICAL PROCESSES	NR. OF GENES	%
cell communication (GO:0007154)	30	9.9%
cellular process (GO:0009987)	47	15.5%
localization (GO:0051179)	2	0.7%
transport (GO:0006810)	20	6.6%
cellular component organization (GO:0016043)	8	2.6%
apoptosis (GO:0006915)	9	3.0%
system process (GO:0003008)	18	5.9%
reproduction (GO:0000003)	6	2.0%
response to stimulus (GO:0050896)	14	4.6%
developmental process (GO:0032502)	29	9.5%
generation of precursor metabolites and energy (GO:0006091)	3	1.0%
metabolic process (GO:0008152)	73	24.0%
cell cycle (GO:0007049)	23	7.6%
immune system process (GO:0002376)	18	5.9%
cell adhesion (GO:0007155)	4	1.3%

Table 5.1: Biological process classification.

METABOLIC PROCESSES	NR. OF GENES	%
nucleobase, nucleoside, nucleotide and nucleic acid metabolic process (GO:0006139)	40	45.5%
lipid metabolic process (GO:0006629)	9	10.2%
cellular amino acid and derivative metabolic process (GO:0006519)	6	6.8%
protein metabolic process (GO:0019538)	26	29.5%
carbohydrate metabolic process (GO:0005975)	7	8.0%

Table 5.2: Metabolic process classification.

CELLULAR PROCESSES	NR. OF GENES	%
cell motion (GO:0006928)	6	8.2%
cell cycle (GO:0007049)	23	31.5%
chromosome segregation (GO:0007059)	2	2.7%
cell adhesion (GO:0007155)	4	5.5%
cell communication (GO:0007154)	30	41.1%
cellular component organization (GO:0016043)	8	11.0%

Table 5.3: Cellular classification.

5.1.2 Molecular function classification

Analysis of the 126 genes by their molecular function revealed that the classes that describe a large fraction of the genes under investigations are binding (35%) and catalytic activity (33%) (Fig.5.1.2 A and Table 5.4). In addition, genes involved in binding are mainly nucleic acid binding proteins (74%) (Fig.5.1.2 B and Table 5.5), while those involved in catalytic activity are mainly involved either in hydrolase activity (31%) or in transferase activity (23%) (Fig. 5.1.2 C and Table 5.6).

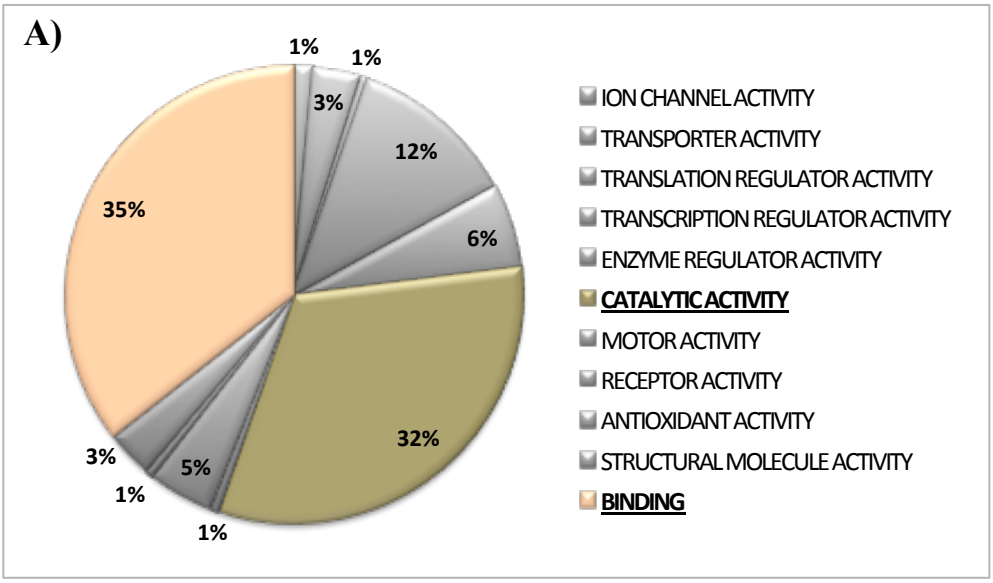

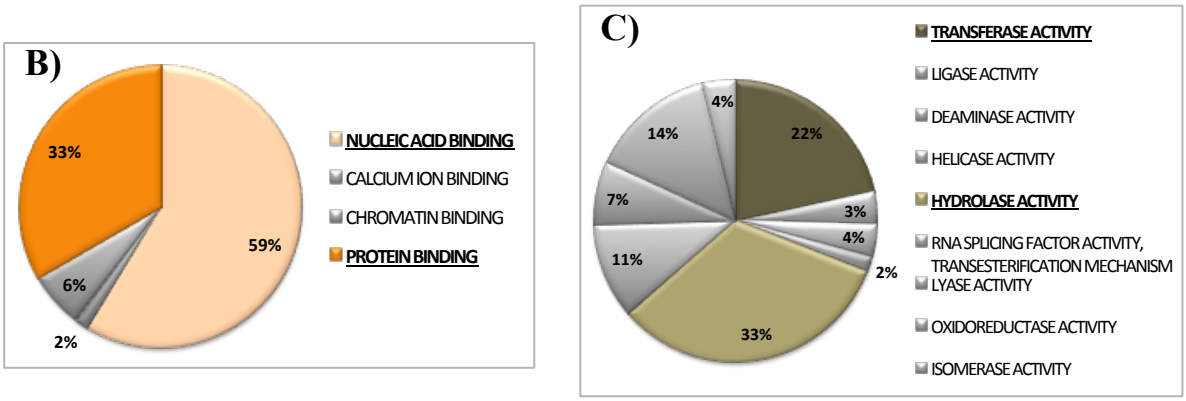

Figure 5.1.2: The 126 genes were classified according to GeneOntologymolecular functions (A), Binding type (B) and Catalitic activity (C) using the panther software (www.pantherdb.org).

MOLECULAR FUNCTIONS	NR. OF GENES	%
ion channel activity (GO:0005216)	2	1.3%
transporter activity (GO:0005215)	5	3.3%
translation regulator activity (GO:0045182)	1	0.7%
transcription regulator activity (GO:0030528)	18	11.8%
enzyme regulator activity (GO:0030234)	9	5.9%
catalytic activity (GO:0003824)	49	32.2%
motor activity (GO:0003774)	1	0.7%
receptor activity (GO:0004872)	7	4.6%
antioxidant activity (GO:0016209)	1	0.7%
structural molecule activity (GO:0005198)	5	3.3%
binding (GO:0005488)	54	35.5%

Table 5.4: Molecular function classification.

BINDING	NR. OF GENES	%
nucleic acid binding (GO:0003676)	37	58.7%
calcium ion binding (GO:0005509)	1	1.6%
chromatin binding (GO:0003682)	4	6.3%
protein binding (GO:0005515)	21	33.3%

Table 5.5: Binding classification.

CATALYTIC ACTIVITY	NR. OF GENES	%
transferase activity (GO:0016740)	12	21.8%
ligase activity (GO:0016874)	2	3.6%
deaminase activity (GO:0019239)	2	3.6%
helicase activity (GO:0004386)	1	1.8%
hydrolase activity (GO:0016787)	18	32.7%
RNA splicing factor activity, transesterification mechanism (GO:0031202)	6	10.9%
lyase activity (GO:0016829)	4	7.3%
oxidoreductase activity (GO:0016491)	8	14.5%
isomerase activity (GO:0016853)	2	3.6%

Table 5.6: Catalytic classification.

5.1.3 BioGPS and PubMed analysis

To further narrow down the number of positive hits to be included in future experiments we established some selection criteria. We chose hits that are involved in one or more key cell function according to the bioinformatic classification reported above. Moreover, we verified the expression profile of the candidate genes in HEK293 cells, in C2C12 cells and in the mouse gastrocnemius, by interrogating the BioGPS database. Then we assigned priority to those genes for which no links with mitochondria are known yet, by performing a research in literature through PubMed. By applying these selection criteria we chose 22 candidates; 3 belonging to the category "catalytic activity", 4 to the category "signal transduction", 11 to the category "transcription processes", 4 genes encoding for structural proteins and 1 whose function has not been annotated yet.

5.2 HTS validation: evaluation of mitochondrial activity in HEK 293 cell

In order to validate the HTS for the selected candidates, the 22 cDNAs were transiently transfected in HEK293 cells and their ability to increase the mitochondrial activity was assessed 60 h after transfection using the MitoTracker® CM-H_2X-ROS dye. We selected this time point to allow transcription and translation of the transfected cDNAs and activation of the mitochondrial machinery. This was an "in-plate" staining instead of flow cytometry-based assay; however this method displays advantages compared with flow cytometry, used in the first screen. The fluorescence relative to mitochondrial activity is detected in live cells directly in the wells with no need of trypsin to allow cells to detach from the well. The latter is a step required in flow cytometry that can alter cell morphology and activities. To evaluate the transfection efficiency we transfected the Green Fluorescent Protein (GFP) and the fluorescence was checked by microscope before performing the experiment. The cell-permeant MitoTracker®CM-H_2X-ROS probe contains a mildly thiol-reactive chloromethyl moiety for labeling mitochondria, the probe passively diffuse across the plasma membrane and accumulate in active mitochondria thus the fluorescence is a quantitative measure of the mitochondrial activity. As shown in Fig. 5.2.1, all the candidates were able to induce the mitochondrial activity with a higher or equal power compared to that of PGC-1α, confirming the data obtained with the previous screening performed in a high throughput format.

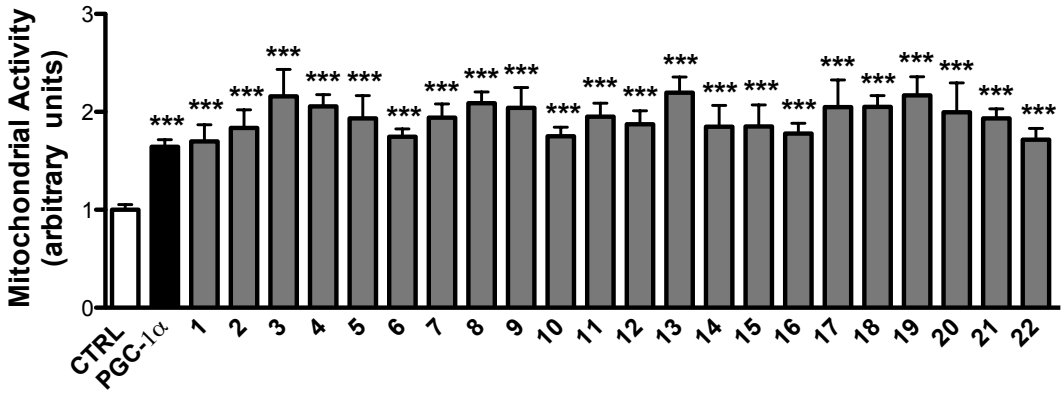

Figure 5.2.1: mitochondrial activity. HEK 293 cells transfected with the empty vector were used as control (CTRL), PGC-1α was used as positive control. Data were normalized against cell number and expressed setting at 1 the signal measured in CTRL samples. Statistical analysis was performed using *t*-test, ***P<0.0001, *vs CTRL.

5.3 Validation of the 22 genes in C2C12 myoblasts

Skeletal muscle is one of the tissues with the strongest levels of dependence on mitochondrial function in regulating the oxidative metabolism, as shown by the severe impacts of mitochondrial diseases on muscle performance in patients [180]. Thus, skeletal muscle is an attractive tissue for analyzing in depth the regulation of mitochondrial biogenesis and function. By this means, we decided to characterize the 22 candidates identified in C2C12 cell line, a mouse skeletal muscle cell line. We used C2C12 myoblasts, since they are very well characterized and easily to manage and to transfect. In addition, in literature they are commonly used for studies dealing with the energetic metabolism. To evaluate the transfection efficiency we transfected the GFP and the fluorescence was detected by microscope before performing each single experiment.

5.3.1 Evaluation of the mitochondrial biogenesis

Taking into consideration the previous results and what is reported in literature, we decided to investigate if the overexpression of the 22 candidates in C2C12 cells could lead to an increase in the mitochondrial DNA copy number [4, 93, 110, 181]. In fact, one of the hallmarks of mitochondrial biogenesis is the increase of mitochondrial DNA content. The 22 hits were individually transfected in C2C12 and after 60 hours total DNA (nuclear and mitochondrial) was extracted. We selected this time point to allow transcription and translation of the transfected cDNAs and to give them enough time to regulate the mitochondrial machinery. The mitochondrial DNA content was evaluated as the ratio between the amount of a mitochondrial encoded gene (cytochrome c oxidase subunit II, COXII) and the amount of a nuclear encoded gene (ribosomal protein large P0, Rplp0 or 36B4). The data were obtained using quantitative real-time polymerase chain reaction (qRT-PCR). As shown in Fig. 5.3.1, all the candidates increased the mitochondrial DNA content at the same or higher levels of those found in cells overexpressing PGC-1α, a very well known mitochondrial regulator [63].

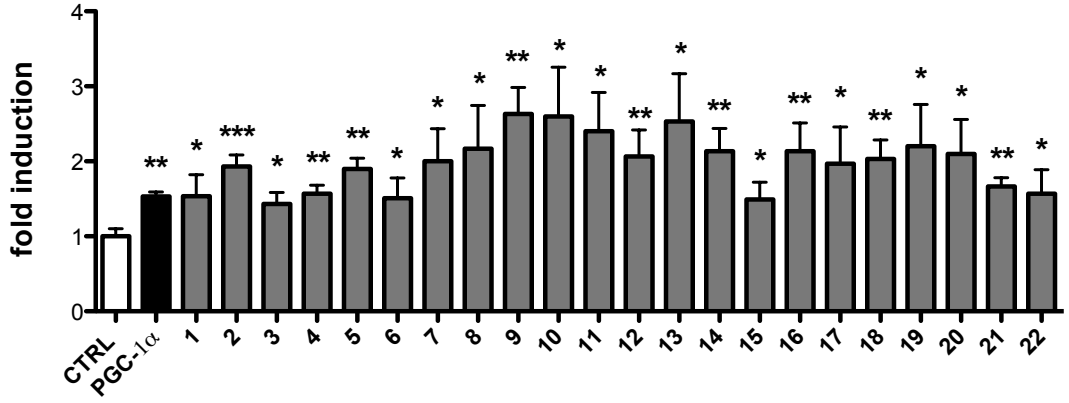

Figure 5.3.1: mtDNA quantification**.** C2C12 myoblasts were transfected with the empty vector (CTRL), with PGC-1α and all the22 cDNAs. Sixty hours after transfection total DNA was extracted from cells. The mtDNA was measured by qRT-PCR and expressed as the ratio between the amount of a mitochondrial gene (COXII) and a nuclear gene (36B4). The data were expressed setting at 1 the ratio found in cells transfected with the empty vector. Statistical analysis was performed using *t*-test, *P<0.05, **P<0.01, ***P<0.0001, *vs CTRL.

5.3.2 Evaluation of the oxygen consumption rate

A potential mitochondrial regulator should increase not only the mtDNA copy number, but also the mitochondrial function. A functional approach to estimate the mitochondrial activity is the evaluation of the respiration, measured as nanomoles of oxygen consumed per minute. Whole C2C12 myoblasts individually transfected with the 22 genes, 60 hours after transfection, were measured for the basal oxygen consumption rate by using a Clark electrode-based oxygraph. As shown in Fig. 5.3.2, the overexpression of 13 out of the 22 candidates enhanced the basal respiration rate. In particular, overexpression of candidate 9, 10, 19 and 22 induced the respiration by 1.7 times compared to the control. It is worth to notice that PGC-1α, our positive control, increased the respiration of 1.5 times, as already reported by other groups [63].

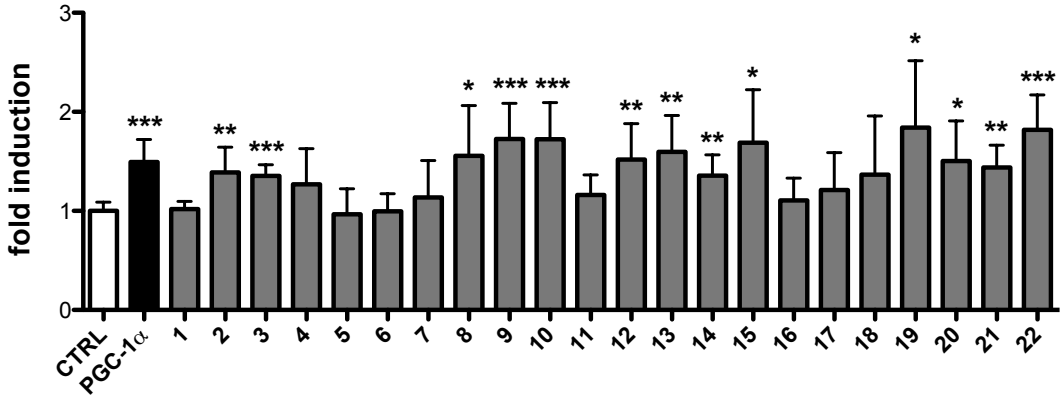

Figure 5.3.2: Oxygen Consumption. C2C12 myoblasts were transfected with the empty vector (CTRL), with PGC-1α and all the22 cDNAs. At 60 hours after transfection the cells were detached from the plates and transferred to a chamber for measurement of oxygen consumption. All data were normalized by protein content and were expressed setting at 1 the respiration rate measured in cells transfected with empty vector. Statistical analysis was performed using *t*-test, *P<0.05, **P<0.01, ***P<0.0001, *vs CTRL.

In the experimental conditions used, we observed that the overexpression of all 22 candidates induced a significant increase of mtDNA, suggesting a positive effect on mitochondrial biogenesis. Nonetheless only 4 of them were able to

increase the basal respiration rate, index of enhanced oxidative function. All together these data indicate that not always an increase mitochondrial DNA couples with higher oxidative capacity in basal conditions.

At this point, we decided to focus our attention on only one candidate gene to deeply characterize its involvement in mitochondrial function. As shown in Fig. 5.3.3, the scatter plot revealed a cluster of four hits able to induce either mitochondrial DNA content and the oxygen consumption at level similar or higher than the known mitochondrial regulator PGC-1α. Among these four new potential mitochondrial regulators the gene number 9 (Zc3h10) was preferred primarily because its function is not yet annotated. This gene is zinc finger CCCH type containing 10 (Zc3h10), and it belongs to a nucleic acid binding protein family.

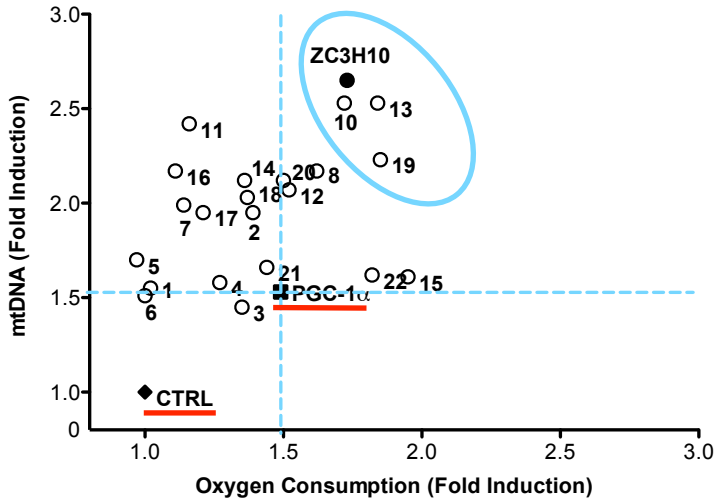

Figure 5.3.3: Scatter plot. This graph correlates the dataset of the mtDNA quantification reported in fig. 9 and the dataset of the Oxygen consumption reported in fig. 10.

5.4 Characterization of Zc3h10 in myoblasts

After choosing our best candidate, we decided to characterize the mitochondrial function of Zc3h10 protein in C2C12 myoblasts. To evaluate the transfection efficiency we transfected the GFP and the fluorescence was detected by microscope before performing each single experiment.

5.4.1 Evaluation of Zc3h10 expression level

C2C12 myoblast either transfected with the empty vector (CTRL) or with the expression vector for Zc3h10 were lysed and a western blot analysis was conducted to evaluate the endogenous expression levels of Zc3h10 and the amount of its overexpression. As shown in Fig. 5.4.1 we were able to detect endogenous Zc3h10 and an increase of two folds the expression level of the overexpressed protein.

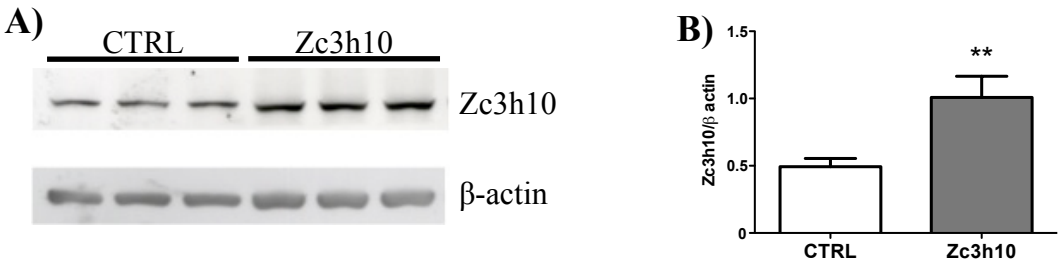

Figure 5.4.1: Western blot of the Zc3h10 protein. (A) Myoblasts transiently transfected with the empty vector (CTRL) and Zc3h10 were collected and the expression level of the Zc3h10 protein was evaluated. (B) Quantification of the Zc3h10 expression level performed using Imagej. Statistical analysis was performed using *t*-test, **P<0.01, *vs CTRL.

5.4.2 Evaluation of Tfam activation by Zc3h10

As we analyzed the Tfam promoter activity in HEK293 cell during the HT screening,

we decided to confirm the data in C2C12 myoblasts. We co-transfected the reporter system (Fig. 5.4.2.1 A), where the luciferase gene is under the control of the Tfam promoter, together with the cDNA encoding PGC-1α, as positive control, or the cDNA encoding Zc3h10. 24 hours after transfection, the promoter activity was evaluated. As shown in Fig. 5.4.2 C the overexpression of PGC-1α stimulated the Tfam promoter activity but also the overexpression of Zc3h10 produced the same effect. Therefore, we can conclude that also in C2C12 myoblasts Zc3h10 stimulated the Tfam transcription, even though at present the molecular mechanism is still unclear.

Wu *et al.* demonstrated that PGC-1α trans-activates Tfam transcription by co-activating the transcription factor NRF1[63]. In fact, they showed that when deleting the NRF1 binding site in the Tfam promoter, the PGC-1α was no longer able to induce the promoter activity. We used the same mutated Tfam reporter system (Tfam MUT, Fig. 5.4.2.1 B), deleted in the NRF1 binding site, to assess if the mechanism of action of Zc3h10 could be similar to that of PGC-1α. We co-transfected the mutated form of the reporter system with the empty vector (CTRL), the cDNA encoding PGC-1α and the cDNA encoding Zc3h10 in myoblasts. As result, the overexpression of PGC-1α did not affect the promoter activity of the mutated reporter system, as expected. While the overexpression of the selected hit induced the promoter activity in both wild type and mutated reporter systems, suggesting a mechanism of action different from that of PGC-1α. It is worth to notice that, if the NRF-1 binding site is deleted (Tfam MUT), the activity of the promoter stimulated by the overexpression of Zc3h10 is lower than that showed when the wild type Tfam promoter (Tfam WT) is transfected (Fig. 5.4.2.1 C). This suggests that Zc3h10 could promote the transactivation of the Tfam promoter through both the NRFs.

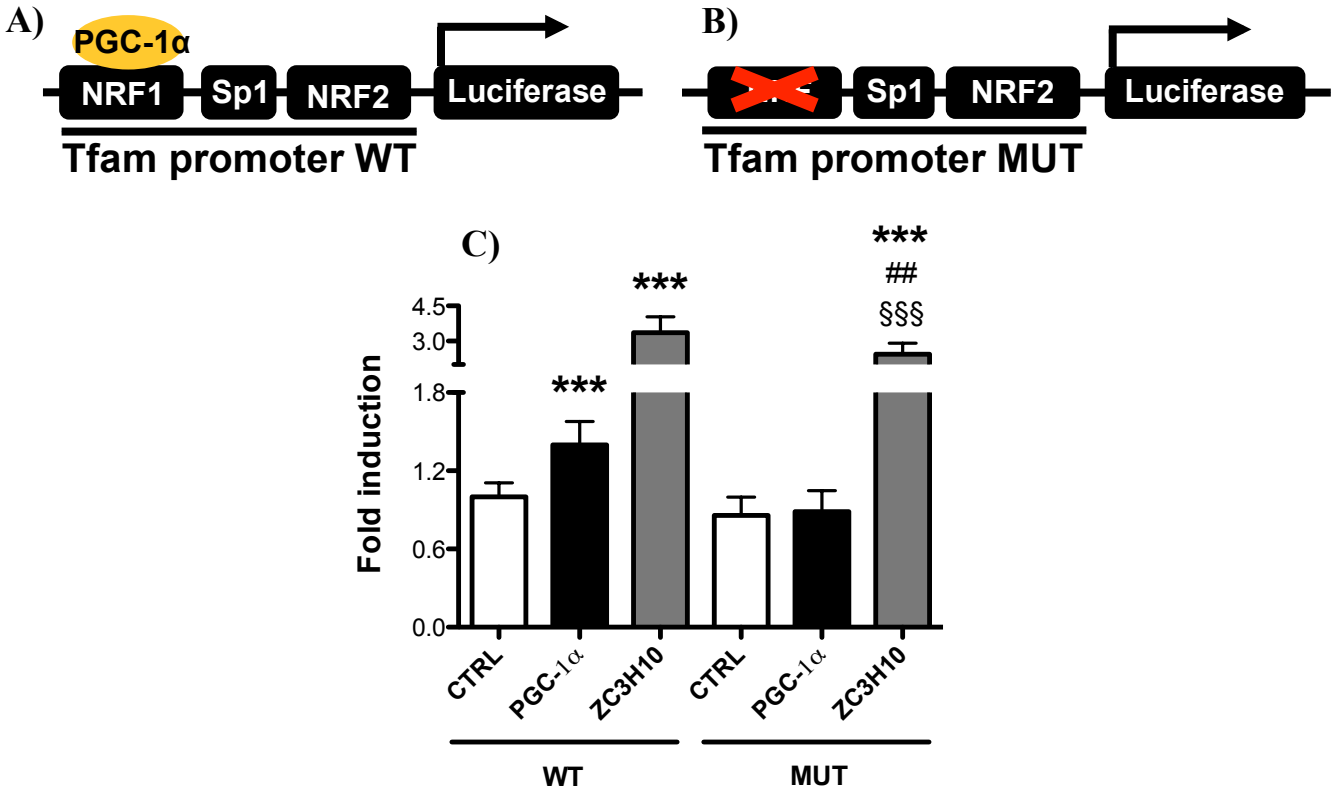

Figure 5.4.2.1:Tfam promoter activity. (A) The scheme of the wild type (WT) Tfam reporter system is shown. (B) The scheme reports the mutated (MUT) Tfam reporter system. (C) Myoblasts were transiently co-transfected with the empty vector (CTRL), PGC-1α cDNA and Zc3h10 cDNA and the wild type and mutated Tfam reporter systems. Twentyfour hours after transfection the luciferase activity was evaluated. Data are expressed as means ± sd, setting at 1 the luciferase activity measured in cells transfected with the empty vector (CTRL). Statistical analysis was performed using *t*-test,**P*<0.05, ***P*<0.01, ****P*<0.001;*vs CTRL WT, §vs CTRL MUT, $^{\#}$vs Zc3h10 WT.

To confirm that the results obtained in Fig. 5.4.2.1 was not an aspecific effect mediated by the interaction of the PGC-1α or Zc3h10 with the backbone of the reporter system (pTK-LUC), we performed the same experiment also with the pTK-LUC vector. Fig.5.4.2.2 showed that PGC-1α and Zc3h10 did not induce pTK-LUC transcriptional activity while these effects are seen when the reporter system contains the Tfam promoter as also previously observed.

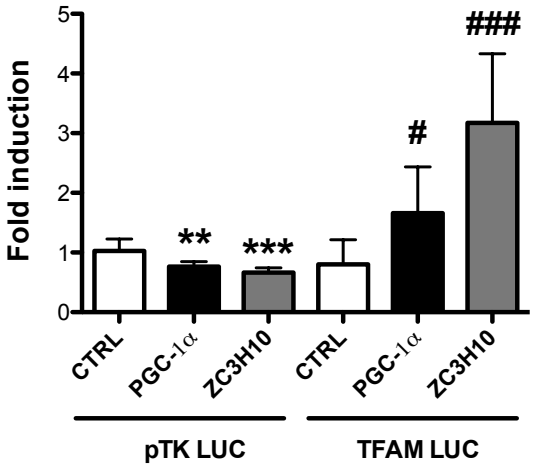

Figure 5.4.2.2: pTK LUC and Tfam promoter activity. Myoblasts were transiently co-transfected with the empty vector (CTRL), PGC-1α cDNA and Zc3h10 cDNA and the WT Tfam reporter system or the pTK LUC vector. 24 hours after transfection the promoter activity was evaluated. All data were expressed setting at 1 the luciferase activity measured in cells transfected with empty vector. Statistical analysis was performed using *t*-test, **P*<0.05, ***P*<0.01, ****P*<0.001;*vs CTRL pTK LUC, #vs CTRL Tfam LUC.

5.4.3 Evaluation of Oxygen Consumption Rate

We decided to deeply characterize the effects produced by overexpression of Zc3h10 analyzing the oxygen consumption rate in uncoupling condition and in maximal respiration. The uncoupled respiration was evaluated adding oligomycin, an ATP synthase inhibitor, which, by blocking the ATP synthase proton channel, uncouples ATP phosphorylation from electron transport chain. In this condition, mitochondria do not produce ATP and the ATPse proton channel does not work, the only way the protons have to enter into the mitochondrial matrix is through the proton leak mediated by UCPs yielding heat (Fig. 5.4.3.1 B). Consequently, the ETC slows down and the cell consumes less oxygen. On the other hand, the maximal respiration was reached adding the carbonyl cyanide m-chlorophenylhydrazone (CCCP), a lipophilic compound that transports the protons through the inner mitochondrial membrane, dissipating the electrochemical gradient and maximizing the mitochondrial respiration

(Fig. 5.4.3.1 C). The CCCP-stimulated oxygen consumption therefore reflects the number of mitochondria and/or the electron transport activity.

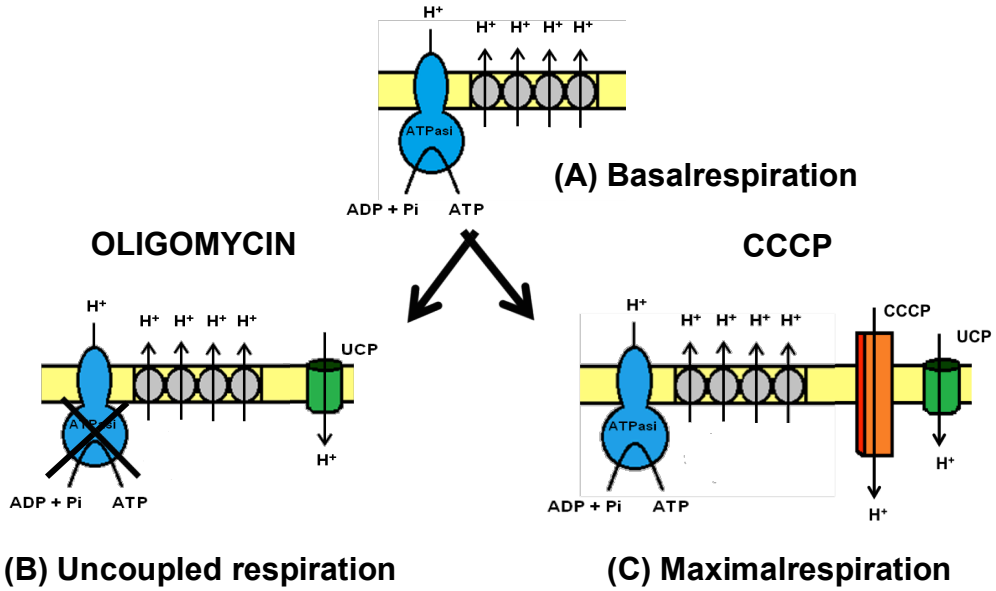

Figure 5.4.3.1: Model illustrating the (A) Basal respiration, (B) Uncoupled respiration and (C) maximal respiration. The figure is adapted from Wu Z. *et al.*, Cell, 1999, Vol 98, 115-124[63].

C2C12 myoblasts were transiently transfected with the different vectors (empty vector, PGC-1α and Zc3h10 cDNAs), and analyzed 60 hours after transfection. The basal, uncoupled and maximal respiration was evaluated in the conditions summarized in. Fig.5.4.3.1 shows that the addition of oligomycin decreased the oxygen consumption as expected, while the addition of CCCP led to a maximal level of respiration in all myoblasts transfected with the different cDNAs. As previously shown (Fig. 5.4.3.2), the overexpression of both PGC-1α and Zc3h10 increased the basal oxygen consumption rate. In addition, we found that the overexpression of PGC-1α increased the uncoupled respiration by 2 folds compared to cells transfected with the empty vector, confirming data already present in literature [63]. In addition, also the overexpression of our selected hit had the same effect (a 2 folds increase), indicating that Zc3h10 stimulates the uncoupling of mitochondria in these cells.

Considering the maximal respiration, the overexpression of our positive control induced the CCCP-stimulated oxygen consumption by around 2 folds [63] while Zc3h10 by 1.5 folds compared to cells transfected with the empty vector. This result indicated that these cells had a higher content and/or electron transport activity of mitochondria.

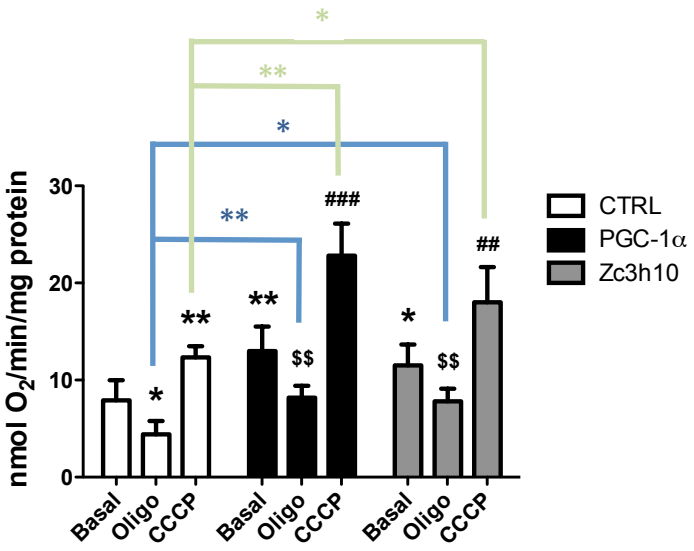

Figure 5.4.3.2: Oxygen Consumption. C2C12 myoblasts transfected with the empty vector (CTRL), with PGC-1α and Zc3h10 cDNAs. At 60 hours after transfection the cells were detached from the plates and transferred to a chamber for measurement of oxygen consumption. The concentration of oligomycin was 1.25 µM and the concentration of the CCCP was 3.75µM. All data were normalized by the protein content. Statistical analysis was performed using t-test,*P<0.05, **P<0.01, ***P<0.001;*vs CTRL Basal,$^{\#}$vs PGC-1α Basal $^{\$}$vs Zc3h10 Basal, *vs CTRL Oligo, *vs CTRL CCCP.

5.4.4 Evaluation of OXPHOS proteins' expression levels

To corroborate the underlying cause of this increased function, we decided to evaluate the expression of the OXPHOS proteins by western blot analyses. As shown in Fig. 5.4.4, the overexpression of Zc3h10 increased the protein level of all the subunits of the OXPHOS complexes to the same extent of the positive control PGC-1α, thus indicating that the increased mitochondrial function is associated with higher

expression of the OXPHOS genes.

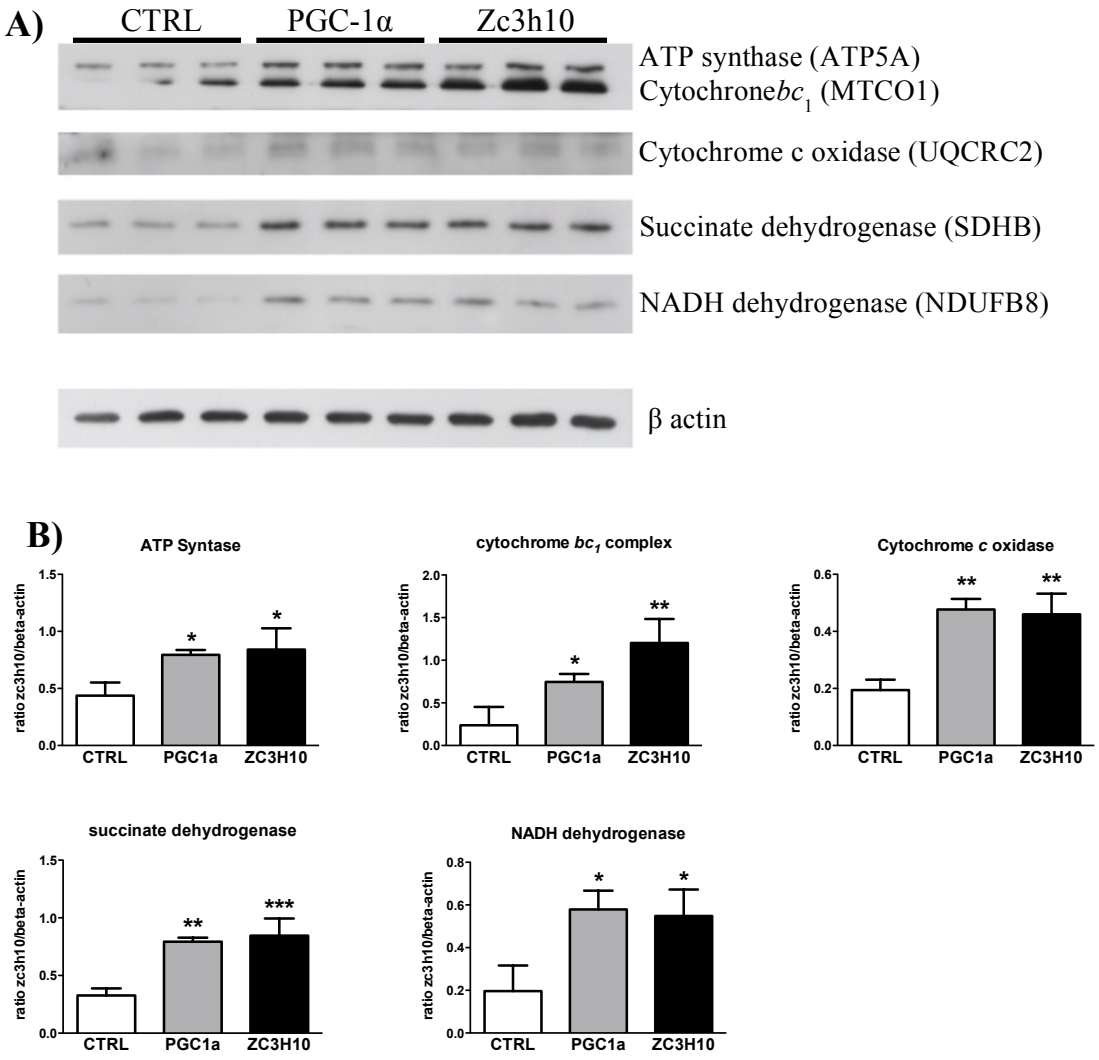

Figure 5.4.4: Western blot of the OXPHOS proteins. (A) Myoblasts transiently transfected with the empty vector (CTRL), PGC-1α and Zc3h10 cDNAswere collected and the expression level of the OXPHOS proteins was evaluated. (B) Quantification of the expression levels of the indicated OXPHOS complexes was performed using Imagej. Statistical analysis was performed using One way ANOVA followed by Dunnett's multiple comparison test,*P<0.05, **P<0.01, ***P<0.001; *vs CTRL.

5.4.5 Evaluation of ATP Production

ATP production is coupled to mitochondrial respiration, therefore, an increased ATP production should be observed in conditions of induced mitochondrial activity. Consequently, we evaluated the total amount of ATP (both mitochondrial and cytosolic) in myoblasts overexpressing our selected hit and the positive control. The

overexpression of both PGC-1α and Zc3h10 increased the total content of ATP (Fig. 5.4.5, sum of the white and black bars). We decided to evaluate if the observed increase was due to the cytosolic or to the mitochondrial fraction. To evaluate the cytosolic ATP, we treated cells with oligomycin (an ATP synthase inhibitor) and we observed no difference in ATP levels (Fig. 5.4.5, white bars). The mitochondrial ATP amount was evaluated as the difference between the total level and the cytosolic fraction. We found increased mitochondrial ATP content both in myoblasts overexpressing PGC-1α and Zc3h10 (Fig.5.4.5, black bars). Once again, these results confirm that the overexpression of both the positive control (PGC-1α) and Zc3h10 stimulate the mitochondrial function.

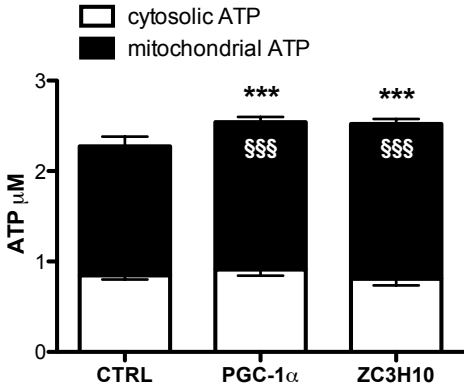

Figure 5.4.5: ATP production. C2C12 myoblasts were transfected with the empty vector (CTRL), with PGC-1α and Zc3h10 cDNAs. At 60 hours after transfection the amount of ATP was evaluated using the ATPlite kit (Perkin Elmer). The concentration of cytosolic ATP was measured treating cells with 10 μM oligomycin for 24 hours. The amount of mitochondrial ATP was calculated as the difference between the total amount of ATP and the cytosolic fraction. Statistical analysis was performed using One way ANOVA followed by Dunnett's multiple comparison test,**P*<0.05, ***P*<0.01, ****P*<0.001; *vs CTRL total ATP amount; §vs CTRL mitochondrial ATP amount.

5.4.6 Evaluation of Reactive Oxygen Species Production

Mitochondrial metabolism is responsible for the majority of the reactive oxygen species (ROS) production in the cell [182]. The formation of ROS occurs when unpaired electrons escape the electron transport chain and react with molecular

oxygen, generating superoxide [183]. Superoxide can react with DNA, proteins, lipids and plays an important role in many physiological and pathophysiological conditions. The maintenance of low ROS levels is critical to normal cell functions, therefore, an increase in mitochondrial activity carry an inherent risk of increasing ROS levels. Consequently, we measured this parameter by a fluorescence-based assay using the 2',7'-dichlorodihydrofluorescein diacetate (CM-H_2DCFDA) probe. The cell-permeant H_2DCFDA is a chemically reduced form of fluorescein used as an indicator of reactive oxygen species in cells. Upon cleavage of the acetate groups by intracellular esterases and oxidation, the non fluorescent H_2DCFDA is converted to the highly fluorescent 2',7'-dichlorofluorescein (DCF). Myoblasts, 60 hours after transfection with the empty vector (CTRL), or the plasmid expressing PGC-1α and Zc3h10 were incubated with the probe. As positive control, we used myoblasts transfected with the empty vector and then treated with H_2O_2, a powerful type of ROS.

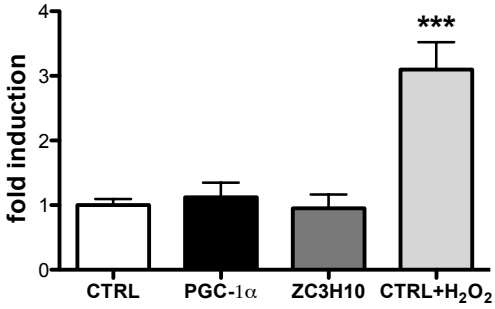

Fig.5.4.6: Reactive Oxygen Species measurement. C2C12 myoblasts were transfected with the empty vector (CTRL), with PGC-1α and ZC3H10 cDNAs. At 60 hours after transfection the cells were treated with CM-H2DCFDA 5μM. As positive control we used myoblasts transfected with the empty vector and treated with 25 μM H_2O_2 for 30 minutes. All data were normalized by the protein content and were expressed setting at 1 the signal measured in cells transfected with empty vector. Statistical analysis was performed using One way ANOVA followed by Dunnett's multiple comparison test,*P<0.05, **P<0.01, ***P<0.001; *vs CTRL.

As shown in Fig. 5.4.6 the overexpression of PGC-1α did not enhance the ROS production, because as reported in literature PGC-1α is able to counterbalance the

ROS production inducing the expression of two enzymes (catalase and superoxide dismutase 2) involved in the catabolism of ROS [184]. The overexpression of Zc3h10 did not increase the ROS level, as well. Despite the increased oxygen consumption rate measured in cells overexpressing either PGC-1α or Zc3h10, we did not observed abnormal level of ROS. This could be due to the activation/induction of antioxidant enzymes, as reported in systems overexpressing PGC-1α.

5.4.7 Measurement of the mitochondrial membrane potential

Apoptosis is a normal process of organismal development. Induction of this process can arise from a variety of stimuli. The intrinsic pathway, also referred to as mitochondrial-mediated apoptosis, is initiated via intracellular signals, such as DNA damage and oxidative stress. Mitochondria own a mitochondrial transition pore that when activated opens a channel in the mitochondrial inner membrane, short circuits proton electrochemical gradient, and initiates programmed cell death (apoptosis). One of the early markers of the mitochondrial-mediated apoptosis is a decrease in the mitochondrial membrane potential. Indeed, we decided to measure this parameter using the JC-1 probe. JC-1 is a cationic dye that exhibits potential-dependent accumulation in mitochondria, indicated by a fluorescence emission shift from green (~525 nm) to red (~590 nm). Consequently, mitochondrial depolarization is indicated by a decrease in the red/green fluorescence intensity ratio. The potential-sensitive color shift is due to concentration-dependent formation of red fluorescent J-aggregates. At 60 hours after transfection the myoblasts transfected with the empty vector (CTRL), or the vectors encoding PGC-1α and Zc3h10 were treated with the JC-1 probe. As positive control, we use myoblasts transfected with the empty vector and then treated with CCCP, which causes quick mitochondrial membrane

depolarization. Fig. 5.4.7 shows that neither the overexpression of PGC-1α nor the overexpression of Zc3h10 affected the membrane potential.

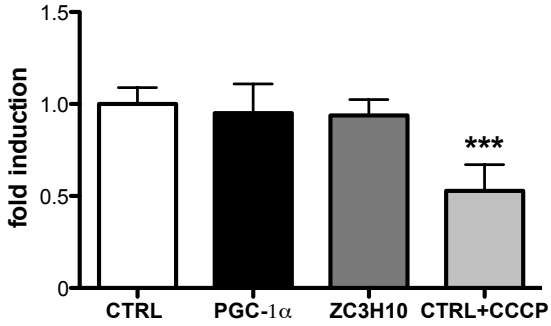

Figure 5.4.7: Inner mitochondrial membrane potential measurement. C2C12 myoblasts were transfected with the empty vector (CTRL), with PGC-1α and ZC3H10 cDNAs. At 60 hours after transfection the cells were treated with 3μM JC-1 probe. As positive control we used myoblasts transfected with the empty vector and treated with 10 μM CCCP for 30 minutes. All data were normalized by the protein amount and were expressed setting at 1 the fluorescence ratio measured in cells transfected with the empty vector. Statistical analysis was performed using One way ANOVA followed by Dunnett's multiple comparison test,*P<0.05, **P<0.01, ***P<0.001; *vs CTRL.

5.4.8 Analysis of the Zc3h10 promoter

Since the function of Zc3h10 is completely unknown till now, no data are present in the literature describing its mechanisms of action or the way it is activated or regulated. Analyzing the Zc3h10 promoter (907 bases) on TFSearch (http://www.cbrc.jp) we found a putative highly conserved binding site for NRF-2 on its sequence (Fig. 5.4.8.1).

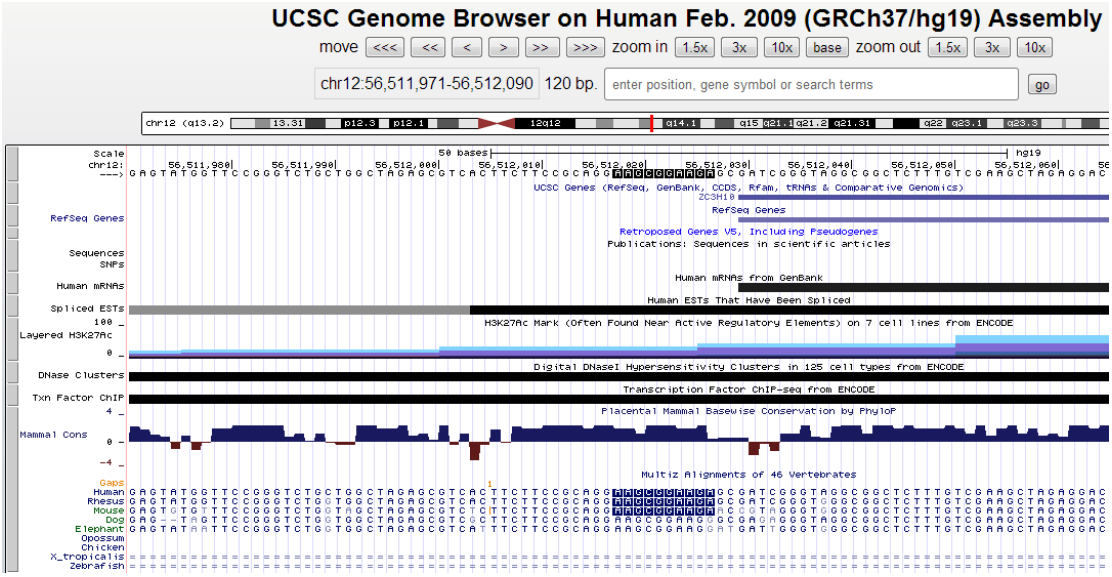

Figure 5.4.8.2: NRF-2 binding site. We searched the sequence of the Zc3h10 promoter purchased from SwitchGear into the Genome Browser (http://genome-euro.ucsc.edu). We found that the Zc3h10 is on the chromosome 12. Underlined in blue there are the NRF-2 putative binding site, that is highly conserved between different species.

We decided to investigate also if some other very well known mitochondrial regulators could in some way also regulate Zc3h10. We co-transfected the reporter system where luciferase was under the Zc3h10 promoter (Zc3h10-LUC), and the empty vector as control or the cDNAs of NRF2, PGC-1α, SIRT1, NRF1 and Zc3h10. 24 hours after the transfection, the promoter activity was evaluated.

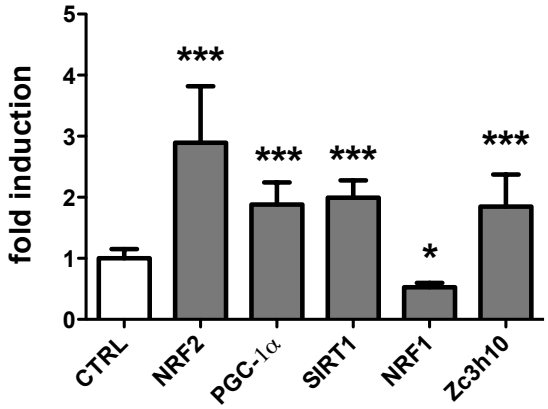

Figure 5.4.8: Zc3h10 promoter activity. Myoblasts were transiently co-transfected with the Zc3h10 reporter system and the empty vector (CTRL), NRF2, PGC-1α, SIRT1, NRF1 or Zc3h10 cDNAs. 24 hours after transfection the promoter activity was evaluated. Statistical analysis was performed using One way ANOVA followed by Dunnett's multiple comparison test,*P<0.05, **P<0.01, ***P<0.001; *vs CTRL.

As shown in Fig. 5.4.8.2, NRF2 induced the Zc3h10 promoter activity about 3 folds,

PGC-1α and SIRT1 increased the promoter activity of 2 folds, Zc3h10 about 1.8 folds suggesting a possible auto-regulation and surprisingly NRF1 seemed to inhibit the activity. These data are very promising, but more experiments should be performed in order to better understand these relationships between Zc3h10 activation and other mitochondrial regulators.

5.4.9 Zc3h10 expression levels in different mice organs

Since Zc3h10 characterization completely lacks, we decided to measure the expression level of this gene by qRT-PCR in different organs of C57BL6/J mice. We chose the organs that are rich in mitochondria mainly correlated in metabolism.

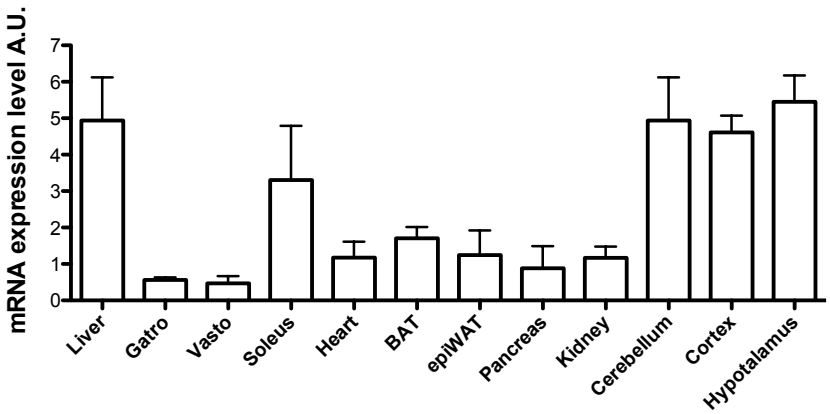

Figure 5.4.9: Zc3h10 gene expression in different tissues. Four 10 weeks old C57 Black 6 mice were sacrificed and the gene expression was measured by qRT-PCR.

As shown in Fig. 5.4.9, the main tissues in which the Zc3h10 is expressed are the liver, the soleus and the central nervous system.

6. Discussion:

Mitochondria are the powerhouse of the cells, since they produce the energy (ATP) necessary for all cellular functions. Apart from this main function, mitochondria are involved in many other metabolic processes like the oxidative catabolism of amino acids, ketogenesis, the urea cycle, the generation of ROS, the control of cytoplasmic calcium and the synthesis of all cellular Fe/S clusters. Consequently, the molecular mechanisms underlying their regulation and functions represent a highly relevant aspect of cell homeostasis.

Mitochondria are organelles possessing their own genome, which codes for some of the subunits of the ETC/OXPHOS complexes. Mitochondrial activities are mediated by thousands of mitochondrial-specific proteins encoded by both the nuclear (nDNA) and the mitochondrial (mtDNA) genome [2, 3]. Hence, the nuclear-mitochondrial crosstalk is at the basis of energy metabolism thus playing a key role in many cellular functions. The mtDNA replication and transcription are regulated by a nuclear-encoded transcription factor, called Tfam. In turn, the Tfam transcription is regulated by other nuclear-encoded factors. For example, PGC-1α, one of the best known among these factors, transactivates Tfam by the coactivation of another nuclear encoded transcription factor such as NRF-1. In fact, as reported in literature the overexpression of PGC-1α increases the basal respiration, a functional parameter to evaluate the mitochondria activity. PGC-1α overexpression increases also the mtDNA content, suggesting an increased mitochondrial biogenesis and also the expression level of the ETC proteins [63]. Many aspects at the basis of mitochondrial biology have not been fully deciphered, like the mechanisms controlling i) mtDNA replication and transcription, ii) the dynamics of mitochondrial fusion and fission and iii) the nuclear-mitochondrial crosstalk.

As mitochondria are so important for whole body metabolism, mitochondrial dysfunction is associated to many diseases such as diabetes, neurodegenerative disorders and aging. Nevertheless, the contribution of mitochondria to the pathogenic mechanisms underlying these pathologies is not completely characterized. Therefore, the aim of this project was to identify new mitochondrial regulators in order to gain knowledge in mitochondrial biology and to get new insights on the role of mitochondria in pathophysiology.

One possible approach for the screening of new regulators could be the yeast two-hybrid system, the same used by Puigserver *et al*. in 1998 for the identification of PGC-1α [115]. They cloned murine PPARγ in-frame into the GAL4 DNA-binding domain (BD) plasmid pAS2. In addition, a HIB 1B (murine brown adipocyte cell line) cDNA expression library was constructed in the GAL4 activation domain (AD) plasmid pACT II. This screening approach is based on the fact that if the PPARγ and one library-encoded protein interact (i.e., bind), then the AD and BD are indirectly connected, bringing the AD in proximity to the transcription start site and transcription GAL4 can occur. If the two proteins do not interact, there is no transcription of the reporter gene. In this way, a successful interaction between the fused proteins is linked to a change in the cell phenotype. Another possible screening methods could be the same used by Puigserver *et al*. to discover if PGC-1α specifically interacts with members of the nuclear hormone receptor superfamily [115]. They used GST-purified fusion proteins of PGC-1α immobilized on glutathione beads and incubated them with PPARγ and other nuclear receptors. The beads were then washed and the sample was processed by electrophoresis. After fixation and enhancement the radiolabeled proteins were visualized by autoradiography. The two screening methods just described, allow isolating proteins

that interact physically, but they are very time consuming and complicated. The sequencing of the human genome in 2003 holds benefits for many fields, from molecular medicine to human evolution. In fact, the Human Genome Project, through its sequencing of the DNA, helped to understand diseases but also allowed the commercial development of genomics research related to DNA based products, like cDNA libraries. These libraries, now commercially available, accounts for all the genes with and without an annotated function present in many organisms, like Homo sapiens, Mus musculus, Drosophila melanogaster and Escherichia coli. These libraries drastically affected all the screening approaches allowing high-tech type of experiments and high throughput screenings.

One of the major challenging nowadays is the identification of the molecular functions and the biological processes in which the proteins encoded by the genome are involved. This project exactly aims at the same objective, even if just related to mitochondria. In fact, we want to identify new mitochondrial regulators whose mitochondrial function was not yet reported. We found three proteins (nr. 10, 13, 19) to be active in mitochondria that are also involved in other pathways. More surprisingly, we discovered the mitochondrial involvement of Zc3h10, a protein whose function where previously completely uncharacterized.

In order to accomplish the aim of finding new mitochondrial factors, we should select a functional assay that could be applied to such a large number of potential regulators, the whole genome. In addition the approach should be relatively fast, allowing an easy deconvolution of results, easy to perform in robotic fashion and robust (i.e., few false negatives/positives). The most suitable approach that fulfills all these requirements is a HTS. The one we set up was also reproducible, as the positive clones identified counted also some very well known mitochondrial regulators as

CREB. We set up a genome-wide HTS, where we arrayed onto 384 wells plate a single cDNA spotted per well (in total 27000 genes were screened); individual cDNAs were co-transfected with a luciferase reporter to measure the activity of Tfam. The HEK 293 was used as cell line. There are many examples in literature of different HTS; nowadays they are widely used for screenings. Nevertheless, they have some limitations. It is not atypical, particularly for initial genome-wide screens in an organism, for the primary screen to be the only experimental data in the study. Apart from the value of the list of genes that are implicated in the process of interest, several systems-wide conclusions can be drawn by looking at the data as a whole rather than focusing on individual genes [185]. In addition, we were aware of the fact that the activation of the Tfam promoter does not automatically imply the discovery of a mitochondrial regulator. Hence, we chose a further assay to get an idea of the effects of these mitochondrial candidate genes. Considering the large number of cDNAs, we used fluorescent probes with a reported mitochondrial selectivity, to evaluate the density (Mitotracker® Green) and the oxidative capacity (Mitotracker® CM-H_2X-ROS). We were aware that the use of these probes is not a method certified and widely accepted, but allowed us to narrow down the number of the positive candidates to 131. To complete the screenings, we got some insights about the 131 positive candidates identified, using bioinformatics tools. We classified the genes for their molecular function and biological process, for their expression level in murine skeletal muscle and C2C12 and assessing they were not yet related with mitochondria. In this project we decided to study a limited number of candidate genes, but sufficient to guarantee to find out a new mitochondrial regulator in a reasonable time. Our choice was to further characterize 22 genes in C2C12 cell lines; 3 involved in the catalytic activity, 4 in signal transduction, 11 in transcription processes, 4 structural

proteins and 1 whose function is not yet annotated. The most abundant class is composed of proteins involved in transcriptional processes, as transcription factors have e regulatory function by definition. Additionally, we chose a gene with a not annotated function, as its identification could be a major finding, too. The use of HEK293 for high throughput screening is very common, in fact these cell are easy to manage and to transfect and in addition, their physiology and metabolism are very well characterized. Nevertheless, the use of skeletal muscle cells is one of the most common used for the study of other mitochondrial regulators, as shown in literature. Skeletal muscle is one of the tissues most highly dependent on mitochondrial function, as shown by the severe impacts of mitochondrial diseases on muscle performance in patients [180]. In addition, mitochondrial dysregulation was demonstrated in muscle of patients suffering from type II diabetes [134]. For this reason we decided to validate the 22 candidates in C2C12, a murine skeletal muscle cell line. In principle we expect that a regulator should affect the mitochondrial biogenesis and/or activity, especially the oxidative activity. In fact, PGC-1α (our positive control) acts on both aspects. One of the most reliable methods for assessing the biogenesis is the measurement of mtDNA. It is a direct measurement, based on the extraction of the DNA, so it has more advantages than the use of the fluorescent probes utilized in the previous screening. Surely, mtDNA measurement is a quite long and complicated procedure, not suitable for high numbers of samples. Regarding the oxidative activity, the biochemical method of excellence is the measure of the respiration. We evaluated the oxygen consumption with a Clark electrode, which is a very complicated and long analysis. We analyzed the respiration of the whole cells. We did not extract mitochondria, as it is a very invasive method that can affect the analysis. Using this approach for hundreds of samples is a very time consuming and

biases-rich methodology. As reported in our results, not always an increased mitochondrial biogenesis reflects an induced mitochondrial activity. This means that an increased mitochondrial biogenesis is necessary but not sufficient to ensure an increased mitochondrial function. We measured the mtDNA content as hallmark of mitochondrial biogenesis, but it could be possible that an increased number of copies of mtDNA do not correlate with an increased in the number of mitochondria; the mtDNA is just more replicated. On the other hand, the increased copies of mtDNA correlate with an increased mitochondrial biogenesis, but the mtDNA is just neither transcribed nor translated. As the mitochondrial genes transcription is under the strictly control of the nucleus [181], a possible explanation may be due to the nucleus that blocks the mtDNA transcription because the cell at that moment does not require an increased mitochondrial function or some other unknown mechanisms controlling the nucleus-mitochondrial crosstalk intervenes. We must not forget that the mtDNA encodes only 13 proteins that are not enough to exploit all the mitochondrial activities; so the transcription and translation of the mitochondrial genome must be coordinated to the expression of nuclear-encoded mitochondrial proteins. For these reasons, we considered as positive mitochondrial regulators only those candidates whose overexpression stimulated both the mitochondrial biogenesis and function as performed by our positive control PGC-1α. Applying these assays, we identified four genes (nr. 9, 10, 13 and 19) that if overexpressed in C2C12 showed a mitochondrial function better than or equal to our positive control PGC-1α.

We decided to prioritize the characterization of the candidate nr. 9, zinc finger CCCH type containing 10 (Zc3h10), because it was a protein with a not yet annotated function. Zc3h10 is very well conserved in all the Eutheria organisms (source http://string90.embl.de) but in literature, were reported only modest amount of articles

that mention this protein. One suggests a possible tumor suppressor function of Zc3h10 as it inhibits anchorage independent growth in soft agar [186], but it is a HTS that do not provide any information about the mechanism. In one other article, a yeast two-hybrid system screening shows that Zc3h10 binds the ataxin-1 (ATXN-1)[187]. The normal function of ATXN-1 is not yet known, but the mutated form of the protein is associated to the Spinocerebellar ataxia type 1, a neurodegenerative disorder [188]. Hence, the major finding of this project was to assess a mitochondrial function to Zc3h10. As shown in our detailed biochemical characterization, Zc3h10 overexpression increased the expression profile of OXPHOS proteins, increased the content and/or electron transport activity of mitochondria (measured by uncoupling and maximal respiration) and increased the mitochondrial ATP production. In addition, the Zc3h10 overexpression was not associated with toxic effects related to the activity of mitochondrial ROS production and induction of apoptosis. It is worth noting that, although ubiquitously expressed, Zc3h10 mRNA levels were high in metabolically active tissues like liver, soleus and brown adipose tissue. These tissues are rich in mitochondria as one of their functions is fuel oxidation, thus this data confirm the mitochondrial function of Zc3h10.

According to our bioinformatics classification, Zc3h10 is a nucleic acid binding protein; even if we do not know if it binds DNA or RNA. This classification is confirmed by some other members of Zc3 protein family; for example Zc3h12a is an essential RNase that prevents immune disorders by directly controlling the stability of a set of inflammatory genes [189]. As a consequence, we could hypothesize that Zc3h10 could act as a transcription factor (like NRF-1/2) or as a factor that regulates in some way the expression of mitochondrial genes (like PGC-1α), but ad hoc experiments should be performed to answer this question. In these regards, we

discovered that Zc3h10 explicates its mitochondrial function activating the promoter of Tfam, as shown in two different cell lines (HEK293 and C2C12) as our positive control PGC-1α. The portion of Tfam used for the analysis contained the binding sites for SP1, NRF-1 and NRF-2. From literature we know that PGC-1α transactivates Tfam by coactivating NRF-1 [63]. Regarding Zc3h10 we found that, mutation of the NRF-1 binding site slightly reduced but did not abolished the Tfam activation by our best candidate, suggesting that the rest of the promoter, including the NRF-2 and SP-1 binding sites, could mediate the effect of Zc3h10. This mode of action is different from that one of PGC-1α, but further experiments should be performed to understand the mechanism of action of Zc3h10.

Complex transcriptional circuitries have been demonstrated to regulate mitochondrial DNA replication and transcription. For example, most of the mitochondrial- or nuclear-encoded OXPHOS subunits have a binding site for NRF-1 or NRF-2 on their promoter; SIRT-1 is a histone deacetylase that affects PGC-1α expression [190]. With this in mind we analyzed the sequence of Zc3h10 promoter *in silico* and we found that it could have a NRF-2 binding site that is highly conserved between organisms. Screening different master mitochondrial regulators for their ability to activate the Zc3h10 promoter activity, we found that NRF-2, PGC-1α and SIRT-1 positively regulates its transcription, while surprisingly NRF-1 seems to have an inhibitory effect. In addition, Zc3h10 seems to have a kind of auto activation, but further experiment should be performed to characterize and explain all these effects and to describe how Zc3h10 is regulated.

As well established in literature, a mitochondrial dysfunction is associated to many diseases; one of the most studied is the T2D. In literature, it is known that the skeletal muscle mitochondria of T2D patients show a reduction in their activity

that reflects a decrease expression profile of many mitochondrial genes [51, 157]. For example, the expression profile of PGC-1α is decreased by nearly 50% in muscle from individual with diabetes [157]. Preliminary results performed in our laboratory, showed that the expression profile of Zc3h10, as well as other mitochondrial-related factors like PGC-1α, Tfam and mtCOXII, is reduced in skeletal muscle of mice with high fat diet-induced diabetes (data not shown). Even if we don't know the molecular mechanisms causing this effect and this result should be supported by other experiments, we can conclude that the expression profile of Zc3h10 follows the same trend of reduction observed in other mitochondrial factors in the skeletal muscle of a mitochondrial dysfunction animal model. This once again sustains the evidence that Zc3h10 has a mitochondrial function.

7. Highlights:

- Integrating different approaches like the high throughput screening, staining assays, bioinformatics tools and functional/biochemical approaches, we were able starting from 27000 cDNAs to identify one gene that is a mitochondrial regulators.
- We assessed the mitochondrial function of Zc3h10. In fact, we demonstrated that its overexpression affected the Tfam promoter activity, increased the mtDNA content (a hallmark of mitochondrial biogenesis) and induced the oxygen consumption rate, the expression of the OXPHOS proteins and the mitochondrial ATP levels (a hallmark of mitochondrial function), without affecting the ROS production or apoptosis.
- We discovered one of the functions of Zc3h10, whose activity was previously completely unknown. Further experiments should be performed in order to understand its mechanism of action, but we were able to frame it in a particular biological context, the mitochondrial regulation.

8. References:

1. Romano, A.H. and T. Conway, *Evolution of carbohydrate metabolic pathways.* Res Microbiol, 1996. **147**(6-7): p. 448-55.
2. Mootha, V.K., et al., *Integrated analysis of protein composition, tissue diversity, and gene regulation in mouse mitochondria.* Cell, 2003. **115**(5): p. 629-40.
3. Pagliarini, D.J., et al., *A mitochondrial protein compendium elucidates complex I disease biology.* Cell, 2008. **134**(1): p. 112-23.
4. Scarpulla, R., *Transcriptional Paradigms in Mammalian Mitochondrial Biogenesis and Function.* Physiol Rev, 2008. **88**: p. 611-638.
5. Balaban, R.S., *Regulation of oxidative phosphorylation in the mammalian cell.* Am J Physiol, 1990. **258**(3 Pt 1): p. C377-89.
6. Hatefi, Y., *The mitochondrial electron transport and oxidative phosphorylation system.* Annu Rev Biochem, 1985. **54**: p. 1015-69.
7. Starkov, A.A., *The role of mitochondria in reactive oxygen species metabolism and signaling.* Ann N Y Acad Sci, 2008. **1147**: p. 37-52.
8. Murphy, M.P., *How mitochondria produce reactive oxygen species.* Biochem J, 2009. **417**(1): p. 1-13.
9. Murgia, M., et al., *Controlling metabolism and cell death: at the heart of mitochondrial calcium signalling.* J Mol Cell Cardiol, 2009. **46**(6): p. 781-8.
10. Rimessi, A., et al., *The versatility of mitochondrial calcium signals: from stimulation of cell metabolism to induction of cell death.* Biochim Biophys Acta, 2008. **1777**(7-8): p. 808-16.
11. Lill, R. and U. Muhlenhoff, *Maturation of iron-sulfur proteins in eukaryotes: mechanisms, connected processes, and diseases.* Annu Rev Biochem, 2008. **77**: p. 669-700.
12. Miller, W.L., *Steroidogenic enzymes.* Endocr Dev, 2008. **13**: p. 1-18.
13. Miller, W.L., *Minireview: regulation of steroidogenesis by electron transfer.* Endocrinology, 2005. **146**(6): p. 2544-50.
14. Miller, W.L., *Steroidogenic acute regulatory protein (StAR), a novel mitochondrial cholesterol transporter.* Biochim Biophys Acta, 2007. **1771**(6): p. 663-76.
15. Gonzalez, I.L., *Barth syndrome: TAZ gene mutations, mRNAs, and evolution.* Am J Med Genet A, 2005. **134**(4): p. 409-14.
16. Muravchick, S., *Clinical implications of mitochondrial disease.* Adv Drug Deliv Rev, 2008. **60**(13-14): p. 1553-60.
17. Gargus, J.J., *Genetic calcium signaling abnormalities in the central nervous system: seizures, migraine, and autism.* Ann N Y Acad Sci, 2009. **1151**: p. 133-56.
18. Gandhi, S., et al., *PINK1-associated Parkinson's disease is caused by neuronal vulnerability to calcium-induced cell death.* Mol Cell, 2009. **33**(5): p. 627-38.
19. Wallace, D.C., *Why do we still have a maternally inherited mitochondrial DNA? Insights from evolutionary medicine.* Annu Rev Biochem, 2007. **76**: p. 781-821.
20. Wallace, D.C. and W. Fan, *Energetics, epigenetics, mitochondrial genetics.* Mitochondrion, 2010. **10**(1): p. 12-31.
21. Benard, G. and R. Rossignol, *Ultrastructure of the mitochondrion and its bearing on function and bioenergetics.* Antioxid Redox Signal, 2008. **10**(8): p. 1313-42.

22. Stuart, R.A., *Supercomplex organization of the oxidative phosphorylation enzymes in yeast mitochondria.* J Bioenerg Biomembr, 2008. **40**(5): p. 411-7.
23. Vonck, J. and E. Schafer, *Supramolecular organization of protein complexes in the mitochondrial inner membrane.* Biochim Biophys Acta, 2009. **1793**(1): p. 117-24.
24. Chan, D.C., *Fusion and fission: interlinked processes critical for mitochondrial health.* Annu Rev Genet, 2012. **46**: p. 265-87.
25. Chen, H., et al., *Mitofusins Mfn1 and Mfn2 coordinately regulate mitochondrial fusion and are essential for embryonic development.* J Cell Biol, 2003. **160**(2): p. 189-200.
26. Chen, H., A. Chomyn, and D.C. Chan, *Disruption of fusion results in mitochondrial heterogeneity and dysfunction.* J Biol Chem, 2005. **280**(28): p. 26185-92.
27. Cipolat, S., et al., *OPA1 requires mitofusin 1 to promote mitochondrial fusion.* Proc Natl Acad Sci U S A, 2004. **101**(45): p. 15927-32.
28. Gandre-Babbe, S. and A.M. van der Bliek, *The novel tail-anchored membrane protein Mff controls mitochondrial and peroxisomal fission in mammalian cells.* Mol Biol Cell, 2008. **19**(6): p. 2402-12.
29. James, D.I., et al., *hFis1, a novel component of the mammalian mitochondrial fission machinery.* J Biol Chem, 2003. **278**(38): p. 36373-9.
30. Yoon, Y., et al., *The mitochondrial protein hFis1 regulates mitochondrial fission in mammalian cells through an interaction with the dynamin-like protein DLP1.* Mol Cell Biol, 2003. **23**(15): p. 5409-20.
31. Smirnova, E., et al., *Dynamin-related protein Drp1 is required for mitochondrial division in mammalian cells.* Mol Biol Cell, 2001. **12**(8): p. 2245-56.
32. Hoppins, S., L. Lackner, and J. Nunnari, *The machines that divide and fuse mitochondria.* Annu Rev Biochem, 2007. **76**: p. 751-80.
33. Elgass, K., et al., *Recent advances into the understanding of mitochondrial fission.* Biochim Biophys Acta, 2013. **1833**(1): p. 150-61.
34. Friedman, J.R., et al., *ER tubules mark sites of mitochondrial division.* Science, 2011. **334**(6054): p. 358-62.
35. Youle, R.J. and A.M. van der Bliek, *Mitochondrial fission, fusion, and stress.* Science, 2012. **337**(6098): p. 1062-5.
36. Rossignol, R., et al., *Energy substrate modulates mitochondrial structure and oxidative capacity in cancer cells.* Cancer Res, 2004. **64**(3): p. 985-93.
37. Tondera, D., et al., *SLP-2 is required for stress-induced mitochondrial hyperfusion.* EMBO J, 2009. **28**(11): p. 1589-600.
38. Rambold, A.S., et al., *Tubular network formation protects mitochondria from autophagosomal degradation during nutrient starvation.* Proc Natl Acad Sci U S A, 2011. **108**(25): p. 10190-5.
39. Gomes, L.C., G. Di Benedetto, and L. Scorrano, *During autophagy mitochondria elongate, are spared from degradation and sustain cell viability.* Nat Cell Biol, 2011. **13**(5): p. 589-98.
40. Ojala, D., J. Montoya, and G. Attardi, *tRNA punctuation model of RNA processing in human mitochondria.* Nature, 1981. **290**(5806): p. 470-4.
41. Clayton, D.A., *Vertebrate mitochondrial DNA-a circle of surprises.* Exp Cell Res, 2000. **255**(1): p. 4-9.

42. Satoh, M. and T. Kuroiwa, *Organization of multiple nucleoids and DNA molecules in mitochondria of a human cell.* Exp Cell Res, 1991. **196**(1): p. 137-40.
43. Bogenhagen, D.F. and D.A. Clayton, *The mitochondrial DNA replication bubble has not burst.* Trends Biochem Sci, 2003. **28**(7): p. 357-60.
44. Clayton, D.A., *Mitochondrial DNA replication: what we know.* IUBMB Life, 2003. **55**(4-5): p. 213-7.
45. Shoubridge, E.A., *Mitochondrial DNA segregation in the developing embryo.* Hum Reprod, 2000. **15 Suppl 2**: p. 229-34.
46. Kaneda, H., et al., *Elimination of paternal mitochondrial DNA in intraspecific crosses during early mouse embryogenesis.* Proc Natl Acad Sci U S A, 1995. **92**(10): p. 4542-6.
47. Schwartz, M. and J. Vissing, *Paternal inheritance of mitochondrial DNA.* N Engl J Med, 2002. **347**(8): p. 576-80.
48. Kraytsberg, Y., et al., *Recombination of human mitochondrial DNA.* Science, 2004. **304**(5673): p. 981.
49. Ashley, M.V., P.J. Laipis, and W.W. Hauswirth, *Rapid segregation of heteroplasmic bovine mitochondria.* Nucleic Acids Res, 1989. **17**(18): p. 7325-31.
50. Scarpulla, R.C., *Transcriptional paradigms in mammalian mitochondrial biogenesis and function.* Physiol Rev, 2008. **88**(2): p. 611-38.
51. Patti, M.E. and S. Corvera, *The role of mitochondria in the pathogenesis of type 2 diabetes.* Endocr Rev, 2010. **31**(3): p. 364-95.
52. Evans, A.R., M. Limp-Foster, and M.R. Kelley, *Going APE over ref-1.* Mutat Res, 2000. **461**(2): p. 83-108.
53. Kelley, M.R. and S.H. Parsons, *Redox regulation of the DNA repair function of the human AP endonuclease Ape1/ref-1.* Antioxid Redox Signal, 2001. **3**(4): p. 671-83.
54. Hansen, J.M., Y.M. Go, and D.P. Jones, *Nuclear and mitochondrial compartmentation of oxidative stress and redox signaling.* Annu Rev Pharmacol Toxicol, 2006. **46**: p. 215-34.
55. Bao, Q. and Y. Shi, *Apoptosome: a platform for the activation of initiator caspases.* Cell Death Differ, 2007. **14**(1): p. 56-65.
56. Suen, D.F., K.L. Norris, and R.J. Youle, *Mitochondrial dynamics and apoptosis.* Genes Dev, 2008. **22**(12): p. 1577-90.
57. Sugioka, R., S. Shimizu, and Y. Tsujimoto, *Fzo1, a protein involved in mitochondrial fusion, inhibits apoptosis.* J Biol Chem, 2004. **279**(50): p. 52726-34.
58. Zamzami, N., et al., *Reduction in mitochondrial potential constitutes an early irreversible step of programmed lymphocyte death in vivo.* J Exp Med, 1995. **181**(5): p. 1661-72.
59. Marcu, R., et al., *Multi-parameter measurement of the permeability transition pore opening in isolated mouse heart mitochondria.* J Vis Exp, 2012(67).
60. Wallace, D.C., *A mitochondrial paradigm of metabolic and degenerative diseases, aging, and cancer: a dawn for evolutionary medicine.* Annu Rev Genet, 2005. **39**: p. 359-407.
61. Virbasius, J.V. and R.C. Scarpulla, *Activation of the human mitochondrial transcription factor A gene by nuclear respiratory factors: a potential regulatory link between nuclear and mitochondrial gene expression in organelle biogenesis.* Proc Natl Acad Sci U S A, 1994. **91**(4): p. 1309-13.

62. Scarpulla, R.C., *Nuclear control of respiratory chain expression in mammalian cells.* J Bioenerg Biomembr, 1997. **29**(2): p. 109-19.
63. Wu, Z., et al., *Mechanisms Controlling Mitochondrial Biogenesis and Respiration through the Thermogenic Coactivator PGC-1.* Cell, 1999. **98**(1): p. 115-124.
64. Lin, J., et al., *Peroxisome proliferator-activated receptor gamma coactivator 1beta (PGC-1beta), a novel PGC-1-related transcription coactivator associated with host cell factor.* J Biol Chem, 2002. **277**(3): p. 1645-8.
65. Andersson, U. and R.C. Scarpulla, *Pgc-1-related coactivator, a novel, serum-inducible coactivator of nuclear respiratory factor 1-dependent transcription in mammalian cells.* Mol Cell Biol, 2001. **21**(11): p. 3738-49.
66. Sonoda, J., et al., *PGC-1beta controls mitochondrial metabolism to modulate circadian activity, adaptive thermogenesis, and hepatic steatosis.* Proc Natl Acad Sci U S A, 2007. **104**(12): p. 5223-8.
67. Vianna, C.R., et al., *Hypomorphic mutation of PGC-1beta causes mitochondrial dysfunction and liver insulin resistance.* Cell Metab, 2006. **4**(6): p. 453-64.
68. Lin, J., et al., *Defects in adaptive energy metabolism with CNS-linked hyperactivity in PGC-1alpha null mice.* Cell, 2004. **119**(1): p. 121-35.
69. Handschin, C., et al., *Abnormal glucose homeostasis in skeletal muscle-specific PGC-1alpha knockout mice reveals skeletal muscle-pancreatic beta cell crosstalk.* J Clin Invest, 2007. **117**(11): p. 3463-74.
70. Handschin, C., et al., *Skeletal muscle fiber-type switching, exercise intolerance, and myopathy in PGC-1alpha muscle-specific knock-out animals.* J Biol Chem, 2007. **282**(41): p. 30014-21.
71. Arany, Z., et al., *Transcriptional coactivator PGC-1 alpha controls the energy state and contractile function of cardiac muscle.* Cell Metab, 2005. **1**(4): p. 259-71.
72. Leone, T.C., et al., *PGC-1alpha deficiency causes multi-system energy metabolic derangements: muscle dysfunction, abnormal weight control and hepatic steatosis.* PLoS Biol, 2005. **3**(4): p. e101.
73. Lehman, J.J., et al., *The transcriptional coactivator PGC-1alpha is essential for maximal and efficient cardiac mitochondrial fatty acid oxidation and lipid homeostasis.* Am J Physiol Heart Circ Physiol, 2008. **295**(1): p. H185-96.
74. Lai, L., et al., *Transcriptional coactivators PGC-1alpha and PGC-lbeta control overlapping programs required for perinatal maturation of the heart.* Genes Dev, 2008. **22**(14): p. 1948-61.
75. Lelliott, C.J., et al., *Ablation of PGC-1beta results in defective mitochondrial activity, thermogenesis, hepatic function, and cardiac performance.* PLoS Biol, 2006. **4**(11): p. e369.
76. Leick, L., et al., *PGC-1alpha is not mandatory for exercise- and training-induced adaptive gene responses in mouse skeletal muscle.* Am J Physiol Endocrinol Metab, 2008. **294**(2): p. E463-74.
77. Vercauteren, K., N. Gleyzer, and R.C. Scarpulla, *Short hairpin RNA-mediated silencing of PRC (PGC-1-related coactivator) results in a severe respiratory chain deficiency associated with the proliferation of aberrant mitochondria.* J Biol Chem, 2009. **284**(4): p. 2307-19.
78. Parker, M.G., M. Christian, and R. White, *The nuclear receptor co-repressor RIP140 controls the expression of metabolic gene networks.* Biochem Soc Trans, 2006. **34**(Pt 6): p. 1103-6.

79. Leonardsson, G., et al., *Nuclear receptor corepressor RIP140 regulates fat accumulation.* Proc Natl Acad Sci U S A, 2004. **101**(22): p. 8437-42.
80. Debevec, D., et al., *Receptor interacting protein 140 regulates expression of uncoupling protein 1 in adipocytes through specific peroxisome proliferator activated receptor isoforms and estrogen-related receptor alpha.* Mol Endocrinol, 2007. **21**(7): p. 1581-92.
81. Christian, M., R. White, and M.G. Parker, *Metabolic regulation by the nuclear receptor corepressor RIP140.* Trends Endocrinol Metab, 2006. **17**(6): p. 243-50.
82. Powelka, A.M., et al., *Suppression of oxidative metabolism and mitochondrial biogenesis by the transcriptional corepressor RIP140 in mouse adipocytes.* J Clin Invest, 2006. **116**(1): p. 125-36.
83. Seth, A., et al., *The transcriptional corepressor RIP140 regulates oxidative metabolism in skeletal muscle.* Cell Metab, 2007. **6**(3): p. 236-45.
84. Fisher, R.P. and D.A. Clayton, *Purification and characterization of human mitochondrial transcription factor 1.* Mol Cell Biol, 1988. **8**(8): p. 3496-509.
85. Fisher, R.P., et al., *DNA wrapping and bending by a mitochondrial high mobility group-like transcriptional activator protein.* J Biol Chem, 1992. **267**(5): p. 3358-67.
86. Parisi, M.A. and D.A. Clayton, *Similarity of human mitochondrial transcription factor 1 to high mobility group proteins.* Science, 1991. **252**(5008): p. 965-9.
87. Antoshechkin, I., D.F. Bogenhagen, and I.A. Mastrangelo, *The HMG-box mitochondrial transcription factor xl-mtTFA binds DNA as a tetramer to activate bidirectional transcription.* EMBO J, 1997. **16**(11): p. 3198-206.
88. Fisher, R.P., M.A. Parisi, and D.A. Clayton, *Flexible recognition of rapidly evolving promoter sequences by mitochondrial transcription factor 1.* Genes Dev, 1989. **3**(12B): p. 2202-17.
89. Dairaghi, D.J., G.S. Shadel, and D.A. Clayton, *Addition of a 29 residue carboxyl-terminal tail converts a simple HMG box-containing protein into a transcriptional activator.* J Mol Biol, 1995. **249**(1): p. 11-28.
90. Larsson, N.G., et al., *Mitochondrial transcription factor A is necessary for mtDNA maintenance and embryogenesis in mice.* Nat Genet, 1998. **18**(3): p. 231-6.
91. Poulton, J., et al., *Deficiency of the human mitochondrial transcription factor h-mtTFA in infantile mitochondrial myopathy is associated with mtDNA depletion.* Hum Mol Genet, 1994. **3**(10): p. 1763-9.
92. Ekstrand, M.I., et al., *Mitochondrial transcription factor A regulates mtDNA copy number in mammals.* Hum Mol Genet, 2004. **13**(9): p. 935-44.
93. Campbell, C.T., J.E. Kolesar, and B.A. Kaufman, *Mitochondrial transcription factor A regulates mitochondrial transcription initiation, DNA packaging, and genome copy number.* Biochim Biophys Acta, 2012. **1819**(9-10): p. 921-9.
94. Antoshechkin, I. and D.F. Bogenhagen, *Distinct roles for two purified factors in transcription of Xenopus mitochondrial DNA.* Mol Cell Biol, 1995. **15**(12): p. 7032-42.
95. Bogenhagen, D.F., et al., *Protein components of mitochondrial DNA nucleoids in higher eukaryotes.* Mol Cell Proteomics, 2003. **2**(11): p. 1205-16.
96. Kukat, C., et al., *Super-resolution microscopy reveals that mammalian mitochondrial nucleoids have a uniform size and frequently contain a single copy of mtDNA.* Proc Natl Acad Sci U S A, 2011. **108**(33): p. 13534-9.

97. Kanki, T., et al., *Architectural role of mitochondrial transcription factor A in maintenance of human mitochondrial DNA.* Mol Cell Biol, 2004. **24**(22): p. 9823-34.
98. Shutt, T.E., M. Bestwick, and G.S. Shadel, *The core human mitochondrial transcription initiation complex: It only takes two to tango.* Transcription, 2011. **2**(2): p. 55-59.
99. Kang, D., S.H. Kim, and N. Hamasaki, *Mitochondrial transcription factor A (TFAM): roles in maintenance of mtDNA and cellular functions.* Mitochondrion, 2007. **7**(1-2): p. 39-44.
100. Kang, D. and N. Hamasaki, *Mitochondrial transcription factor A in the maintenance of mitochondrial DNA: overview of its multiple roles.* Ann N Y Acad Sci, 2005. **1042**: p. 101-8.
101. Uchiumi, T. and D. Kang, *The role of TFAM-associated proteins in mitochondrial RNA metabolism.* Biochim Biophys Acta, 2012. **1820**(5): p. 565-70.
102. Rebelo, A.P., L.M. Dillon, and C.T. Moraes, *Mitochondrial DNA transcription regulation and nucleoid organization.* J Inherit Metab Dis, 2011. **34**(4): p. 941-51.
103. Legros, F., et al., *Organization and dynamics of human mitochondrial DNA.* J Cell Sci, 2004. **117**(Pt 13): p. 2653-62.
104. Wai, T., D. Teoli, and E.A. Shoubridge, *The mitochondrial DNA genetic bottleneck results from replication of a subpopulation of genomes.* Nat Genet, 2008. **40**(12): p. 1484-8.
105. Wang, Y. and D.F. Bogenhagen, *Human mitochondrial DNA nucleoids are linked to protein folding machinery and metabolic enzymes at the mitochondrial inner membrane.* J Biol Chem, 2006. **281**(35): p. 25791-802.
106. Ngo, H.B., J.T. Kaiser, and D.C. Chan, *The mitochondrial transcription and packaging factor Tfam imposes a U-turn on mitochondrial DNA.* Nat Struct Mol Biol, 2011. **18**(11): p. 1290-6.
107. Rubio-Cosials, A., et al., *Human mitochondrial transcription factor A induces a U-turn structure in the light strand promoter.* Nat Struct Mol Biol, 2011. **18**(11): p. 1281-9.
108. Pohjoismaki, J.L., et al., *Alterations to the expression level of mitochondrial transcription factor A, TFAM, modify the mode of mitochondrial DNA replication in cultured human cells.* Nucleic Acids Res, 2006. **34**(20): p. 5815-28.
109. Matsushima, Y., Y. Goto, and L.S. Kaguni, *Mitochondrial Lon protease regulates mitochondrial DNA copy number and transcription by selective degradation of mitochondrial transcription factor A (TFAM).* Proc Natl Acad Sci U S A, 2010. **107**(43): p. 18410-5.
110. Kelly, D.P. and R.C. Scarpulla, *Transcriptional regulatory circuits controlling mitochondrial biogenesis and function.* Genes Dev, 2004. **18**(4): p. 357-68.
111. Scarpulla, R.C., *Nuclear activators and coactivators in mammalian mitochondrial biogenesis.* Biochim Biophys Acta, 2002. **1576**(1-2): p. 1-14.
112. Scarpulla, R.C., *Transcriptional activators and coactivators in the nuclear control of mitochondrial function in mammalian cells.* Gene, 2002. **286**(1): p. 81-9.
113. Braidotti, G., I.A. Borthwick, and B.K. May, *Identification of regulatory sequences in the gene for 5-aminolevulinate synthase from rat.* J Biol Chem, 1993. **268**(2): p. 1109-17.

114. Aizencang, G.I., et al., *Uroporphyrinogen III synthase. An alternative promoter controls erythroid-specific expression in the murine gene.* J Biol Chem, 2000. **275**(4): p. 2295-304.
115. Puigserver, P., et al., *A cold-inducible coactivator of nuclear receptors linked to adaptive thermogenesis.* Cell, 1998. **92**(6): p. 829-39.
116. Puigserver, P., *Tissue-specific regulation of metabolic pathways through the transcriptional coactivator PGC1-alpha.* Int J Obes (Lond), 2005. **29 Suppl 1**: p. S5-9.
117. Lin, J., C. Handschin, and B.M. Spiegelman, *Metabolic control through the PGC-1 family of transcription coactivators.* Cell Metab, 2005. **1**(6): p. 361-70.
118. Gleyzer, N., K. Vercauteren, and R.C. Scarpulla, *Control of mitochondrial transcription specificity factors (TFB1M and TFB2M) by nuclear respiratory factors (NRF-1 and NRF-2) and PGC-1 family coactivators.* Mol Cell Biol, 2005. **25**(4): p. 1354-66.
119. Schreiber, S.N., et al., *The estrogen-related receptor alpha (ERRalpha) functions in PPARgamma coactivator 1alpha (PGC-1alpha)-induced mitochondrial biogenesis.* Proc Natl Acad Sci U S A, 2004. **101**(17): p. 6472-7.
120. Mootha, V.K., et al., *Erralpha and Gabpa/b specify PGC-1alpha-dependent oxidative phosphorylation gene expression that is altered in diabetic muscle.* Proc Natl Acad Sci U S A, 2004. **101**(17): p. 6570-5.
121. Herzig, S., et al., *CREB regulates hepatic gluconeogenesis through the coactivator PGC-1.* Nature, 2001. **413**(6852): p. 179-83.
122. Nisoli, E., et al., *Mitochondrial biogenesis in mammals: the role of endogenous nitric oxide.* Science, 2003. **299**(5608): p. 896-9.
123. Nisoli, E., et al., *Mitochondrial biogenesis by NO yields functionally active mitochondria in mammals.* Proc Natl Acad Sci U S A, 2004. **101**(47): p. 16507-12.
124. Terada, S., et al., *Effects of low-intensity prolonged exercise on PGC-1 mRNA expression in rat epitrochlearis muscle.* Biochem Biophys Res Commun, 2002. **296**(2): p. 350-4.
125. Terada, S., et al., *Effects of high-intensity intermittent swimming on PGC-1alpha protein expression in rat skeletal muscle.* Acta Physiol Scand, 2005. **184**(1): p. 59-65.
126. Terada, S. and I. Tabata, *Effects of acute bouts of running and swimming exercise on PGC-1alpha protein expression in rat epitrochlearis and soleus muscle.* Am J Physiol Endocrinol Metab, 2004. **286**(2): p. E208-16.
127. Baar, K., et al., *Adaptations of skeletal muscle to exercise: rapid increase in the transcriptional coactivator PGC-1.* FASEB J, 2002. **16**(14): p. 1879-86.
128. Akimoto, T., et al., *Exercise stimulates Pgc-1alpha transcription in skeletal muscle through activation of the p38 MAPK pathway.* J Biol Chem, 2005. **280**(20): p. 19587-93.
129. Dimauro, S. and G. Davidzon, *Mitochondrial DNA and disease.* Ann Med, 2005. **37**(3): p. 222-32.
130. Wallace, D.C., *Diseases of the mitochondrial DNA.* Annu Rev Biochem, 1992. **61**: p. 1175-212.
131. Shoubridge, E.A., *Nuclear genetic defects of oxidative phosphorylation.* Hum Mol Genet, 2001. **10**(20): p. 2277-84.
132. Suomalainen, A. and J. Kaukonen, *Diseases caused by nuclear genes affecting mtDNA stability.* Am J Med Genet, 2001. **106**(1): p. 53-61.

133. Schon, E.A. and G. Manfredi, *Neuronal degeneration and mitochondrial dysfunction.* J Clin Invest, 2003. **111**(3): p. 303-12.
134. Lowell, B.B. and G.I. Shulman, *Mitochondrial dysfunction and type 2 diabetes.* Science, 2005. **307**(5708): p. 384-7.
135. Dufour, E. and N.G. Larsson, *Understanding aging: revealing order out of chaos.* Biochim Biophys Acta, 2004. **1658**(1-2): p. 122-32.
136. Andersen, J.K., *Oxidative stress in neurodegeneration: cause or consequence?* Nat Med, 2004. **10 Suppl**: p. S18-25.
137. Spillantini, M.G., et al., *Alpha-synuclein in Lewy bodies.* Nature, 1997. **388**(6645): p. 839-40.
138. Davis, G.C., et al., *Chronic Parkinsonism secondary to intravenous injection of meperidine analogues.* Psychiatry Res, 1979. **1**(3): p. 249-54.
139. Langston, J.W., et al., *Evidence of active nerve cell degeneration in the substantia nigra of humans years after 1-methyl-4-phenyl-1,2,3,6-tetrahydropyridine exposure.* Ann Neurol, 1999. **46**(4): p. 598-605.
140. Winklhofer, K.F. and C. Haass, *Mitochondrial dysfunction in Parkinson's disease.* Biochim Biophys Acta, 2010. **1802**(1): p. 29-44.
141. Parihar, M.S., et al., *Alpha-synuclein overexpression and aggregation exacerbates impairment of mitochondrial functions by augmenting oxidative stress in human neuroblastoma cells.* Int J Biochem Cell Biol, 2009. **41**(10): p. 2015-24.
142. Tabrizi, S.J., et al., *Expression of mutant alpha-synuclein causes increased susceptibility to dopamine toxicity.* Hum Mol Genet, 2000. **9**(18): p. 2683-9.
143. Song, D.D., et al., *Enhanced substantia nigra mitochondrial pathology in human alpha-synuclein transgenic mice after treatment with MPTP.* Exp Neurol, 2004. **186**(2): p. 158-72.
144. Hsu, L.J., et al., *alpha-synuclein promotes mitochondrial deficit and oxidative stress.* Am J Pathol, 2000. **157**(2): p. 401-10.
145. Stichel, C.C., et al., *Mono- and double-mutant mouse models of Parkinson's disease display severe mitochondrial damage.* Hum Mol Genet, 2007. **16**(20): p. 2377-93.
146. Ellis, C.E., et al., *Mitochondrial lipid abnormality and electron transport chain impairment in mice lacking alpha-synuclein.* Mol Cell Biol, 2005. **25**(22): p. 10190-201.
147. Mortiboys, H., et al., *Mitochondrial function and morphology are impaired in parkin-mutant fibroblasts.* Ann Neurol, 2008. **64**(5): p. 555-65.
148. Rothfuss, O., et al., *Parkin protects mitochondrial genome integrity and supports mitochondrial DNA repair.* Hum Mol Genet, 2009. **18**(20): p. 3832-50.
149. Wood-Kaczmar, A., et al., *PINK1 is necessary for long term survival and mitochondrial function in human dopaminergic neurons.* PLoS One, 2008. **3**(6): p. e2455.
150. Gautier, C.A., T. Kitada, and J. Shen, *Loss of PINK1 causes mitochondrial functional defects and increased sensitivity to oxidative stress.* Proc Natl Acad Sci U S A, 2008. **105**(32): p. 11364-9.
151. Gegg, M.E., et al., *Silencing of PINK1 expression affects mitochondrial DNA and oxidative phosphorylation in dopaminergic cells.* PLoS One, 2009. **4**(3): p. e4756.
152. Chomyn, A. and G. Attardi, *MtDNA mutations in aging and apoptosis.* Biochem Biophys Res Commun, 2003. **304**(3): p. 519-29.

153. Kujoth, G.C., et al., *Mitochondrial DNA mutations, oxidative stress, and apoptosis in mammalian aging.* Science, 2005. **309**(5733): p. 481-4.
154. Schriner, S.E., et al., *Extension of murine life span by overexpression of catalase targeted to mitochondria.* Science, 2005. **308**(5730): p. 1909-11.
155. Patti, M.E., *Gene expression in humans with diabetes and prediabetes: what have we learned about diabetes pathophysiology?* Curr Opin Clin Nutr Metab Care, 2004. **7**(4): p. 383-90.
156. Petersen, K.F., et al., *Mitochondrial dysfunction in the elderly: possible role in insulin resistance.* Science, 2003. **300**(5622): p. 1140-2.
157. Patti, M.E., et al., *Coordinated reduction of genes of oxidative metabolism in humans with insulin resistance and diabetes: Potential role of PGC1 and NRF1.* Proc Natl Acad Sci U S A, 2003. **100**(14): p. 8466-71.
158. Mootha, V.K., et al., *PGC-1alpha-responsive genes involved in oxidative phosphorylation are coordinately downregulated in human diabetes.* Nat Genet, 2003. **34**(3): p. 267-73.
159. St-Pierre, J., et al., *Bioenergetic analysis of peroxisome proliferator-activated receptor gamma coactivators 1alpha and 1beta (PGC-1alpha and PGC-1beta) in muscle cells.* J Biol Chem, 2003. **278**(29): p. 26597-603.
160. Vondra, K., et al., *Enzyme activities in quadriceps femoris muscle of obese diabetic male patients.* Diabetologia, 1977. **13**(5): p. 527-9.
161. Kelley, D.E., et al., *Dysfunction of mitochondria in human skeletal muscle in type 2 diabetes.* Diabetes, 2002. **51**(10): p. 2944-50.
162. Maechler, P. and C.B. Wollheim, *Mitochondrial function in normal and diabetic beta-cells.* Nature, 2001. **414**(6865): p. 807-12.
163. Maassen, J.A., et al., *Mitochondrial diabetes: molecular mechanisms and clinical presentation.* Diabetes, 2004. **53 Suppl 1**: p. S103-9.
164. Goto, Y., I. Nonaka, and S. Horai, *A mutation in the tRNA(Leu)(UUR) gene associated with the MELAS subgroup of mitochondrial encephalomyopathies.* Nature, 1990. **348**(6302): p. 651-3.
165. Holt, I.J., et al., *A new mitochondrial disease associated with mitochondrial DNA heteroplasmy.* Am J Hum Genet, 1990. **46**(3): p. 428-33.
166. Holt, I.J., A.E. Harding, and J.A. Morgan-Hughes, *Deletions of muscle mitochondrial DNA in patients with mitochondrial myopathies.* Nature, 1988. **331**(6158): p. 717-9.
167. Shoffner, J.M., et al., *Myoclonic epilepsy and ragged-red fiber disease (MERRF) is associated with a mitochondrial DNA tRNA(Lys) mutation.* Cell, 1990. **61**(6): p. 931-7.
168. Wallace, D.C., et al., *Familial mitochondrial encephalomyopathy (MERRF): genetic, pathophysiological, and biochemical characterization of a mitochondrial DNA disease.* Cell, 1988. **55**(4): p. 601-10.
169. Wallace, D.C., et al., *Mitochondrial DNA mutation associated with Leber's hereditary optic neuropathy.* Science, 1988. **242**(4884): p. 1427-30.
170. Arany, Z., et al., *The transcriptional coactivator PGC-1beta drives the formation of oxidative type IIX fibers in skeletal muscle.* Cell Metab, 2007. **5**(1): p. 35-46.
171. Lin, J., et al., *Transcriptional co-activator PGC-1 alpha drives the formation of slow-twitch muscle fibres.* Nature, 2002. **418**(6899): p. 797-801.
172. Aza-Blanc, P., et al., *Identification of modulators of TRAIL-induced apoptosis via RNAi-based phenotypic screening.* Mol Cell, 2003. **12**(3): p. 627-37.

173. Chanda, S.K., et al., *Genome-scale functional profiling of the mammalian AP-1 signaling pathway.* Proc Natl Acad Sci U S A, 2003. **100**(21): p. 12153-8.
174. Conkright, M.D., et al., *TORCs: transducers of regulated CREB activity.* Mol Cell, 2003. **12**(2): p. 413-23.
175. Harada, J.N., et al., *Identification of novel mammalian growth regulatory factors by genome-scale quantitative image analysis.* Genome Res, 2005. **15**(8): p. 1136-44.
176. Huang, Q., et al., *Identification of p53 regulators by genome-wide functional analysis.* Proc Natl Acad Sci U S A, 2004. **101**(10): p. 3456-61.
177. Sato, T.K., et al., *A functional genomics strategy reveals Rora as a component of the mammalian circadian clock.* Neuron, 2004. **43**(4): p. 527-37.
178. Fan, M., et al., *Suppression of mitochondrial respiration through recruitment of p160 myb binding protein to PGC-1alpha: modulation by p38 MAPK.* Genes Dev, 2004. **18**(3): p. 278-89.
179. Franko, A., et al., *CREB-1alpha is recruited to and mediates upregulation of the cytochrome c promoter during enhanced mitochondrial biogenesis accompanying skeletal muscle differentiation.* Mol Cell Biol, 2008. **28**(7): p. 2446-59.
180. Taylor, R.W. and D.M. Turnbull, *Mitochondrial DNA mutations in human disease.* Nat Rev Genet, 2005. **6**(5): p. 389-402.
181. Scarpulla, R.C., *Nuclear control of respiratory gene expression in mammalian cells.* J Cell Biochem, 2006. **97**(4): p. 673-83.
182. Balaban, R.S., S. Nemoto, and T. Finkel, *Mitochondria, oxidants, and aging.* Cell, 2005. **120**(4): p. 483-95.
183. Turrens, J.F., *Superoxide production by the mitochondrial respiratory chain.* Biosci Rep, 1997. **17**(1): p. 3-8.
184. !!! INVALID CITATION !!!
185. Carpenter, A.E. and D.M. Sabatini, *Systematic genome-wide screens of gene function.* Nat Rev Genet, 2004. **5**(1): p. 11-22.
186. Guardiola-Serrano, F., et al., *Gene trapping identifies a putative tumor suppressor and a new inducer of cell migration.* Biochem Biophys Res Commun, 2008. **376**(4): p. 748-52.
187. Suter, B., et al., *Development and application of a DNA microarray-based yeast two-hybrid system.* Nucleic Acids Res, 2013. **41**(3): p. 1496-507.
188. Bergeron, D., et al., *An out-of-frame overlapping reading frame in the ataxin-1 coding sequence encodes a novel ataxin-1 interacting protein.* J Biol Chem, 2013. **288**(30): p. 21824-35.
189. Matsushita, K., et al., *Zc3h12a is an RNase essential for controlling immune responses by regulating mRNA decay.* Nature, 2009. **458**(7242): p. 1185-90.
190. Nemoto, S., M.M. Fergusson, and T. Finkel, *SIRT1 functionally interacts with the metabolic regulator and transcriptional coactivator PGC-1{alpha}.* J Biol Chem, 2005. **280**(16): p. 16456-60.